Structure-dependent relative toxic potencies of selected pyrrolizidine alkaloids

Vom Fachbereich Chemie der Technischen Universität Kaiserslautern zur Verleihung des akademischen Grades „Doktor der Naturwissenschaften“ genehmigte

Dissertation

D386

Vorgelegt von

Diplom-Lebensmittelchemikerin Lan Gao

Betreuer der Arbeit: **Prof. Dr. Dr. Dieter Schrenk**

Kaiserslautern, 2022

Der experimentelle Teil der vorliegenden Arbeit entstand in der Zeit von September 2016 bis September 2019 im Fachbereich Chemie, Fachrichtung Lebensmittelchemie und Toxikologie der Technischen Universität Kaiserslautern, in der Arbeitsgruppe von Professor Dr. Dr. Dieter Schrenk.

Promotionskommission:

Vorsitzender: Prof. Dr. Werner R. Thiel

1. Berichterstatter: Prof. Dr. Dr. Dieter Schrenk

2. Berichterstatter: Prof. Dr. Jörg Fahrer

Datum der wissenschaftlichen Aussprache: 05.05.2022

Eidesstattliche Erklärung

Hiermit versichere ich, dass ich die vorliegende Arbeit eigenständig verfasst, keine anderen als die angegebenen Quellen und Hilfsmittel verwendet und Literaturzitate kenntlich gemacht habe. Ich erkläre außerdem, dass diese Arbeit weder in gleicher noch in ähnlicher Form bereits in einem andren Prüfungsverfahren vorgelegen hat.

Kaiserslautern, den _____ _____

Lan Gao

TABLE OF CONTENTS

LIST OF TABLES

LIST OF FIGURES

KURZFASSUNG

Bei Pyrrolizidinalkaloiden (PA) handelt es sich um sekundäre Pflanzeninhaltsstoffe, die überwiegend in Pflanzen der Familien *Asteraceae*, *Boraginaceae* und *Fabaceae* vorkommen. Chemisch gesehen bestehen PAs aus einer Necinbase und Mono- oder Dicarbonsäuren, sogenannten Necinsäure(n). 1,2-ungesättigte PAs können im Organismus, insbesondere in der Leber, von Cytochrom P450 Monooxygenasen (CYPs) metabolisch aktiviert werden, wobei Pyrrol-Alkaloide entstehen. Diese hochreaktiven Metaboliten können kovalent mit nukleophilen Zentren von DNA, Proteinen oder Aminosäuren reagieren, wodurch hepatotoxische, genotoxische oder karzinogene Effekte induziert werden könnten. Das Vorkommen von PAs als Verunreinigung in einer Vielzahl von Lebens- und Futtermitteln muss als Gesundheitsgefahr betrachtet werden.

Die Risikobewertung von PAs orientierte sich bisher vor allem an Lasiocarpin und Riddelliin, denen die höchste toxische Wirkung zugeschrieben wurde. Es gibt jedoch Hinweise auf eine strukturabhängige Toxizität, weshalb sich die induzierten toxischen Wirkungen möglicherweise deutlich voneinander unterschieden. Deswegen könnte das karzinogene Risiko von PA-haltigen Produkten in der Vergangenheit überschätzt worden sein.

In einer Übersichtarbeit leiteten Merz und Schrenk nach Analyse zahlreicher Daten „interim Relative Potency (iREP)“ Faktoren für eine Reihe relevanter PAs ab, um die strukturellen Unterschiede besser mit der entsprechenden Toxizität zu korrelieren. Die Verwendung solcher iREP Faktoren könnte eine wissenschaftlichere Grundlage für die Risikobewertung bieten, wenn eine ausreichende Anzahl experimenteller Daten der Toxizität von einzelnen PAs generiert wird.

Um die Beziehung zwischen Struktur und Toxizität von PAs besser zu verstehen sowie die Anwendbarkeit von iREP Faktoren zu überprüfen und zu verfeinern, wurden die *in vitro* Zytotoxizität, Genotoxizität und Mutagenität ausgewählter PAs (Lasiocarpin, Monocrotalin‡, Retrorsin, Senecionin, Seneciphyllin‡, Echimidin‡, Europin‡, Heliotrin‡, Indicin und Lycopsamin) in einem Forschungsprojekt von Kooperation Phytopharmaka untersucht. Von mir wurden dabei die Untersuchungen mit Lasiocarpin, Retrorsin, Senecionin, Indicin und Lycopsamin durchgeführt.

Die Zytotoxizität wurde mittels *Alamar Blue Assay* an primären Rattenhepatozyten, an HepG2 Zellen und an Zellen einer transfizierten HepG2 (CYP3A4) C9 Zelllinie bestimmt. Eine strukturabhängige Toxizität wurde sowohl mit Rattenhepatozyten als auch mit HepG2 (CYP3A4) Zellen nachgewiesen. An HepG2 Zellen zeigte keines der ausgewählten PAs eine zytotoxische Wirkung, vermutlich aufgrund der fehlenden CYP-Expression. Weiterhin wurde die Rolle der CYP450-Enzyme bei der metabolischen Aktivierung mit einer Inhibitionsstudie bestätigt. Zur Messung der CYP-

Aktivität wurde ein kinetischer Assay verwendet, wobei die 7-Benzyloxyresorufin-*O*-Dealkylierung (BROD) analysiert wurde. Schließlich konnte mit dem *Glutathione-reductase-DTNB recycling assay* gezeigt werden, dass Glutathion offenbar keine wichtige Rolle bei der PA-induzierten Zytotoxizität spielt. Zur Überprüfung der Gentoxizität wurde der Mikrokern-Test durchgeführt. Alle ausgewählten PAs zeigten eine konzentration-abhängige Genotoxizität in transfizierten HepG2 Zellen. Im *Alamar blue Assay* und im Mikrokern Test ergibt sich für die relativen toxischen Potenzen der ausgewählten PAs folgende Reihenfolge: Lasiocarpin > Senecionin > Seneciphyllin ⩾ Retrorsin > Heliotrin (?) Echimidin ⩾ Europin ≈ Indicin ≈ Lycopsamin ≈ Monocrotalin. Die in diesem Projekt festgestellten relativen toxischen Potenzen der PAs stimmen nicht vollständig mit den iREP Faktoren von Merz und Schrenk überein, wobei sich für Monocrotalin and Echimidin deutliche Abweichungen ergaben. Monocrotalin war weniger und Echimidin potenter als es die iREP Faktoren aussagen. Weiterhin wurde die Mutagenität der PAs im Ames-Fluktuationstest an *Salmonella typhimurium* geprüft. Es konnte dabei keine mutagene Wirkung nachgewiesen werden, auch nicht in Anwesenheit einer externen metabolischen Aktivierung (S9-Mix).

ABSTRACT

Pyrrolizidine alkaloids are naturally occurring secondary plant metabolites mainly found in plant families of *Asteraceae, Boraginaceae,* and *Fabaceae*. Chemically, PAs consist of a pyrrolizidine core bearing hydroxyl groups, the so-called necine base, and mono- or dicarboxylic necine acids bound to the pyrrolizidine core via ester linkages. 1,2-unsaturated PAs are hepatotoxic, genotoxic, and carcinogenic due to the highly reactive pyrrolic metabolites formed by cytochrome P450 monooxygenases (CYPs) primarily in the liver. The presence of PAs as frequent contaminants in the wide variety of food and feed products has to be considered a relevant safety issue.

Based on the currently available data, the risk assessment of PAs was mainly approached using the two most toxic potent congeners, i.e., lasiocarpine and riddelliine. However, it is well recognized that toxicity is differing significantly between the congeners related to their structural features. The risk of PA-containing products is indeed overestimated, and a comprehensive risk assessment should take these differences into account.

After analyzing the data of many PAs, Merz and Schrenk derived interim Relative Potency (iREP) factors to present the differences in their toxicity between the sub-groups of PA congeners concerning their structural features. The use of such iREP factors could probably provide a more scientific basis for PA risk assessment until sufficient experimental analysis of the toxicities of individual congeners is applied.

To obtain a better understanding of the relationship between structure and toxicity of PA congeners and provide more evidence for further refinement of relative (toxic) potency factors, data of the *in vitro* cytotoxicity, genotoxicity, and mutagenicity of diverse individual PA congeners (lasiocarpine, monocrotaline‡, retrorsine, senecionine, seneciphylline‡, echimidine‡, europine‡, heliotrine‡, indicine, and lycopsamine) has been generated in our project supported by Kooperation Phytopharmaka. Among them, lasiocarpine, retrorsine, senecionine, indicine and lycopsamine have been investigated on my part.

Cytotoxicity was assessed using the Alamar blue assay in primary rat hepatocytes, HepG2 cells, and the HepG2 (CYP3A4) cell line. In HepG2 cells, none of the selected PAs exhibited cytotoxic effects, probably due to the lack of CYPs. In primary rat hepatocytes as well as in HepG2(CYP3A4) cells, a clear structure dependent cytotoxicity could be demonstrated. The role of CYP450 enzymes in metabolic activation was further confirmed using an inhibition assay. A kinetic assay analyzing 7-benzyloxyresorufin-*O*-dealkylation (BROD) was used for measuring the activity of CYP450 enzymes. Furthermore, the utilization of a glutathione-reductase-DTNB recycling assay indicated that glutathione might not play a critical role in PA-induced cytotoxicity. A micronucleus test was used for determining the PA-induced clastogenic

genotoxicity. All selected PA congeners exhibited concentration-dependent toxicity in the HepG2 (CYP3A4) cells. The relative potencies of PA congeners estimated from Alamar blue assay and micronucleus assay are generally consistent with the following ranking: lasiocarpine > senecionine > seneciphylline ≥ retrorsine > heliotrine (?) echimidine ≥ europine ≈ indicine ≈ lycopsamine ≈ monocrotaline. The relative toxic potencies evaluated based on our findings were not completely consistent with the iREP classification previously reported by Merz and Schrenk. Monocrotaline in both assays exhibited considerably lower toxic potency. Echimidine, however, was more toxic than expected. On the other hand, mutagenicity was measured in Ames fluctuation assay with *Salmonella typhimurium* strains TA98 and TA100. None of the selected PA congeners up to 300 µM showed mutagenic effects despite metabolic activation with S9-mix.

ABBREVIATIONS

ASB	assay stock buffer
BCA	bicinchoninic acid
BfArM	ger: Bundesinstitute für Arzneimittel und Medizinprodukte
BfR	German Federal Institute for Risk Assessment
BMD	benchmark dose
$BMDL_{10}$	benchmark dose lower confidence limit 10%
BMDL	benchmark doses with lower confidence limits
BMDU	benchmark doses with upper confidence limits
BSA	bovine serum albumin
BROD	7-benzoxyresorufin-*O*-dealkylase
bw	body weight
COE	Council of Europe
COT	Committee on Toxicity of Chemicals in Food, Consumer Products and The Environment
CYP450	Cytochrome P450
DMEM-LG	Dulbecco´s modified Eagle´s medium-low glucose
DMEM-HG	Dulbecco´s modified Eagle´s medium-high glucose
DMF	dimethylformamide
DMSO	dimethylsulfoxide
DTNB	5,5´-dithiobis-2-nitrobenzoic acid
EC_{50}	effective concentration 50%
EDTA	ethylene diamine tetraacetate
EFSA	European Food Safety Authority
et al.	lat: *et alii*
FCS	fetal calf serum
FAU	formazine attenuation unit
FDA	U.S. food and drug administration
G6P	glucose-6-phosphate
G6PDH	glutathione-6-phosphate dehydrogenase
GR	glutathione-*S*-reductase
GSH	glutathione reduced form
GSSG	glutathione oxidized form
GST	glutathione S-transferase
GSx	total glutathione, i.e., the sum of GSH and GSSG

HEPES	4-(2-hydroxyethyl)-1-piperazineethanesulfonic acid
HMPC	Committee on Herbal Medicinal Products
HPLC	high-performance liquid chromatography
HVOD	hepatic veno-occlusive disease
i.p.	lat: *intra peritoneum*
IPCS	International Programme on Chemical Safety
iREP	interim relative potency
i.v.	lat: *intra vena*
JECFA	joint FAO/WHO expert committee on food additives
LD50	median lethal dose
MN	Micronucleus
MOE	margin of exposure
β-$NADP^+$	β-nicotinamide adenine dinucleotide phosphate
β-NADPH	β-nicotinamide adenine dinucleotide phosphate hydrate
n.s.	not significant
NC	negative control
NO(A)EL	no observed (adverse) effect level
n.t.	not tested
NTP	National Toxicology Program
PBS	phosphate-buffered saline
PC	positive control
PoD	point of departure
SCE	sister chromatid exchange
SD	standard deviation
SSA	5-sulfosalicylic acid
TDI	tolerable daily intake
TTC	Threshold of Toxicology Concern
UDS	unscheduled DNA synthesis
WHO	World Health Organization

1 INTRODUCTION

Pyrrolizidine alkaloids as secondary metabolites occur in a variety of plants distributed widely in the world. They are found as contaminants in various food sources, such as wheat, honey, tea, milk, and meat products, and also present in plant extracts used in phytopharmaceuticals and homeopathic preparations (BfR, 2015, 2013; Bodi et al., 2014; Mulder et al., 2018; Mulder et al., 2015). Due to the toxic action, PAs represent a possible concern for human health. With a further increase in the production and consumption of herbal teas and medicinal plants, contamination of PAs may become more critical.

In recent years, their potent hepatotoxicity, genotoxicity, and particularly carcinogenicity have been extensively studied. Similar to many other toxic chemicals, PAs exert their toxicities only after metabolic activation. The liver, which contains abundant metabolic essential enzymes, especially the cytochrome P450 (CYP) family, plays a primary role in PAs metabolism. Based on numerous toxic studies, certain metabolites of the 1,2-unsaturated PAs are assumed to be responsible for the toxic effects.

Owing to the genotoxic and carcinogenic properties exhibited in chronic animal studies, there is thought to be no safe threshold dose. In the beginning, the exposure of PAs was suggested to be minimized or avoided (WHO-IPCS, 1989, 1988). When the "Margin of Exposure (MoE)" approach was applied, a reference dose $BMDL_{10}$ (10% increase in the tumor incidence in animal experiments) combined with an MoE >10,000 (low level of concern) was used to derive a tolerable daily intake of toxic unsaturated PAs (COT, 2008; EFSA Panel on Contaminants in the Food Chain, 2011; WHO-IPCS, 1989, 1988).

Because of the inadequate data on the toxicity of individual PA congeners, current risk assessments are mainly based on the carcinogenicity of lasiocarpine or riddelliine, the most potent PA congeners, precautionary assuming the toxic potency of all the PA congeners equal and sharing the same mode of action. But numerous animal experiments and *in vitro* studies demonstrated that the toxic potencies of PA congeners probably differ by orders of magnitude. Many other PAs are plausible as expected lower potent compared to lasiocarpine and riddelliine. Therefore, it possibly misleads to overestimate the risk of PAs in foods and herbal medicines, resulting in excessively restricted limitations for the intake. An appropriate evaluation assists the risk assessment and contributes to guaranteeing the safety of marketed PA-containing products.

After analyzing available literature on congener-specific toxicity, including acute toxicity, cytotoxicity, and genotoxicity, a considerable structure dependence has been found by Merz and Schrenk (2016). According to this strong indication of a relationship

between toxic potency and structural features, the concept of interim relative (toxic) potency (iREP) factors was proposed, whereby PA congeners have been divided into four different subgroups with respect to their toxic potencies and structural characteristics. However, due to the limited data of individual PA congeners and poor comparability between studies with various endpoints, at the moment, the assigned provisional REP factors still could not be reliably estimated the relative toxic potency of all PA congeners.

Our project aimed to apply an improved data basis to understand better the relationship between structure and toxicity of individual PA congeners and provide more evidence for further refinement of REP factors. Ten PA congeners (lasiocarpine, monocrotaline‡, retrorsine, senecionine, seneciphylline‡, echimidine‡, europine‡, heliotrine‡, indicine, and lycopsamine) with different structural features from four relative potency subgroups have been selected for our project. They were determined by a series of *in vitro* test systems with different endpoints to quantify their hepatotoxicity, genotoxicity, and mutagenicity. The results of five congeners (lasiocarpine, retrorsine, senecionine, indicine, and lycopsamine) were presented in my work. The same protocol was also applied to five other PA congeners, including echimidine‡, europine‡, heliotrine‡, monocrotaline‡, and seneciphylline‡, which have been measured by Mr. Rutz. Therefore, the data from Mr. Rutz were not reported in the results of this work. Only the values already published, such as EC_{50}s or BMDs, being cited in discussion help better understand the probable relationship between the structural features and the relative toxic potencies.

In the first instance, the cytotoxicity was investigated by Alamar blue assay in primary rat hepatocytes and HepG2 cells. All PA congeners exhibited a concentration-dependent manner in the primary culture. In contrast, almost no detectable cytotoxic effects could be found in the HepG2 cell line, likely because of the lack of CYP enzymes. To investigate whether CYP450 enzymes play a critical role in the metabolic activation involved in PA-induced toxicity, an inhibition study on CYP450 enzyme activity was also accomplished with primary rat hepatocytes. In addition, it is well known that intracellular glutathione is typically related to the detoxification of xenobiotics. Thus, the glutathione-reductase-DTNB recycling assay has been applied to determine whether this mechanism was associated with PA-induced cytotoxicity. Afterwards, HepG2 (CYP3A4) clone 9 cell line transducing with recombinant lentivirus for constitutive and stable overexpression of CYP3A4 obtained from the University of Technology Cottbus-Senftenberg was also used to investigate the cytotoxicity. It exhibited similar behavior as primary rat hepatocytes. Tests for genotoxicity, including the mutagenicity and clastogenicity, Ames-fluctuation assay and micronucleus test have been utilized, respectively. In the Ames-fluctuation assay, all PA congeners exhibited no detectable mutagenic effects in strains TA98 and TA100

of *Salmonella typhimurium* despite the S9 mix as an external metabolic activation. Due to the overexpression and relative higher activity of CYPs, the permanent cell line HepG2 (CYP3A4) C9 was chosen for the micronucleus test (Herzog et al., 2015).

In summary, whether in cytotoxic tests or genotoxic assays, all selected PA congeners in our project showed a concentration-dependent manner. The relative toxic potencies of all these congeners were generally consistent with the proposed iREP factors suggested by Merz and Schrenk but with two apparent exceptions of monocrotaline and echimidine. The variation from the proposed concept might be related to congener-specific metabolism, different susceptibilities among species, or other toxicokinetic factors. It is necessary to accumulate more convenient and efficient data on individual PA congeners while taking the particular toxicokinetics of PAs into account to refine REP factors further.

2 THEORETICAL FRAMEWORK

2.1 Pyrrolizidine alkaloids

2.1.1 Occurrence and exposure

Pyrrolizidine alkaloids are secondary plant metabolites that occur in hundreds of plants species from up to 13 families widespread worldwide (Mattocks, 1986; Smith and Culvenor, 1981). Up to now, more than 660 different PAs and their corresponding *N*-oxides derivates have been identified in over 6000 plants mainly belonging to families of *Asteraceae, Boraginaceae, and Fabaceae*, half of them have been estimated hepatotoxic, carcinogenic, mutagenic, or teratogenic (Roeder, 2000; Stegelmeier et al., 1999). In plants, PAs play a role as a constitutive protection mechanism to defense against fungal, bacterial pathogens, and the attack by herbivores (Chen et al., 2017; Hartmann, 1999; Hartmann and Witte, 1995). The composition and concentration of PAs in different plants eventually in different parts of the plants is related to species, location, season, also environmental conditions (Bull et al., 1968; Mattocks, 1986).

Due to their universal distribution of toxic PA-containing plants, PAs could be found from foods containing PA constituents or as contaminants in various food items, such as wheat, tea, honey, eggs, milk, meat, etc. (BfR, 2015; Crews et al., 1997a; Crews et al., 1997b; Edgar et al., 2002; Edgar and Smith, 2000; Kempf et al., 2010; Kowalczyk and Kwiatek, 2018; Mohabbat et al., 1976; Mulder et al., 2016; Tandon et al., 1978; Tandon et al., 1976; Wang et al., 2019). Among them, honey originated from PA-containing plants was estimated to be one of the principal exposure sources and has been investigated using different measurement methods. Echimidine and lycopsamine were found to be the main contributors (Edgar et al., 2002; EFSA Panel on Contaminants in the Food Chain, 2016; Kempf et al., 2010; Kowalczyk and Kwiatek, 2018; Wang et al., 2019). EFSA also recommended the exposure route through a carry-

over effect from feed containing toxic PAs into animal products, such as milk and milk products. Mulder et al. reported that 11 out 118 milk samples were contaminated with PAs but with relatively low levels between 0.05 and 0.17 µg/l (EFSA Panel on Contaminants in the Food Chain, 2007; Mulder et al., 2015). With regard to the PA exposure from tea and herbal infusions intermedine, intermedine-*N*-oxide, lycopsamine, retrorsine-*N*-oxide, senecionine, senecionine-*N*-oxide, seneciphylline, and seneciphylline-*N*-oxide were reported by Bodi et al. (Bodi et al., 2014) as the most frequent observed congeners with the highest concentrations. In addition, herbal remedies and folk teas for medicinal purposes popular in many underdeveloped countries are made from PA-containing plants. In China, Sri Lanka, and other countries, many herbal plants with certain natural contents of PAs have been used for traditional homeopathic medicine (Arseculeratne et al., 1985, 1981; Bah et al., 1994; Edgar et al., 1992; Roeder, 2000). About 38 Chinese herbal plants containing PAs were well characterized by Roeder (2000). In recent years, more reports revealed the exposure by consumption of teas and herbal infusions even prepared from no PA-containing plants due to cross-contamination during harvesting, storage, or transport. At the same time, the use of dietary supplements has become increasingly popular in the world.

Based on the PA-content in a great number of food samples (s. Tab. 1) and the consumption of differently exposed populations, the dietary exposure to PAs via honey, tea, or herbal infusion, and pollen-based supplements has been estimated by EFSA. For the adult population average customers, the mean chronic exposure from honey ranged between 0.1 and 7.4 ng/kg bw per day, while in the young population, it was between 0.3 and 27.0 ng/kg bw per day. Among the highly exposed customers, the maximal exposure was estimated at 17.6 and 31.0 ng/kg bw per day, respectively, for the adult and young populations. For the different sorts of teas and herbal infusions, the mean chronic dietary exposure to PAs was estimated for average customers with a range of 34.5 – 48.4 and 31.1 – 41.8 ng/kg bw per day in the young and adult population, respectively, according to the data reported in EFSA Art 36 grant. When considering the highly exposed population, the highest estimates were 153.8 – 214.0 and 87.7 – 127.2 ng/kg bw per day. Using the data submitted by Tea & Herbal Infusions Europa, the estimated chronic exposure was significantly lower. Regarding pollen-based supplements, based on limited data, the chronic exposure could be estimated between 0.7 and 11.5 ng/kg bw per day among customers (EFSA Panel on Contaminants in the Food Chain, 2016).

Table 1: PA-content and main contributors in different food samples

Product	Concentrations and main PA contributors
Milk	0.05 – 0.17 µg/l echimidine, jacoline, lycopsamine, otosenine, retrorsine, and senkirkine
Honey (retail)	0 – 248.0 µg/kg

	echimidine and lycopsamine
Tea (dry products)[1]	
Black tea	1.2 – 1155.5 µg/kg intermedine-*N*-oxide, intermedine, lycopsamine, retrorsine-*N*-oxide, and senecionine-*N*-oxide
Chamomile	0 – 3441.2 µg/kg senecionine-*N*-oxide, intermedine, senecionine, and lycopsamine
Green tea	0 – 486.9 µg/kg senecionine-*N*-oxide, retrorsine-*N*-oxide, intermedine, and lycopsamine
Peppermint	0 – 887.2 µg/kg seneciphylline-*N*-oxide, senecionine-*N*-oxide, retrorsine-*N*-oxide, and seneciphylline
Rooibos	79.8 – 498.4 µg/kg senecionine-*N*-oxide, restrorsine-*N*-oxide, and senecionine
Pollen-based supplements	235 – 253 µg/kg (average) lycopsamine, intermedine, and their *N*-oxides
Plant extracts (dry products)[2]	
Borage (*Borago officinalis*)	31.1 / 28.7 mg/kg
Comfrey (*Symphytum officinale*)	29.7 / 17.6 mg/kg
Coltsfoot (*Tussilago farfarae*)	15.8 mg/kg
Gremil (*Lithospermum officinale*)	14.6 mg/kg

1. Range of content in different sorts of tea estimated based on the minimum lower and maximum upper bound;
2. All plant extracts were prepared as tea infusion (2 g in 150 ml).
(BfR, 2013; Bodi et al., 2014; EFSA Panel on Contaminants in the Food Chain, 2017, 2007; Mathon et al., 2014; Mulder et al., 2015).

2.1.2 Structure characteristics

PAs are a large class of heterocyclic compounds with a general structure of PAs called necine base classified into four common types: platynecine, retronecine, heliotridine, and otonecine (s. Fig. 1), among which retronecine- and heliotridine-types are enantiomers at the C7 position. Only platynecine-type contains a saturated necine base. Retronecine-, heliotridine- and otonecine-type with a double bond between C1- and C2-position are considered as toxic PAs. The PA congeners (s. Fig. 2) selected in our project belong to retronecine- and heliotridine-types. The necine base of these types consists of two five-membered rings sharing a typical nitrogen atom at position 4 and fitted with an unsaturated bond between the C-atoms in position 1 and 2. Most PAs naturally occurring in plants are esterified. The acids that are esterified with the necine base are called necine acids. PAs can be divided according to the esterification pattern of necine acids into mono-ester, open-chain di-ester, and cyclic di-ester. Except for the otonecine-type, the other three types of PAs in plants are presented as corresponding *N*-oxides.

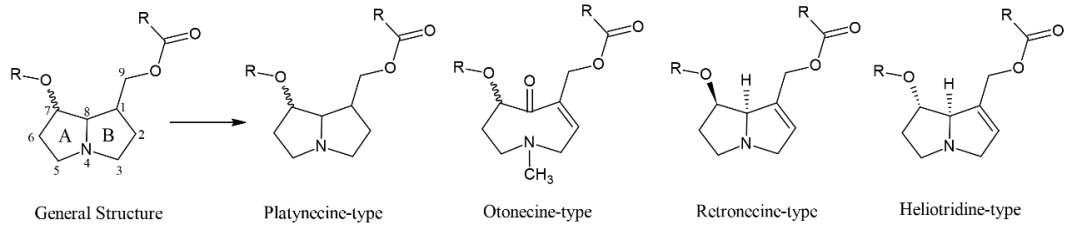

Figure 1: Structure features of different PA-types based on necine bases

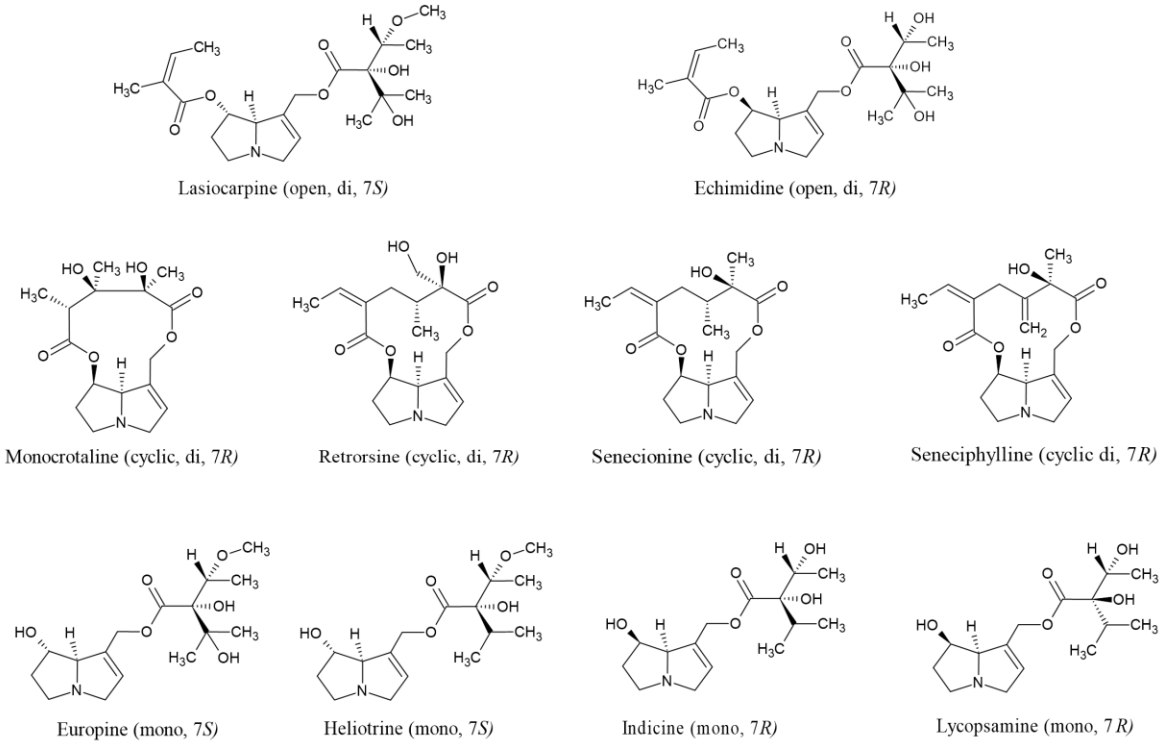

Figure 2: Structures of selected pyrrolizidine alkaloids in our project

2.1.3 Metabolism pathway

Similar to the majority of other chemical compounds, PAs require metabolic activation to exert their toxicity. The metabolic activation pathway of PAs was proposed only based on studies of some individual PAs, and the generally accepted theory assumed the highly reactive "pyrrolic ester" to be the most potential toxic metabolite responsible for the toxicity. Hence the metabolism of PAs to dehydro-pyrrolizidine alkaloids is considered as an essential metabolic activation pathway. Therefore, platynecine-type containing a saturated necine base does not generate the chemically reactive intermediate pyrrolic ester after CYP450-mediated oxidation and is less toxic (Lester et al., 2019; Ruan et al., 2014a). The retronecine- and heliotridine-type PAs with 1,2-unsaturated structures due to their potential to undergo metabolic activation leading to a formation of reactive pyrroles, which are unstable and difficult to be detected, are considered to be relevant for safety assessment (Fu et al., 2001; Mattocks, 1986;

Stegelmeier et al., 1999). The otonecine-type is also unsaturated but undergoes an initial oxidative *N*-demethylation of the necine base followed by ring closure and dehydration to achieve metabolic activation (Fu et al., 2004). The retronecine- and heliotrine-types have been reported to be more toxic than otonecine-type due to the higher amount of pyrrole-protein adducts generated and more CYPs involved in the metabolic activation (Ruan et al., 2014b).

In my work, the *in vitro* systems were treated with five PAs belonging to the most toxic retronecine- and heliotridine-types. The inferred metabolic pathways for PAs (s. Fig. 3) are shown using the general structure of these two types.

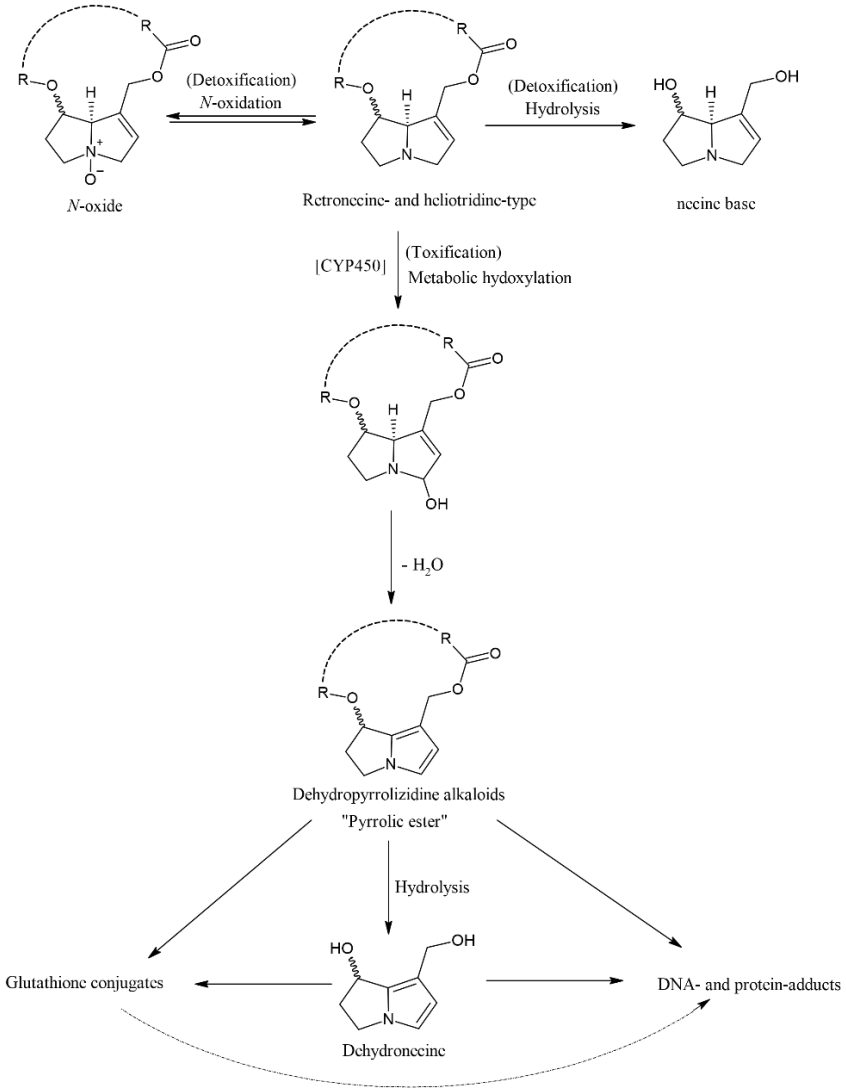

Figure 3:Proposed principal metabolism pathways of retronecine- and heliotridine-types.

According to the studies of the metabolism of individual PA congeners, a principal metabolism pathway could be proposed. After oral intake, the lipophilic PAs can be resorbed via specific favin-dependent monooxygenases in intestinal mucosa by forming more hydrophilic corresponding *N*-oxides, which can be easier excreted through urine

to detoxify. However, *N*-oxides may possibly be converted back to parent PAs by intestinal flora to form the identical adducts but with less formation rate and are thus considered to be less potent (Chou et al., 2003; Fu et al., 2001; He et al., 2017; Mattocks, 1971; Wang et al., 2005c; Yang et al., 2017). When PAs enter the circulatory system, they could be hydrolyzed by unspecific esterase to the corresponding necine bases and acids without developing any toxic effect. On the other hand, the majority of PAs with unsaturated structure along into the liver is most likely oxidized by cytochrome P450 monooxygenases primarily to 3-hydroxy-PAs then forming a reactive "pyrrolic ester", i.e., (±)-6,7-dihydro-7-hydroxy-1-hydroxymethyl-5*H*-pyrrolizine ester, which could rapidly bind covalently to nucleophilic centers of DNA or non-specifically to cellular proteins leading to the formation of genotoxic adducts (Chen et al., 2010; Fu et al., 2002; Fu et al., 2001; Ruan et al., 2014b; Yang et al., 2001b).

There is another possible pathway via dehydronecine, which is produced by "pyrrolic ester" upon hydrolysis. In addition, since "pyrrolic esters" are highly unstable, more adducts are probably derived from dehydronecine rather than through dehydro-PA. On the other hand, dehydronecines are more persistent with lower chemical and biological activity. They are not acutely toxic but can cause extensive extrahepatic injury, especially in young animals (ANZFA, 2001; Fu et al., 2001; Stegelmeier et al., 1999).

"Pyrrolic ester" and dehydronecine both capable of binding to glutathione to form GSH-conjugates that could be readily excreted have generally been considered a detoxification pathway. However, 7-GS-dehydronecine and 7-cysteine-dehydronecine could also bind to DNA and protein to produce genotoxic adducts similar to "pyrrolic esters" which suggests that GSH conjugated adducts of PAs are also potential carcinogenic (He et al., 2017). In the study of Geburek et al. (2020b), GSH conjugates were observed with higher levels formed by di-esters than that by less toxic mono-esters.

Besides the generally accepted metabolic pathway and the corresponding formed metabolites, *trans*-4-hydroxy-2-hexenal was also reported as the primary metabolite in an *in vitro* hepatic microsomal metabolism of senecionine (Segall et al., 1985). It was likely formed by the metabolism of the retronecine base from cleavage of the bonds between C1-C2, C5-N, and C8-N. In addition, *trans*-4-hydroxy-2-hexenal subjected to lipid peroxidation is well known for carcinogenicity and mutagenicity. It suggests that other intermediates and metabolites might also be associated with the toxicity of PAs, and the formation of other compounds should also be considered a possible activation pathway.

PAs undergoing metabolic activation exhibit their toxicity primarily in the liver because they require metabolic bioactivation via different CYP450 isoforms, among which CYP3A and CYP2B subfamilies showed the most pronounced effects (Buhler and

Kedzierski, 1986; Chung et al., 1995; Huan et al., 1998; Li et al., 2011; Miranda et al., 1991), but also occurs in other organs such as the lung, pancreas, or blood vessels.

Additionally, the metabolic pattern of individual PA congeners is species- and tissue-dependent. In inhibition studies with sheep and hamster microsomes, it was revealed that CYP3A was the critical enzyme mediating the metabolic activation in both species (Huan et al., 1998). In comparison, the CYP2B isoform was more important in the biotransformation with hepatic microsomes from guinea pigs. Many PAs have been indicated in human liver microsomes to be catalyzed mainly by CYP3A4 except for monocrotaline, which was metabolized predominantly by CYP2A6 and CYP2E1 (Li et al., 2011; Miranda et al., 1991; Ruan et al., 2014b). The susceptibility of PA intoxication related to species was reported in numerous studies. In general, humans, rats, mice, cattle, and horses are more sensitive to PAs than sheep, goats, rabbits, and guinea pigs. The differences probably arise from the toxicokinetics including various distributions of CYP isoforms, transport of the compounds, as well as the balance between the intoxication and detoxification (Cheeke and Pierson-Goeger, 1983; Huan et al., 1998; Mattocks, 1986; Molyneux et al., 2011; Shull et al., 1976; White et al., 1973; Winter et al., 1988). Although the metabolism-dependent toxicity of PA congeners varies between species (Geburek et al., 2020b; Geburek et al., 2020a), the prominent and fundamental metabolic processes are generally common to all PAs.

2.1.4 Toxicity

(Sub)acute and chronic toxicity

The PA-induced livestock and human poisoning from the intake of herbs or foods containing PAs have been reported in different countries. In some severe poisonings, the outbreak resulted in a high mortality rate. Acute toxicity, i.e., short-term toxicity caused by consuming foods or herbal products containing high amounts of PAs, was commonly associated with hepatic sinusoidal obstruction syndrome (hepatic veno-occlusive disease, HVOD). It is characterized by ascites and hepatomegaly, possibly progressing to cirrhosis, even induced mortality due to hepatic failure or haematemesis caused esophageal varices (Kakar et al., 2010; Kumana et al., 1985; Mohabbat et al., 1976; Roulet et al., 1988; Tandon et al., 1976).

The median lethal dose (LD_{50}), i.e., 50% lethality of animal experiments, was commonly investigated in acute toxicity studies. Oral LD_{50} value was reported in mice for senecionine of 57 mg/kg bw. It was determined in rats for retrorsine of 34- 38 mg/kg bw, for echimidine of 518 mg/kg bw, and for heliotrine of 510 mg/kg bw (Dalefield et al., 2015; Dalefield et al., 2012; EFSA Panel on Contaminants in the Food Chain, 2011; Mattocks, 1971; Wang et al., 2011). The LD_{50} values after intraperitoneal (*i.p.*) or intravenous (*i.v.*) administration were also available but not relevant for the risk assessment of PAs in food.

The short-term toxicity of riddelliine was determined in F344 rats and B6C3F1 mice in a 2-week and a 13-week study (Chan, 1993). These results are part of a 2-year bioassay from the National Toxicology Program (NTP). In another 2-year chronic study from NTP, lasiocarpine was also demonstrated to induce liver tumors with F344 rats (NTP, 1978).

Chronic toxicity happens when food or herbal medicines contain minor PAs but are consumed for the long term. It could result in damages such as megalocytosis, hyperplasia, veno-occlusion, cirrhosis, and even adenomas or carcinomas, mainly in the liver, lungs, and blood vessels, but also possibly in other organs (Mattocks, 1986). Since PAs are mostly eliminated rapidly, the chronic damage lack of specific clinical features is easily misinterpreted caused by other toxicants. It could not be easy to relate to the PAs. Consequently, not much information on chronic studies on humans is available to assure the chronic effects of PAs exposure. Due to the excellent repair capacity of the liver, if with low doses over an extended period, it possibly leads to a pulmonary disease rather than liver damage (Edgar et al., 2011).

Hepatotoxicity

PAs induced human hepatoxicity is most frequently associated with the consumption of herbal remedies. Outbreaks of PA-induced human poisoning in Afghanistan and India caused by intake of PA-containing plants demonstrated its hepatotoxicity (Kakar et al., 2010). It is well known that PA-induced hepatotoxicity is processed via CYP-mediated metabolic activation followed by the formation of pyrrole-protein adducts, which damage the normal function of specific proteins in the liver. Pyrrole-protein adducts of PAs were demonstrated in the liver of mice and *in vitro* using rat liver microsomes and the recombinant human CYPs (Ruan et al., 2014a; Ruan et al., 2014b). Hence Pyrrol-protein was suggested as a biomarker for PA-induced liver injury. In addition, the pyrrole-protein adducts of the PA *N*-oxides after biotransformation to their corresponding PAs and followed by common metabolic pathway were also determined and confirmed by Yang et al. (2017).

Time- and concentration-dependent apoptosis involving the extrinsic death receptor pathway and the intrinsic mitochondrial pathway in HepaRG cells after PA exposure have been reported by Waizenegger et al. (2018). It suggested that retronecine-type PAs (senecionine, echimidine) were more potent than heliotridine- (heliotrine) or otonecine-type (senkirkine).

Genotoxicity

Plenty of naturally occurred flowers, leaves, stalks, roots, or seeds from many plants containing PAs those widely used in herbal remedies or some foodstuffs, as well as their fractions, were to be found carcinogenic (Hirono et al., 1983; Hirono et al., 1978; Hirono et al., 1976; Schoental et al., 1971; Schoental et al., 1970). In addition, a number

of purified PAs, including clivorine, heliotrine, petasitenine, retrorsine, senkirkine, and symphytine were also indicated in many animal experiments to induce tumors, not only in the liver but also in other organs such as lung, kidney, pancreas, or even in the brain (Hirono et al., 1979; Hirono et al., 1977; Kuhara et al., 1980; Rao and Reddy, 1978; Schoental, 1975; Schoental et al., 1971; Schoental et al., 1954; Schoental and Cavanagh, 1972).

The 2-year long-term studies by NTP revealed that riddelliine and lasiocarpine induced liver tumors in F344 rats and/or B6C3F1 mice (Chan, 1993; NTP, 2003, 1978). At the same time, the PA congeners belonging to retronecine-type were confirmed as the most genotoxic.

A variety of genotoxic effects such as DNA binding, DNA cross-linking, DNA-protein cross-linking, formation of micronuclei, sister chromatid exchanges, chromosomal aberrations, mutations, or teratogenicity was determined *in vivo* or *in vitro* studies.

DNA adducts of riddelliine were found in rodent (female F344 rats and B6C3F1 mice) liver after feeding (Chou et al., 2004; Yang et al., 2001a; Yang et al., 2001b). Based on the excellent correlation between the level of the dehydronecine-derived DNA adducts and the tumorigenic potencies presumed that riddelliine-induced liver tumor could be mediated by dehydronecine-DNA adducts (Yang et al., 2001b). The adducts, which possibly lead to hemangiosarcomas, were generated in liver endothelial cells significantly more than in the parenchymal cells (Chou et al., 2004). The formation of DNA adducts by oral gavages of retrorsine with a daily dose of 1.0 mg/kg bw for three consecutive days to F344 female rats or monocrotaline with a single orally dose of 10 mg/kg bw also supported that these dehydronecine-derived DNA adducts might be responsible for PA-induced liver tumorigenicity and genotoxicity (Wang et al., 2005b; Wang et al., 2005a). Afterward, dehydronecine-derived DNA adducts were also determined in the liver of rats after oral gavage with clivorine, heliotrine, lasiocarpine, monocrotaline, retrorsine, and riddelliine. At the same time, the di-esters formed higher levels of DNA-adducts than the mono-esters, which indicated that the DNA-adducts could be potential biomarkers of PA-induced tumorgenicity (Xia et al., 2013). The PA-derived DNA adducts have also been found in the blood of F344 female and male rats after a single dose of gavaging with riddelliine (Yan et al., 2002).

DNA cross-linking or DNA-protein cross-linking induced by different PA congeners and their pyrrolic derivatives have also been determined. *In vivo*, after *i.p.* injection of monocrotaline to adult male Sprague-Dawley rats, DNA-DNA interstrand cross-linking and DNA-protein cross-linking were observed. Still, it was shown no evidence for the DNA single-strand break (Petry et al., 1984). In *in vitro* studies, congeners including heliosupine, latifoline, monocrotaline, retrorsine, riddelliine, senecionine, and seneciphylline, have been reported to induce DNA-DNA or DNA-protein cross-linking

to varying degrees in cultured Madin-Darby bovine kidney epithelial cells. Similar to the finding of Petry et al., none of these PA congeners led to detectable DNA single-strand breaks (Hincks et al., 1991). Using the same cell line, Kim et al. investigated a series of corresponding pyrrolic derivatives of the congeners belonging to cyclic di-ester PAs and found the cross-linking activity of these derivatives in general consistent with the potencies of the parent PAs (Kim et al., 1999; Kim et al., 1995). The PAs or their reactive metabolites in cross-linking the DNA or protein have also been proved in human breast carcinoma cells, as well as in cross-linking with DNA from E.coli, M13, and pBR322 plasmid (Coulombe et al., 1999; Kim et al., 1999; Pereira et al., 1998; Reed et al., 1988; White and Mattocks, 1972). Although DNA strand breaks could not be demonstrated using alkaline elution assay, with the Comet assay, isatidine and monocrotaline exhibited positive effects on human hepatoma (HepG2) cells and human glioblastoma cell line (GL-15), respectively (Silva-Neto et al., 2010; Uhl et al., 2000). Furthermore, many PA congeners have been identified by Louisse et al. (2019) to induce DNA strand breaks but using γH2AX assay.

Unscheduled DNA synthesis (UDS) found in rat liver induced by riddelliine, in hepatocytes from different species caused by lasiocarpine, senecionine, seneciphylline, and monocrotaline was also reported (Mori et al., 1985; Williams et al., 1980).

PA-induced chromosomal alteration has also been frequently investigated. Clastogenic damage, i.e., formation of micronuclei, was evaluated in the bone marrow of adult mice and their fetal liver after exposure to heliotrine and monocrotaline (Sanderson and Clark, 1993). *In vitro*, retrorsine, monocrotaline, and isatidine were demonstrated to induce micronuclei in primary rat hepatocytes (Müller-Tegethoff et al., 1997). Using HepaRG cell line, the positive response was also found to lasiocarpine, retrorsine, monocrotaline, echimidine, europine, heliotrine, indicine, lycopsamine, and other 6 PAs as well as several corresponding *N*-oxides (Allemang et al., 2018). Lasiocarpine and senkirkine could induce chromatid gaps, while heliotrine and petasitenine caused interchromosomal exchanges in V79 cells (Takanashi et al., 1980). Additionally, sister chromatid exchange (SCE) induced by senechiphylline, senkirkine, heliotrine, and monocrotaline, was also demonstrated in V79 cells when co-cultured with primary chick embryo hepatocytes.

The carcinogenic activity appears frequently accompanied by mutagenic behavior. Mei et al. reported a G:C to T:A predominantly transversal mutation pattern of riddelliine *in vivo* using liver *cII* gene of transgenic big blue rats (Mei et al., 2004a; Mei et al., 2004b). Using standard or modified Ames test with pre-incubation, the PA congeners, such as clivorine, fukinotoxin, heliotrine, ligularidine, LX-201, lasiocarpine, monocrotaline, retrorsine, senkirkine, seneciphylline, and senecivernine were found mutagenic or weakly mutagenic to the strain TA100 of *Salmonella typhimurium* in the presence of S9 metabolic activation system (Rubiolo et al., 1992; Yamanaka et al.,

1979). For retrorsine, the mutagenic activity was additionally observed in the strains of TA1535 and 1537 (Wehner et al., 1979).

2.1.5 Regulatory rules of PAs and PA-containing products

Based on the limited data, only lasiocarpine, monocrotaline, and riddelliine were classified to category 2B, i.e., possibly carcinogenic to humans, by the International Agency for Research on Cancer (IARC). Other PAs were not classifiable (IARC, 2002).

The World Health Organization - International Programme on Chemical Safety (WHO-IPCS) stated that human PA poisoning might lead to acute HVOD. According to literature data of *Symphytum* poisoning over about six months (Ridker et al., 1985), it was estimated that a PA dose equivalent to 0.01 mg heliotrine/kg bw per day may lead to liver disease in humans, indicating even intake of low doses if over some time also possibly cause a health risk. Based on the genotoxic properties observed in chronic animal studies, the actual human cancer risk could not be evaluated. Thus the exposure should be avoided or minimized (WHO-IPCS, 1989, 1988).

German Federal Institute for Risk Assessment (BfR) also emphasized that the exposure to 1,2-unsaturated PAs from different foods should have complied with the "As Low As Reasonable Achievable (ALARA)" principle and not exceed an intake of 0.007 µg/kg bw per day (BfR, 2011). In agreement with the value issued by the Committee on Toxicity of Chemicals in Food, Consumer Products and The Environment (COT) in 2008, which was based on a benchmark dose lower confidence limit for 10% extra cancer risk ($BMDL_{10}$) of 73 µg/kg bw per day established from a two years carcinogenicity study of lasiocarpine in male rats (NTP, 1978) with applying a margin of exposure (MOE) of 10,000 (COT, 2008).

The European Food Safety Authority (EFSA) Panel on Contaminants in the Food Chain (CONTAM) concluded that 1,2-unsaturated PAs might act as genotoxic carcinogens in humans. However, since it was impossible to estimate a tolerable daily intake (TDI) from the food other than honey, CONTAM Panel decided to implement also the MOE approach, which was recommended by COT (EFSA Panel on Contaminants in the Food Chain, 2011).

Following the more data of PAs on other food supplements, in 2017, EFSA established a $BMDL_{10}$ of 237 µg/kg bw per day for induction of liver haemangiosarcomas in female rats exposed to riddelliine as the new reference point of departure (PoD) to access the cancer risk of PAs (EFSA Panel on Contaminants in the Food Chain, 2017). The assumption was summarized all cumulative PA exposures and supposed all PA congeners are as potent as the known most potent representatives lasiocarpine or riddelliine.

To reduce the risks caused by PA-containing herbal medicinal products, BfArM restricted that the exposure of medicinal products containing 1,2-unsaturated PAs should not exceed 100 µg/day with external application and 1 µg/day if internal use. Still, if the application period is longer than six weeks, the limits should be reduced respectively to 10 µg and 0.1 µg per day (BfArM, 1992).

In the public statement EMA/HMPC/893108/2011, Committee on Herbal Medicinal Products (HMPC) deduced a short-term (maximum 14 days) acceptable daily intake of 0.35 µg/day of toxic 1,2-unsaturated PAs related to the final product for a 50 kg person derived from the permitted daily intake of 0.007 µg/kg bw per day stated by COT and EFSA (COT, 2008; EFSA Panel on Contaminants in the Food Chain, 2011; EMA, 2014).

In 2016, BfArM implemented a risk assessment which divided the contamination with PA-producing plants into the following three risk categories: Category A – very low or no concern, amount of PAs in 90% of the measured samples below 0.1 µg/day or none more than 0.35 µg/day; Category B – low concern, amount of PAs in 90% of the measured samples below 0.35 µg/day or none more than 1.0 µg/day; Category C – relevant concern, no data available or classification to categories A and B is not possible. It also clarified an upper limit of 1 µg PAs per day to be valid for the next three-year transition period. After that, a limitation of 0.35 µg per day proposed by HPMC should be applied (BfArM, 2016). In January 2019, HMPC decided to extend the deadline another two years (EMA, 2020).

Briefly, risk assessment for PAs using the MOE approach performed by COT was currently adopted by EFSA and HMPC. The regulatory limits were established generally based on the data of the most potent PA congeners, lasiocarpine or riddelliine. The MOE approach can be used for a risk assessment of genotoxic and carcinogenic substances but is not appropriate to estimate a TDI. Alternatively, the Threshold of Toxicology Concern (TTC) concept, which is based on a lifelong exposure and an acceptable lifetime cancer risk of 10^{-5}, was also proposed to establish the limits for PAs. According to this concept, a TDI threshold of 1.5 µg/day is acceptable for the compounds with the toxicological concern but lack available data on its carcinogenicity. The threshold should be reduced to 0.15 µg/day when with the structural alert for genotoxicity. However, this concept cannot be applied to PAs since they are genotoxic, mutagenic, and have available carcinogenicity data.

To date, few regulatory guidance approaches applied limits of PAs intake either for the PA-containing medicinal products or food supplements, and the limits were estimated only based on the most potent congeners. Instead, appropriate and reasonable limit values should be established according to more available data on the toxic potencies of individual PA congeners.

2.1.6 Relative potency factors (REP factors)

The toxicological potencies of individual congeners, even from the same chemical group, can be extraordinarily different. Thus the concept of relative potency (REP) factors was developed to describe the relative toxic potency of each compound in comparison to the reference compound, usually the most toxic congener of the group. The relative potency factor of the latter is assigned chiefly as 1.0, presenting their toxic potency as 100%, and the others ≤ 1.0.

Currently, the most risk assessment applying MOE approach of PAs presented based on the exposure of 1,2-unsaturated PAs combined the $BMDL_{10}$ of lasiocarpine or riddelliine, which are the most toxic congeners of PA. For this reason, the MOE approach might lead to an overestimation of risk to human health. Thus, using REP factors to take the relative toxic potencies of different PA congeners into account might be a way forward.

Based on available composite data of a short-term study in adult rodents, genotoxicity data in *Drosophila*, and *in vitro* cytotoxicity data, Merz and Schrenk (Merz and Schrenk, 2016) proposed interim relative potency (iREP) factors for a series of 1,2-unsaturated PA congeners and *N*-oxides to differentiate structurally related subgroups of toxic potency. Open-chain di-esters with 7*S*-configuration (e.g., lasiocarpine) and cyclic di-esters (e.g., monocrotaline‡, retrorsine, senecionine, and seneciphylline‡; ‡not in my work) assigned a REP factor of 1.0, mono-esters with 7*S* configuration (e.g., europine‡ and heliotrine‡; ‡not in my work) were like 0.3, REP factor of 0.1 for open-chain di-esters with 7*R* configuration (e.g., echimidine‡, ‡not in my work), and the last group of mono-esters with 7*R* configuration (e.g., indicine and lycopsamine) defined as 0.01. For the corresponding *N*-oxides, it was suggested using the iREP factors equal to their parent PA congener, assuming that *N*-oxides could be reduced entirely.

In a later approach considering tumor formation *in vivo*, Chen et al. (2017) calculated further RPFs using $BMDL_{10}$ of 0.07 and 0.18 mg/kg bw per day for lasiocarpine and riddelliine, which was evaluated from the studies of NTP (2003, 1978). Or otherwise, T10※ values, an alternative point for MOE approach, derived from *in vivo* data on the incidence of tumors in rats for a few PAs with insufficient data for dose-response modeling $BMDL_{10}$ values (Hirono et al., 1979; Kuhara et al., 1980; Shumaker et al., 1976), resulted in RPFs of 1.0, 0.39, 0.23, 0.05, 0.03 and 0.02, respectively for lasiocarpine, riddelliine, monocrotaline, clivorine, senkirkine, and symphytine. MOE values obtained with and without iREP factors proposed by Merz and Schrenk were also compared in the report. It revealed that the MOE values estimated without iREP factors were generally lower than those with iREP factors, especially for the samples that contained major PAs with low iREP factors.

(T10※: an alternative point for MOE approach, e.g., if the incidence in the control group was 5/50 (10%), and in the group with exposure of 30 mg/kg bw per day was 30/50 (60%), the extra risk was [(60-10)/(100-10)]/100 = 55.6%, T10 = 10/55.6 x 30 mg/kg bw per day (Benford et al., 2010).)

In 2019, HepaRG as a cell model was used by Louisse et al. (2019) to determine *in vitro* genotoxicity associated phosphorylation of histone H2AX, which is well known related to double-strand DNA breaks. γH2Ax formed after exposure to different PAs with increasing concentrations was quantified in Cell Western assay. Data of concentration-response were analyzed using PROAST to apply the Benchmark concentration (BMC), e.g., BMC_{50} corresponding to a 1.5 fold γH2AX over the background level. Louisse et al. assigned the potency of riddelliine as 1.0, subsequently evaluated the relative potencies using the BMC_{50} of respective PA dividing the value of riddelliine. Based on the results from the calculation, PAs were grouped into four classes. The class with the highest potency ($0.3 < REP \leq 1.2$), including senecionine (1.24), seneciphylline (1.20), lasiocarpine (1.08), riddelliine (1.0), retrorsine (0.9), echimidine (0.61), etc., mostly are open-chain and cyclic di-esters. However, not all cyclic di-ester are similarly potent, some of them belong to the second group ($0.1 < REP \leq 0.3$) and such as monocrotaline (0.06) eventually was classified into the third group ($0.01 < REP \leq 0.1$). Lycopsamine (0.02) and indicine (≤ 0.01), the two mono-esters investigated in my study, respectively, belong to Class 3 and Class 4 ($REP \leq 0.01$) of least potency.

Additionally, the ratio of DHP-DNA adducts at adenine and guanine and the metabolic rate in culture, i.e., area under the concentration versus time curve (AUC) for the depletion of parent PA *in vitro* in a rat sandwich-cultured hepatocytes system, was used to represent the intrinsic relative genotoxic potency among congeners (Lester et al., 2019). It demonstrated after an incubation of 24 h that lasiocarpine was the most potent congener displaying with a ratio of 1.0, then followed the ranking: lasiocarpine (1.0) > echimidine (0.7) ≈ riddelliine (0.4) ≈ heliotrine (0.3) > europine (0.1) ≈ monocrotaline (0.09) ≈ lycopsamine (0.08) ≈ indicine (0.04). Riddelliine and monocrotaline had adduct/AUC ratios of 0.4 and 0.09, which were much lower than the assigned iREP factor of 1.0, europine with a ratio of 0.1 was also not as potent as predicted. In contrast, echimidine displayed a much higher intrinsic potency than that proposed iREP factor.

These findings were almost consistent with the results published by Allenmang et al. (2018), which exhibited the genotoxic potencies analyzing the PA-induced amount of micronuclei in pre-differentiated HepaRG cells as following rank lasiocarpine > echimidine ≥ retrorsine ≥ heliotrine > europine > indicine > lycopsamine ≥ monocrotaline.

All these approaches support the concept of relative potency factors and further explain the wide range of the toxic potency of different PA congeners. It is not appropriate to directly use the most potent congeners to estimate the realistic toxicity of total PA content in foods or herbal medicinal products. According to iREP factors, the risk assessment applied to distinguish toxic potencies between different individual PA congeners, hence adjusting the potential toxicity of total PA content in different samples, could give a more realistic estimation.

The provisional REP factors proposed by Merz and Schrenk (2016) or the other approaches were still not entirely adequate for the risk assessment of pyrrolizidine alkaloids due to the limited available data or the design limitations on studies, suggesting there is space for further refinement of the values. It is also necessary to summarize the quantitative data of PA content and distribution in different products.

2.1.7 Selected PA congeners

Lasiocarpine (LaC)

(Ref. substance: lasiocarpine; CAS No.: 303-34-4; m.w.: 411.50 g/mol)

Lasiocarpine, an open-chain di-ester belonging to heliotridine-type distributed in *Heliotropioideae* (Boraginaceae), can also be found in *Boraginoideas* (Boraginaceae) and *Eupatorieae* (Asteraceae). It is well known for its hepatotoxicity, genotoxicity, and carcinogenicity (Smith and Culvenor, 1981). Due to the carcinogenicity it was classified as Class 2B (IARC, 2002).

The metabolism of lasiocarpine is mainly catalyzed by CYP3A, particularly CYP3A4 isoform in humans. In general, humans, pigs, rats, and mice were more susceptible to lasiocarpine-induced toxicity than the species rabbit and sheep (Fashe et al., 2015).

In Afghanistan, acute human poisoning was caused by exposure to wheat flour contaminated with seeds of *Heliotropium*, which possibly contains about 0.1% PAs, and lasiocarpine is the primary component (Eröksüz et al., 2001; Kakar et al., 2010).

The LD_{50} of lasiocarpine, when *i.p.* administered with a single dose in male rats, was 77 mg/kg bw (WHO-IPCS, 1988). A 2-year carcinogenicity bioassay from NTP showed that lasiocarpine induced liver tumors in F344 rats (NTP, 1978).

The genotoxicity has also been studied using several *in vitro* assays. For instance, induction of chromosomal aberrations was found in V79 hamster cells without external metabolic activation with high concentrations between 500 µM and 10 mM (Takanashi et al., 1980). In HepaRG cells, lasiocarpine only with a concentration of 0.59 µM could induce a statistically significant increase in micronuclei compared to the control (Allemang et al., 2018). In addition, dehydronecine-derived DNA-adducts involved in

the metabolism of lasiocarpine to exert its genotoxicity were demonstrated in rat livers and liver microsomes after orally gavaged (Xia et al., 2013; Xia et al., 2006).

Retrorsine (ReS)

(Ref. substance: retrorsine; CAS No.: 480-54-6; m.w.: 351.40 g/mol)

Retrorsine is a cyclic di-ester with an unsaturated double bond that occurs mainly in plants of the *Senecio genus* (Fu et al., 2004). It was found that mice, hamsters, and rats were the more susceptible species than guinea pigs. After feeding with retrorsine, dehydroretrorsine, dehydroretronecine, and corresponding *N*-oxides could be formed as main metabolites (Chu and Segall, 1991), which were also found *in vitro* via human or rat liver microsomal metabolism (Couet et al., 1996). Furthermore, retrorsine exposure could enhance or induce the expression of CYP1A1, CYP1A2, CYP2E1, and CYP2B1/2 in the liver of rats (Gordon et al., 2000).

In 1954, liver tumorigenicity in rats induced by retrorsine was firstly reported by Schoental et al. (1954). Oral LD_{50} was demonstrated in rats for 34-38 mg/kg bw (EFSA Panel on Contaminants in the Food Chain, 2011; Mattocks, 1971). According to the LD_{50} values calculated from data on male rats dying from acute haemorrhagic necrosis of the liver 3 – 7 days after a single *i.p.* dose (34 mg/kg bw), retrorsine was even more potent than lasiocarpine (77 mg/kg bw) (WHO-IPCS, 1988).

The retrorsine-induced toxic effect has been reported in several studies. For instance, in V79 cells, cytotoxic effects, i.e., low number and poor quality of metaphases, were only evident when hepatocytes were used for metabolic activation. Without an external metabolization system, retrorsine showed only a slightly genotoxic effect of inducing chromosomal aberrations at the concentrations of 1000 µM. But the addition of an S9 mix or cocultivation with primary rat hepatocytes resulted in a drastic increase in chromosomal aberration rate. It decreased the active dose to 32 and 3.2 µM, respectively (Müller et al., 1992). In HepaRG cells, a chromosomal aberration was exhibited only at 9.5 µM (Allemang et al., 2018). Additionally, retrorsine could induce megalocyte formation at 500 µM and DNA cross-linking at doses from 50-500 µM in cultured bovine kidney epithelial cells when co-incubated for 2 h with an NADPH-generating system and rat liver S9 fraction (Hincks et al., 1991; Kim et al., 1993).

Senecionine (SeC)

(Ref. substance: senecionine; CAS No.: 130-01-8; m.w.: 335.40 g/mol)

Senecionine is a structural analog to retrorsine, also a typical cyclic di-ester with an α,β-unsaturated double bond from *Senecioneae* (Asteraceae). As one of the most toxic PA congeners, it is hepatotoxic, genotoxic, and tumorigenic (Mattocks, 1986).

Like most other PA congeners, the primary metabolic pathway of senecionine was believed to form a reactive alkylating metabolite responsible for the toxicity. Therefore, it was found as predicted to covalently bind to macromolecules such as protein and DNA (Green et al., 1981). Meanwhile, senecionine could be metabolized in primary rat hepatocytes to form corresponding water-soluble *N*-oxides and other conjugates. Besides, Segall et al. found that trans-4-hydroxy-2-hexanal from the hepatic microsomal metabolism might also involve in senecionine-induced hepatotoxicity or carcinogenicity since this compound was proved not only to be cytotoxic in primary rat hepatocytes but also could bind to DNA (Griffin and Segall, 1986; Segall et al., 1985; Winter et al., 1988).

In humans, rats, sheep, and hamsters, it was found that the CYP3A subfamily is the primary enzyme responsible for its metabolic activation (Huan et al., 1998; Miranda et al., 1991; Stegelmeier et al., 1999; Williams et al., 1989). CYP2B subfamily was the primary catalyst for PA pyrroles formation in guinea pigs (Chung et al., 1995). Except for the species or strains differences in the distribution of CYP enzymes resulting in various susceptibilities to PAs, Chung and Buhler (Chung and Buhler, 2004) also mentioned a possible gender dependence using F344 and SD rats.

It was reported an oral LD_{50} value of 57 mg/kg bw in mice (Wang et al., 2011), and *i.p.* LD_{50} value of 50 mg/kg bw in male rats by the IPCS-Health and Safety Guideline of pyrrolizidine alkaloids with a single dose.

The cytotoxic potency of senecionine has been evidenced by the leakage of lactate dehydrogenase (LDH) assay with rat hepatocytes in primary culture (Green et al., 1981).

Like retrorsine, senecionine could also induce megalocytosis and DNA cross-linking in cultured bovine kidney epithelial cells in the presence of the S9 fraction in combination with an NADPH-generating system (Hincks et al., 1991). The stimulation of DNA repair measured as unscheduled DNA synthesis has also been demonstrated in primary rat hepatocytes (Green et al., 1981).

Indicine (InC)

(Ref. substance: indicine hydrochloride; CAS No.: 1195140-94-3; m.w.: 335.83 g/mol)

Allenmang et al. (2018) found that in HepaRG cells, a significant concentration of 133 μM for micronucleus formation.

There is not so much available data about indicine due to its low toxic potency.

Lycopsamine(LyA)

(Ref. substance: lycopsamine; CAS No.: 10284-07-1; m.w.: 299.37 g/mol)

Lycopsamine induced a significant increase in micronuclei in HepaRG cells at doses of 74 µM, which was 125-fold higher than lasiocarpine (Allemang et al., 2018).

There is not so much available data related to the toxicity of lycopsamine due to its low toxic potency. On the contrary, it was observed that acting as an anti-lung cancer candidate (Yu et al., 2020).

2.2 Measuring systems

2.2.1 Cell cultures

(Rat) hepatocytes in primary culture

The primary culture of hepatocytes is an effective in *vitro* model that has been widely used to investigate the biotransformation, cytotoxic and genotoxic properties of xenobiotics and new pharmaceuticals, also used to establish new biomarkers. Hepatocytes, especially human hepatocytes, in primary culture are considered a gold standard for investigating the metabolism and toxicity of compounds.

In primary culture, the non-proliferated hepatocytes, which are known to contain the high activity of metabolizing enzymes, could remain a variety of major metabolic properties and differentiated functions of the liver *in vivo* for several days (Bissell et al., 1973; Jeejeebhoy and Phillips, 1976).

However, many liver-specific enzymes, including cytochrome P450, which is essential for the metabolism of a variety of endogenous substrates and xenobiotic, decline rapidly to low levels within a few days in primary culture under conventional conditions (Acosta et al., 1979; Fahl et al., 1979; Guzelian et al., 1977). The most rapid decrease of CYP450 was demonstrated during the initial 24 hours after isolation in the culture, followed by a slower rate in the next 24 hours. Therefore, the more extended periods the cells cultivated, the less CYP450 could anticipate the metabolism of substrates. (Bissell and Guzelian, 1979; Evarts et al., 1984; Fahl et al., 1979; Guzelian et al., 1977; Maslansky and Williams, 1982)

Due to the limited life span, availability, and the complexity of isolation from animals, even human organs make *in vitro* assays with primary cells time-consuming. Results of many studies using primary cells reported poor reproducibility mainly because of the donor variation (Guillouzo, 1998). It is also well known that the reproducibility of assays is essential for estimating the toxicity of chemicals. Therefore, the conditions to acquire more stable recovery and optimal attachment have been intensively investigated and established (Bissell et al., 1973; Seglen, 1976; Seglen and Fosså, 1978; Williams et al., 1977). On the other hand, various methods for the isolation were reported that achieved high cell yields and good viability (Berry and Friend, 1969; Bissell et al., 1973; Labrecque and Howard, 1976; Seglen, 1976).

Additionally, primary hepatocytes derived from diverse species were characterized for the different distributions of enzymes and corresponding metabolism pathways and the responses to the substances (Mitchell and Jollows, 1975; Williams, 1978, 1974). Thus the results of rat hepatocytes in primary culture cannot be directly transmitted to other species or humans.

HepG2 naïve cell line

HepG2 is a human hepatocellular carcinoma cell line with epithelial-like morphology frequently used *in vitro* in metabolism and hepatotoxicity studies alternative to primary hepatocytes. HepG2 cells have shown high proliferation rates and maintain many differentiated hepatic functions. The expression of phase II metabolizing enzymes, such as glutathione *S*-transferase and sulfotransferase, is almost identical to that in primary hepatocytes, except for UDP-glucuronyltransferase. The major limitation of this cell line is the markedly lower expression of many transporters and enzymes, especially the hepatic cytochrome P450 isoenzymes, which are involved in phase I metabolic bioactivation of many drugs and xenobiotics (Donato et al., 2013; Guo et al., 2011; Hilgendorf et al., 2007; Javitt, 1990; Knowles et al., 1980; Westerink and Schoonen, 2007). Organic anion transports were also poorly expressed in HepG2 cells (Hilgendorf et al., 2007). However, unlimited life span, stable phenotype, easy handling, and stock availability are advantages for *in vitro* research.

HepG2 (CYP3A4) C9 cell line

The deficiency of essential enzymes required for biotransformation is the most common cause of false-negative results of many potentially toxic compounds. In most hepatoma cell lines, the metabolizing enzymes are limitedly expressed. Thus, cells transformed with virus genes or oncogenes enabling expression of CYP450 enzymes have been developed and extensively used in the research of metabolic properties. CYP3A4 is one of the most abundant CYP450 enzymes expressed in the human liver and was also found probably to be one of the most important enzymes for the bioactivation of PAs (Fashe et al., 2015; Ruan et al., 2014b). HepG2 (CYP3A4) clone 9 cells obtained from the University of Technology Cottbus-Senftenberg were transduced with recombinant lentivirus for constitutive and stable protein overexpression of CYP3A4 showing more than 10,000-fold compared to HepG2 parental cell presented an activity of about 600 pmol/mg total cellular protein per minute determined by testosterone 6β-hydroxylation that could be additionally induced via rifampicin, maintained the morphological properties of the parental cells (Herzog et al., 2015).

2.2.2 7-Benzyloxyresorufin-*O*-dealkylase (BROD) multi-well plate assay and inhibition study

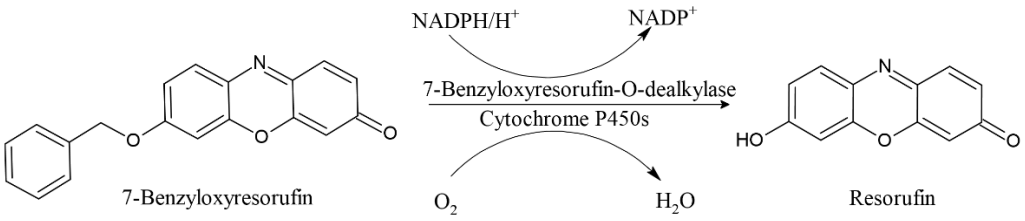

Figure 4: The principle of 7-benzyloxyresorufin-*O*-dealkylase (BROD) assay. In the presence of NADPH, 7-benzyloxyresorufin is catalyzed by Cytochrome P450 to produce resorufin.

This assay is based on metabolism by CYP isoforms in cell culture of appropriated non-fluorescent substrate 7-benzyloxyresorufin (s. Fig. 4). After incubation with cells, the fluorescent product resorufin is formed and then quantified automatically. The fluorescence-based alkoxyresorufin-*O*-dealkylation assays are measured in the presence of S9 fractions, with microsomes or cultured cells. It usually requires a relatively lengthy procedure for harvesting, disruption, and preparation of cells or fractions. In the BROD multi-plate assay to determine CYP450 activities, the substrate 7-benzyloxyresorufin has been directly added to the multi-well plates in intact living cells and metabolized by monolayers. Since there was no need to disrupt the cells, the handling time was reduced. Meanwhile, cellular damage and the loss of biological activity have been minimized. This method is convenient, quick, sensitive, and cost-efficient.

However, most fluorometric substrates are not specific or selective for a single CYP450 isoform. 7-Benzyloxyresorufin can be dealkylated by more than one CYP450 isoforms including CYP1A2, CYP2B1 also CYP3A1/2 in rats, if in humans, it has been suggested more likely as an indicator of CYP3A, but also appeared to be catalyzed by CYP1A and CYP2A (Burke et al., 1994; Chen and Eaton, 1991; Namkung et al., 1988).

To investigate whether CYP450 enzymes play a crucial role in metabolic activation, i.e., metabolic-based toxicity of chemicals, CYP450s being inhibited or induced by some compounds should affect the metabolic pathway. Numerous substrates have been identified as competitive, non-competitive, or irreversible CYP450 inhibitors.

In my inhibition study, ketoconazole was chosen as a broad inhibitor of rat cytochrome P450 enzymes. Ketoconazole was a potent and selective inhibitor of CYP3A4 activity in the human liver, by contrast, in rat cells act as a far less specific inhibitor, being able to inhibit many different isoforms (Baldwin et al., 1995; Eagling et al., 1998; Novotná et al., 2014).

2.2.3 Glutathione-reductase-DTNB recycling assay

Glutathione (γ-*L*-glutamyl-*L*-cysteinyl glycine; GSH), a tripeptide of glutamate, cysteine, and glycine, occurs in the cytosol and the organelles and plays an important role in the detoxification of many chemicals and antioxidant defense. GSH can be oxidized by electrophilic substances (e. g., free radicals, reactive oxygen/nitrogen) or electrophilic metabolites of chemicals to glutathione disulfide (GSSG). GSH deficiency typically contributes to oxidative stress (Wu et al., 2004).

The determination of glutathione is based on a reduction of 5,5-dithiobis (2-nitrobenzoic acid) (DTNB; Ellmann`s reagent) with reduced glutathione (GSH), leading to chromophoric 5-thio-2-nitrobenzoic acid (TNB). In the presence of NADPH, the glutathione disulfide (GSSG) can also be reduced to GSH by adding glutathione reductase (GR) and then reacting in the same way (s. Fig. 5). The rate of TNB formation is proportional to the amount of total glutathione (GSx), i.e., the sum of GSH and GSSG, measurable at 412 or 405 nm (Anderson, 1985).

The samples were acidified at first to inactivate γ-glutamyl transferase and reduced the non-enzymatic oxidation of GSH to GSSG (Anderson, 1985). Since DTNB as a sulfhydryl reagent also reacts with the other thiol groups (Ellman and Lysko, 1979), proteins were precipitated with 5-sulfosalicylic acid (SSA) (Hamilton, 1962). NADPH is well known as an essential coenzyme for many redox reactions. In the pentose phosphate pathway, the oxidation of glucose-6-phosphate (G6P) by glucose-6-phosphate dehydrogenase (G6PDH) is a source of NADPH (Berg et al., 2017). Instead of pure NADPH, in this work, a mix of $NADP^+$, G6P, G6PDH was used as the NADPH-generating system. $MgCl_2$ was added as a source of Mg^{2+} ions to stimulate CYP activity.

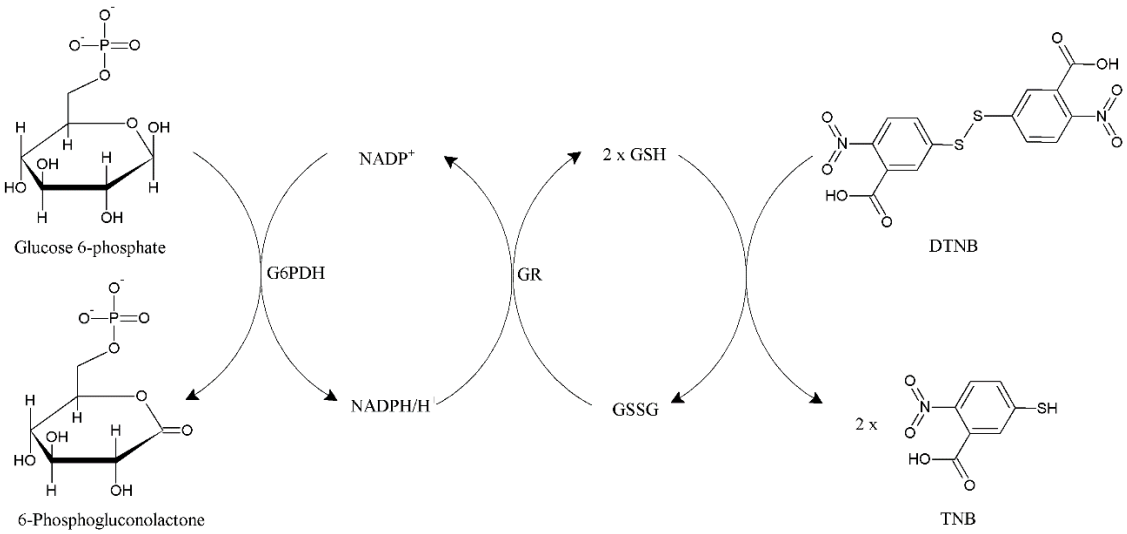

Figure 5: Schematic mechanism of glutathione reductase-DTNB recycling assay.a) NADPH-regenerating system: G6P is oxidized by G6PDH to produce NADPH; b) in the presence of NADPH, GSSG is reduced to GSH by adding GR; c) GSH reacts with thiol reagent DTNB to form GSSG and chromophoric TNB.

GSSG can be determined after derivatization of GSH by 2-vinyl pyridine (2-VP) followed by reduction with GR (s. Fig. 6) (Griffith, 1980). The content of GSH is calculated as the difference between the GSx and GSSG (GSH = GSx – 2 x GSSG).

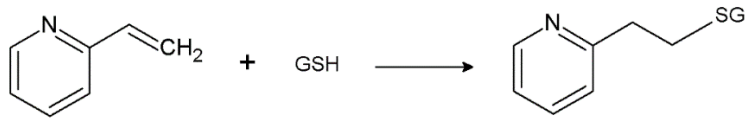

Figure 6: Derivatization of pre-existing GSH with 2-VP. The 2-VP blocks the thiol group of GSH.

2.2.4 Alamar blue (Resazurin) assay

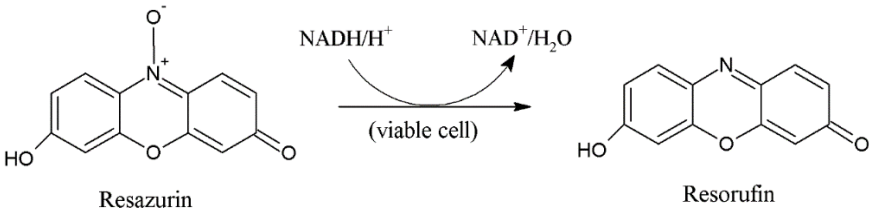

Figure 7: The principle of Alamar blue (resazurin) assay. Blue, non-fluorescent resazurin is reduced to pink-colored, highly fluorescent resorufin in living cells.

Alamar blue assay has been used to measure cell proliferation of various cell lines, bacteria, and fungi and estimate the cytotoxicity of agents (Page et al., 1993). Alamar blue (synonym: resazurin) is a non-toxic, cell-permeable chemical indicator which in oxidized form is blue in color and non-fluorescent. Upon entering viable cells in the presence of NAD(P)H resazurin is reduced to a pink-colored, highly fluorescent resorufin, which can be quantitatively determined by fluoroscan (λ_{Ex} = 544 nm, λ_{Em} = 590 nm) (s. Fig. 7). Since NAD(P)H is the complex organic molecule found only in vital, metabolically competent cells, the generated resorufin is proportional to the number of living cells. However, it is not clear whether this reduction occurs intracellularly in response to mitochondrial enzymes (Fries and Mitsuhashi, 1995) or extracellularly via a chemical reaction of the medium resulting from cell growth (O'Brien et al., 2000). In addition, resorufin can be further reduced to colorless hydroresorufin. The inversion to resorufin is irreversible, whereas the following reduction to hydroresorufin is reversible (VanDemark et al., 1945).

In this study, Alamar blue assay was used to determine the viability of different cell lines and assure bacteria viability in the Ames fluctuation assay. However, the viability could only be measured without the S9 mix since resazurin would be immediately reduced to resorufin via NADPH generated from the added compounds in the S9 mix, even without any vital bacteria.

2.2.5 Ames fluctuation assay

The Ames fluctuation assay, a high throughput variant of the classical Ames test, modified according to ISO 11350:2011 was used to detect the mutagenicity of PAs.

The constructed mutants of *Salmonella typhimurium* are reverted from a histidine-requiring (autotrophy) bacterial strain back to histidine-independent (prototrophy) strain by chemical mutagens (s. Fig. 8).

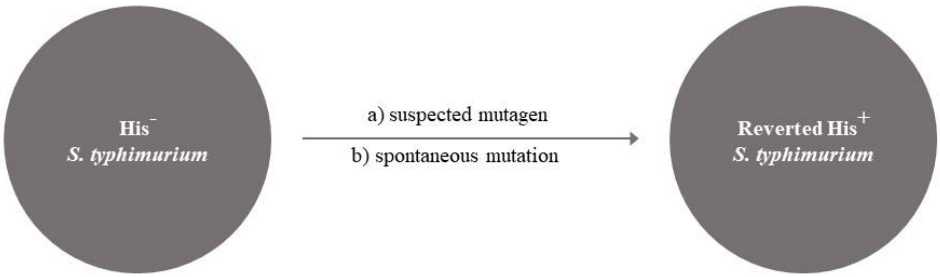

Figure 8: The principle of Ames fluctuation assay. A strain of *S. typhimurium* that carries a defective gene to synthesize histidine (His) can be reversed by a mutagen. With back mutation, the bacteria regain the function that can grow in the medium lacking histidine.

The test compounds are measured with and without exogenous metabolic activation in different strains. Each strain contains a different type of mutation in the histidine operon (s. Tab. 2). Furthermore, other mutations increase their sensitivity to mutagens. The *rfa*-mutation causes a partial defect of the lipopolysaccharide barrier, which leads to a higher permeability of the cell membrane and therefore enables large mutagenic compounds to penetrate the cells more efficiently. This character can be confirmed by demonstrating crystal violet sensitivity. Due to the *rfa*-mutation, large molecules such as crystal violet were permitted to enter the cells and inhibit the growth. Another *uvrB*-mutation increases sensitivity by defecting the DNA excision system (Ames et al., 1973). TA102 does not contain this mutation, so it is primarily sensitive to the mutagens that require intact DNA repair (Levin et al., 1982). This mutation can be tested for UV sensitivity. Except for strain TA102, the other strains with *uvrB*-mutation will not grow after exposure to UV-C light because they cannot repair the DNA damage (Ames et al., 1973). The R-factor plasmid, pKM101, which is contained in all test strain enhances the cell´s error-prone response and repair system, thus also increasing the susceptibility to mutagenesis. Because an ampicillin resistance has been identified of pKM101 DNA, accordingly the ampicillin resistance could be tested to prove the presence of the plasmid, although this resistance was not related to increased sensitivity of the R-factor strains (Langer et al., 1981; McCann et al., 1975). TA102 is also the only strain that carries the multicopy plasmid pAQ1, besides the hisG428 mutation also a tetracycline resistance gene (Levin et al., 1982). The genotypes of test strains should be confirmed before using a new set of frozen bacterial cultures.

Table 2: Genotypes of the used strains in Ames fluctuation assay

Strain	Histidine operon	LPS	Repair	R-factor
TA97a	hisD6610	*rfa*	*uvrB*	+ R
TA98	hisD3052	*rfa*	*uvrB*	+ R
TA100	hisG46	*rfa*	*uvrB*	+ R
TA102	hisG428 (pAQ1)	*rfa*	--	+ R

A variety of chemical mutagens requiring metabolic activation can be confirmed *in vitro* as mutagens only after adding a liver extract of rat (or human), i.e., S9, that contains active phase I and II metabolic enzymes (Hayes and Kruger, 2014). S9 mix has been reported as a valuable bioactivation for testing cytotoxicity and genotoxicity.

Since a wide variety of chemicals to exert their toxicities require metabolic activation, it is essential that the S9 fraction, i.e., 9000 g supernatant fraction of rat liver homogenates, prepared from induced animals and used for the exogenous metabolic activation. Although other tissues or species could also be used, the rat liver is the most convenient source of enzymes. It contains not only notable cytochrome P450s but also sulfotransferase, glutathione transferase, *N*-acetyltransferase, and many other cytosolic enzymes. In general, the S9 mix from Aroclor 1254-induced rat liver, a polychlorinated biphenyl (PCB), is traditionally used in *in vitro* assays. The induction can also be produced after a combined injection of phenobarbital with *β*-naphthoflavone. One disadvantage of the S9 fraction is that it requires exogenous cofactors such as NADPH and GSH to exert enzyme activities (Hayes and Kruger, 2014).

2.2.6 Micronucleus assay

In a complete risk assessment of chemical compounds, genotoxicity is typically evaluated as an important endpoint. The micronucleus test *in vivo* or *in vitro* is routinely included in many genotoxic testing guidelines. This assay is a standard tool in genotoxicity hazard identification (OECD, 2016).

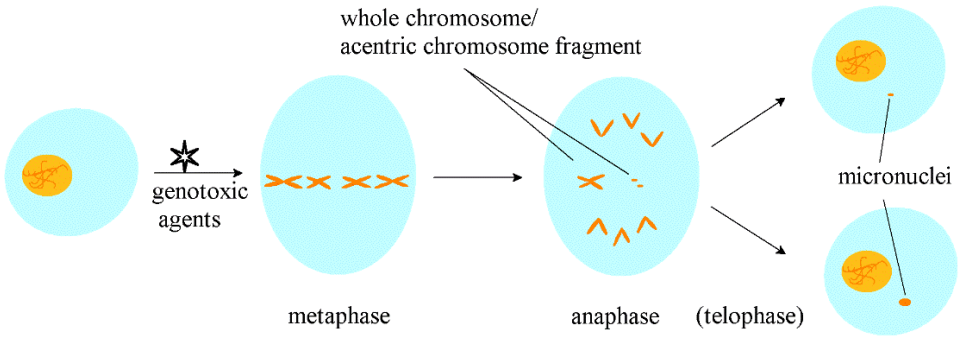

Figure 9: Micronucleus formation. The MN originate during anaphase/telophase of mitosis from either the lagging acentric fragment or whole chromosome.

Micronucleus formation indicates chromosomal damage potential in cells that have undergone division after exposure to clastogenic agents or aneugenic compounds as colchicine or vinblastine (Kirsch-Volders et al., 1997). After exposure, the cells should be grown for sufficient time to lead to micronuclei formation in the interphase cells (s. Fig. 9). DAPI (s. Fig. 10) is a fluorescent nucleic acid dye used to stain an A-T-rich cluster in DNA. When DAPI enter the cells and bind to DNA, the fluorescence of DAPI yield increases more than 20-fold (Kapuscinski, 1995). Microscopy is a method for visualizing and counting the staining nuclei and micronuclei based on their specific features. Countryman and Heddle have established the criteria for identifying micronuclei (a) form smooth, round or oval; (b) diameter less than 1/3 of the nuclei; (c) color same as or lighter than the nuclei; (d) position within 3 – 4 nuclear diameters but no connection, and at the same focus plane as the nucleus; (e) no more than two associated with one nucleus (Countryman and Heddle, 1976).

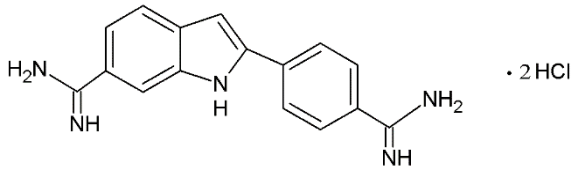

Figure 10: Structure of DAPI.

The micronucleus assay has been widely used as the most reliable testing to evaluate the induction of chromosomal aberration. But it can not be suggested as an alternative method for a chromosomal aberration assay since it does not directly exhibit the chromosomes in the metaphase. Therefore, two or more genotoxic assays should be combined with multiple endpoints to approach a more convincing risk assessment or hazard identification. Except that, cytotoxicity should be determined to ensure sufficient cell viability. The highest concentration should aim to achieve a viability $\geqslant$ 50% compared to the solvent control. Otherwise, it is capable of producing a false-negative response due to excessive cytotoxicity.

2.2.7 Bicinchoninic acid (BCA) assay for protein quantification

Bicinchoninic acid (BCA) assay, also known as Smith assay (Smith et al., 1985), is a simple, rapid, and sensitive method for measuring the protein content. It is based on a biuret reaction in which Cu^{2+} to Cu^{+} is reduced by protein with cysteine, cystine, tyrosine, tryptophan amino acid residues under alkaline conditions. Each cuprous cation (Cu^{+}) chelates then with two molecules of BCA forming a purple-colored water-soluble complex that strongly exhibits an absorbance at the wavelength of 562 nm (s. Fig. 11). The protein concentrations are generally interpreted with reference to a standard curve from a typical protein bovine serum albumin (BSA).

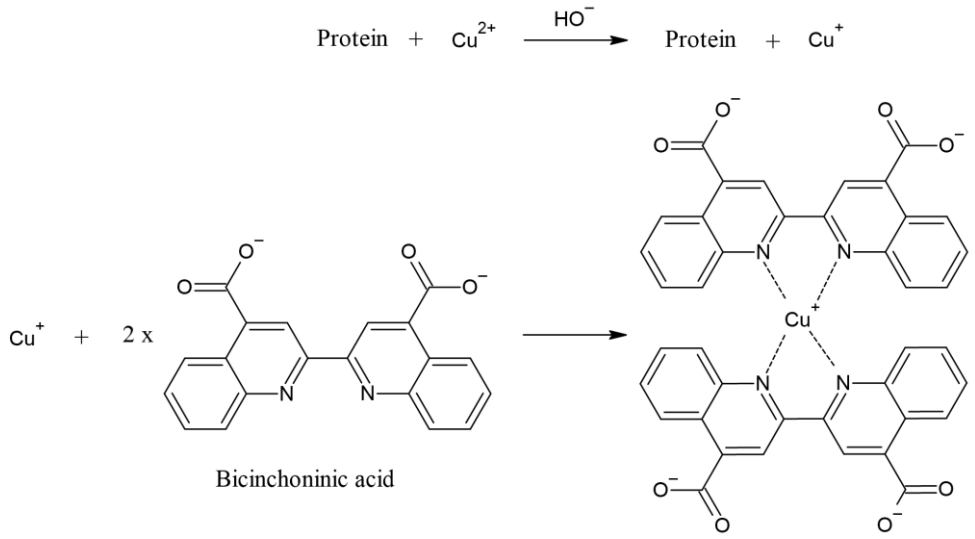

Figure 11: Overview of the basic reaction in the bicinchoninic acid (BCA) assay. a) biuret reaction: cupric ions (Cu^{2+}) are conversed to cuprous ions (Cu^{+}) by protein in an alkaline environment; b) two molecules of BCA bind to each molecule of cuprous cation formed in biuret reaction.

3 **RESULTS**

3.1 7-Benzyloxyresorufin-*O*-dealkylase (BROD) assay

PAs require metabolic activation to exert their toxic effects. Whether the activity of enzymes in different cell lines is strong enough to lead the metabolism plays an essential role in their toxicity. Therefore, the activity of CYPs was determined using a BROD assay.

As shown in Fig. 12, the BROD activity in primary rat hepatocytes was measured up to 72 h after seeding. The formed resorufin is quantified employing a multi-well plate fluorescence reader and related to the total amount of protein (pmol resorufin/mg protein per min). Since the enzyme activity in hepatocytes from different perfusions initially differed, for comparison, the BROD activity 3 h after seeding as initial activity was defined as 100% to compare the enzyme activity of different perfusions. After that, measured enzyme activities were presented as the percentage of initial activity. The BROD activity in primary rat hepatocytes decreased rapidly during the culture. Over up to 6 h after seeding, there was a noticeable loss in activity , falling approximately half. After 24 hours, the activity remained was less than 15% and after 72 h it was virtually absent. Therefore, the decrease in toxicity of several PA congeners with longer pre-incubation is most likely due to a loss in relevant CYP activity.

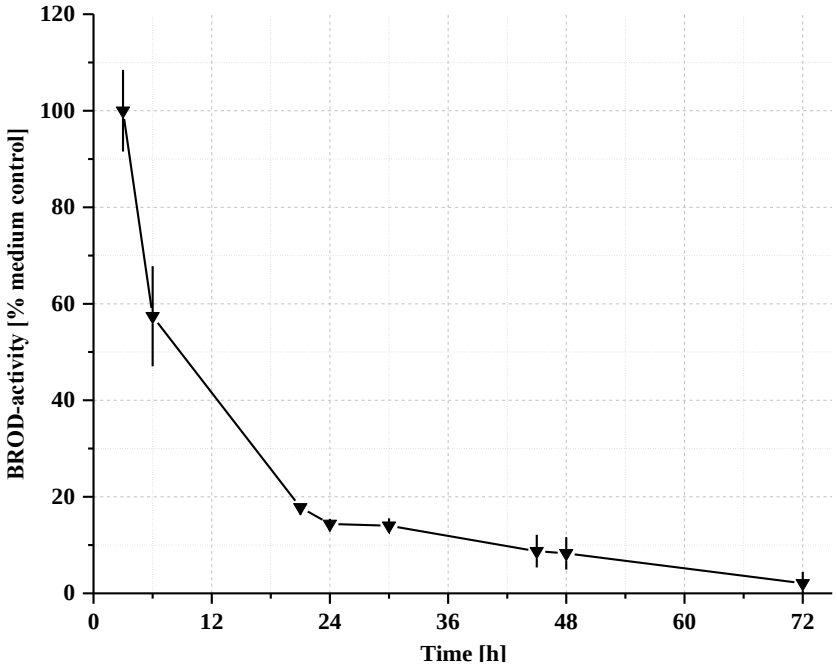

Figure 12: 7-Benzoxylresorufin *O*-dealkylase (BROD) activity in primary rat hepatocytes up to 72 h after seeding. The point represents the mean ± SD of three different preparations. Each measurement was detected triplicate in independent culture wells.

Furthermore, the initial CYP activity in non-transformed HepG2 cells and in CYP3A4 over-expressed human HepG2 cells were also measured and compared to that in primary rat hepatocytes. A mean BROD activity of 0.44 ± 0.18 pmol resorufin/mg protein per minute in the human HepG2 cell line over-expressing the CYP3A4 gene was determined (s. Fig. 13). In contrast, the activity in non-transformed HepG2 cells was 0.09 ± 0.01 pmol resorufin/mg protein per minute (s. Fig. 13). In the culture of primary rat hepatocytes, the BROD activity was 21.9 ± 11.9 (data not shown) 3 h after seeding and 2.1 ± 0.3 pmol resorufin/mg protein per minute after 24 h (s. Fig. 13; data from 3 different perfusions). When comparing cultured cells 24 h after seeding, the activity determined in primary rat hepatocytes was about five times and more than 20 times, respectively, as much in HepG2 (CYP3A4) C9 cell line and in naïve HepG2 cells. Therefore, instead of frequently handling naïve HepG2 cells, the permanent HepG2 (CYP3A4) C9 cell line was chosen for further genotoxic investigation in the micronucleus test.

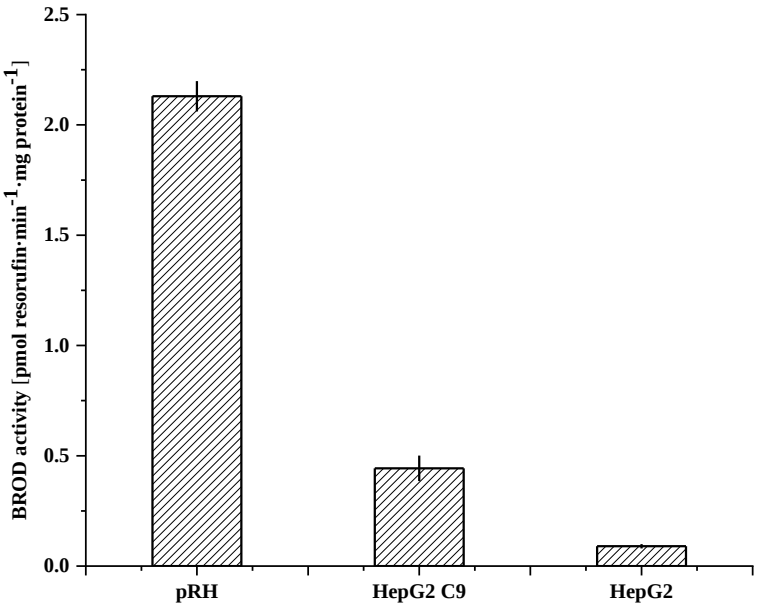

Figure 13: Comparison of BROD activity 24 h after seeding in primary rat hepatocytes, CYP3A4 over-expressed and non-transformed human HepG2 cell lines. The point represents the mean ± SD of three different preparations. Each measurement was detected triplicate in independent culture wells.

In order to investigate the effects of inhibition of CYP activity on the cytotoxicity of PA congeners, ketoconazole, well known as a cytochrome P450 inhibitor, was selected. Its inhibition potency on BROD activity at concentrations of 1, 5, 10, and 40 µM was determined (s. Fig. 14). The results showed that after incubation for 2 h, the BROD activity was inhibited concentration-dependently. Expressed as a percentage of the control activity value, IC_{50} was calculated to be less than 1 µM. It was confirmed that ketoconazole at 5 µM led to an 80% decrease in BROD activity without causing cytotoxicity. Hence this concentration was chosen for the pre-treatment in further investigations.

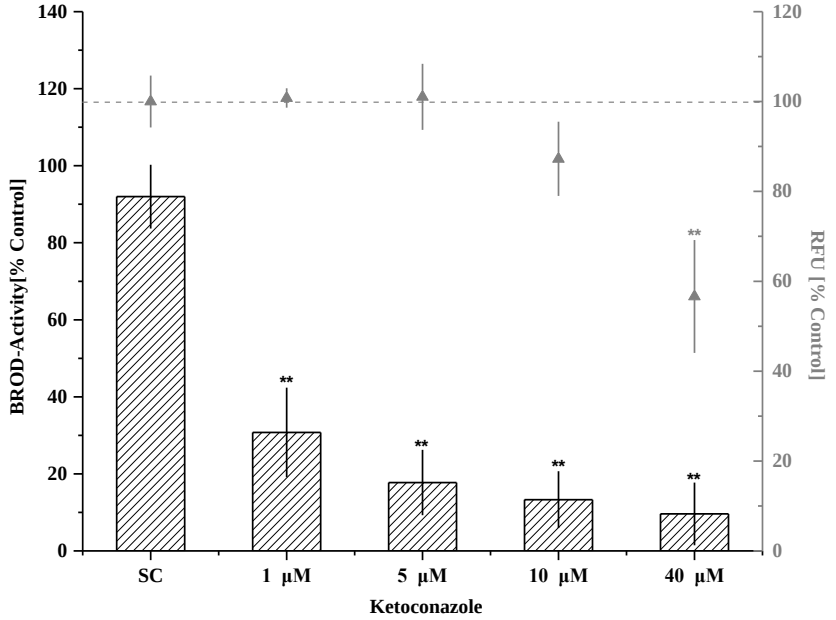

Figure 14: Effect of ketoconazole on BROD activity and cell viability. (Bar) BROD activity. (Triangle) cell viability. After 3 h of adherence, the primary rat hepatocytes were incubated with 1, 5, 10, and 40 µM ketoconazole for 2 h. Data are shown the mean ± SD of three different experiments. Each measurement was detected triplicate in independent culture wells. BROD activity differed significantly from the solvent control at *p<0.05 or **p<0.01.

3.2 Glutathione reductase-DTNB recycling assay

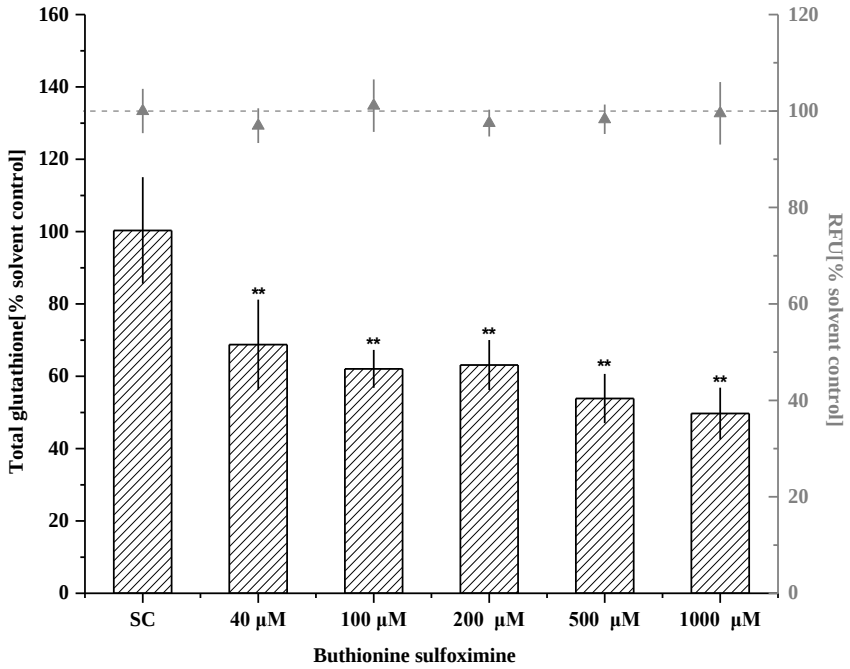

Figure 15: Effect of BSO on glutathione levels and cell viability. (Bar) total glutathione levels. (Triangle) cell viability. After 3 h of adherence, the primary rat hepatocytes were incubated with 40, 100, 200, 500 µM, and 1mM BSO for 2 h. Data are shown the mean ± SD of three different experiments. Each measurement was detected triplicate in independent culture wells. Total glutathione levels differed significantly from the solvent control at *p<0.05 or **p<0.01.

Similar to ketoconazole, buthionine sulfoximine (BSO) was used to investigate the influence of glutathione depletion on the cytotoxicity of PAs. Total glutathione levels were measured after incubation with 40, 100, 200, 500 µM, and 1 mM of BSO for 2 h. Glutathione amount was depleted about 50% via treatment with 1 mM BSO without being cytotoxic to the cells (s. Fig. 15).

3.3 Alamar blue (Resazurin) assay

3.3.1 Rat hepatocytes in primary culture (pRH)

The results of the Alamar blue assay in the culture of primary rat hepatocytes after incubation with different PA congeners for 24 and 48 hours are shown in Fig. 16 to 20. Decreased cell viability in a concentration-dependent manner was demonstrated generally with all tested compounds. Furthermore, cytotoxicity was more pronounced after 48 h of incubation compared to a 24 h incubation time. In addition, it was found that the cytotoxicity considerably depended on the individual PA congener.

Rat hepatocytes were initially cultured following a 24 h pre-incubation period before adding the alkaloids. Lasiocarpine above 25 µM, retrorsine, and senecionine above 75 µM showed a statistically highly significant reduction of cell viability to about 50 - 70% after both incubation times (s. Fig. 16 to 20, filled bars).

When the protocol was changed, the cells were pre-incubated for only 3 hours (s. Fig. 16 to 20, scattered bars). After 24 hours of incubation with PAs, the cytotoxicity was almost unaffected by shorter pre-incubation time, but with 48 h, cytotoxicity was generally more pronounced. Lasiocarpine even showed highly significant cytotoxicity at the concentration of 1 µM. After exposure to 300 µM lasiocarpine, with an incubation time of 24 h, the viability of cells was 17.5 ± 5.1%, which was reached at the concentration of 25 µM if incubated for 48 h. The highly significant cytotoxic effect of lasiocarpine was shown above 1 µM, of retrorsine and senecionine above 5 µM for an incubation time of 48 h. In addition, with the highest measured concentration of 300 µM of all these three di-ester alkaloids, the viability decreased below 30% after 24 h. It even led to almost complete mortalities after 48 h. The cytotoxic effects of di-esters, including cyclic and open-chained, were more pronounced than those of the mono-esters indicine and lycopsamine. After incubation with indicine or lycopsamine of 300 µM for 48 h, cell viability was still greater than 30%.

It was found that individual PAs differ considerably in their cytotoxic potency in the primary culture of rat hepatocytes. Lasiocarpine, an open-chained di-ester with a 7*S*-structure, proved to be the most cytotoxic, followed by the di-ester retrorsine and senecionine. The mono-esters indicine and lycopsamine were much less cytotoxic.

The analysis of BROD activity during the period showed that the less toxicity of most PA congeners with a longer pre-incubation is maybe due to the loss of CYP activity

also the decrease in sensitivity of the primary rat hepatocytes towards PA congeners. The cytotoxicity was affected by the pre-incubation time variously for different PA congeners, likely because of the other influences of diverse CYP enzymes on their metabolic activation.

Furthermore, the effects of inhibition of CYP and GSH depletion on the cytotoxicity of PAs were also investigated. Using ketoconazole as a CYP inhibitor (s. Fig. 16 to 20, dotted bars), after adherence, the primary rat hepatocytes were pre-incubated with 5 µM ketoconazole for 2 hours before incubating with alkaloids. The cytotoxicity of indicine and lycopsamine was only slightly weaker after 48 h than that without pre-treatment, whereas lasiocarpine, retrorsine, and senecionine were significantly less cytotoxic. However, the influence of ketoconazole for the cytotoxicity of lasiocarpine, retrorsine, and senecionine could be only observed at low concentrations, due to the extreme cytotoxicity of these alkaloids at high concentrations, especially after the incubation time of 48 h, the viability of cells was too low to reflect the inhibition.

Total glutathione was depleted by about 50% via 2 h pre-incubation with 1 mM BSO. There was only some slight effect on the cytotoxicity of indicine at the concentrations of 75 and 300 µM after 24 h incubation. For other congeners, GSH depletion had almost no significant impact on their cytotoxicity (s. Fig. 16 to 20, open bars). The effect of glutathione depletion on cytotoxicity of retrorsine was not determined.

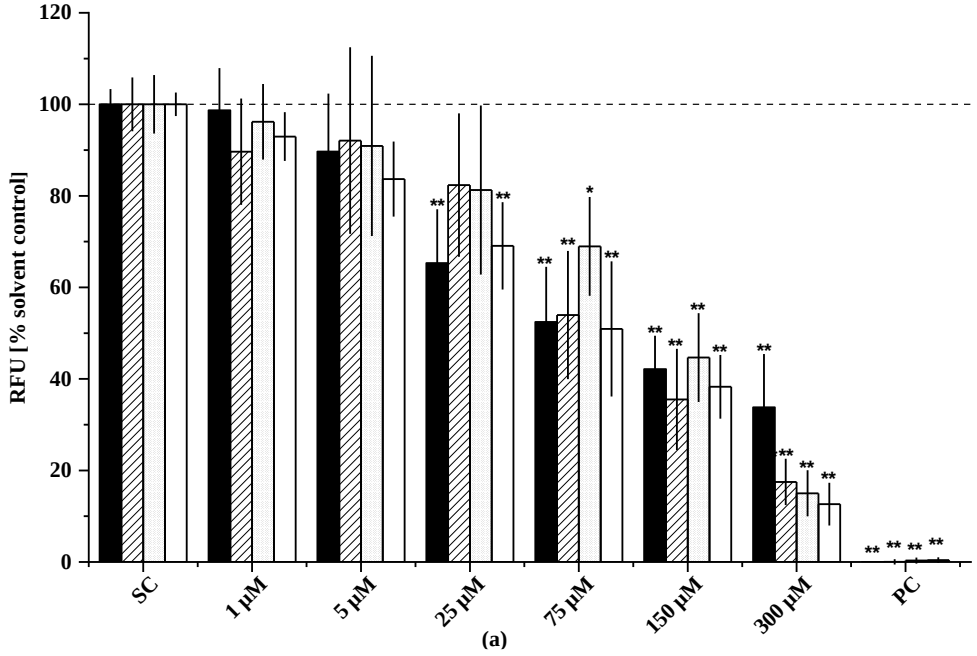

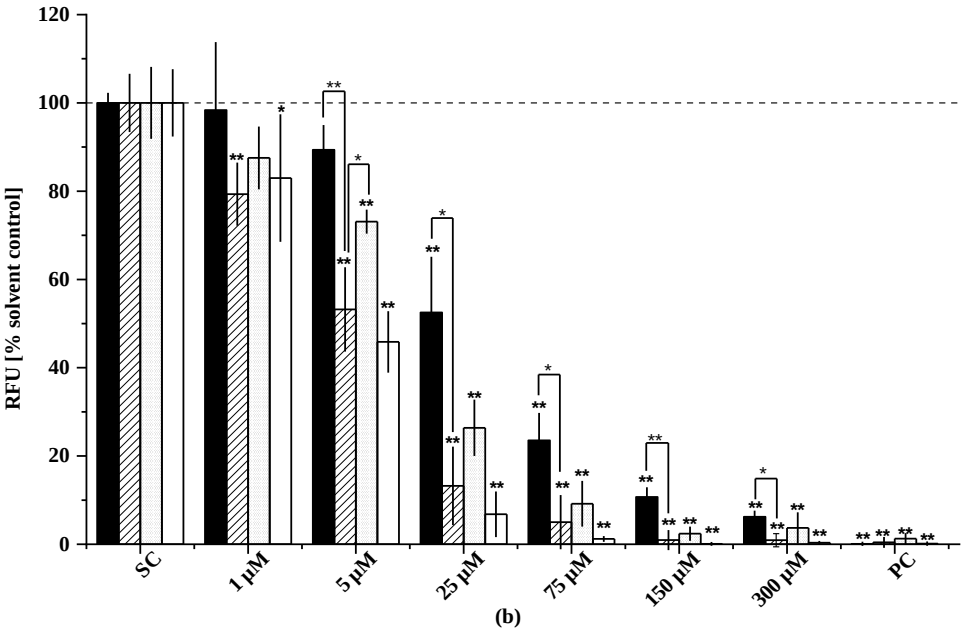

Figure 16: Cytotoxicity (Alamar blue assay) of lasiocarpine in the culture of primary rat hepatocytes, expressed as relative resorufin units (RFU). (a) Incubation with alkaloid for 24 hours. (b) Incubation with alkaloid for 48 hours. The cells were incubated with lasiocarpine at different concentrations after 24 h of pre-incubation (filled bars), or after 3 h of pre-incubation (scattered bars), or after 3 h of pretreatment with 5 µM of ketoconazole (dotted bars) or with 1 mM BSO (open bars) for 2 h. Data are shown the mean ± SD of three different experiments. Each measurement was detected triplicate in independent culture wells. Resorufin reduction levels were significantly different from the solvent control at *p<0.05 or **p<0.01 or from each other, as indicated, at *p<0.05 or **p<0.01.

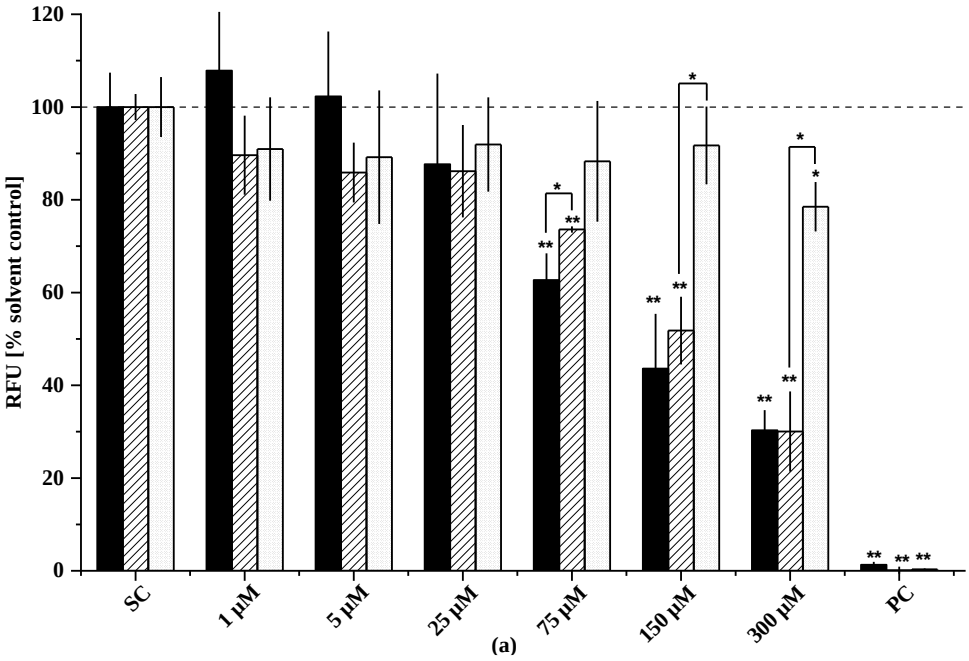

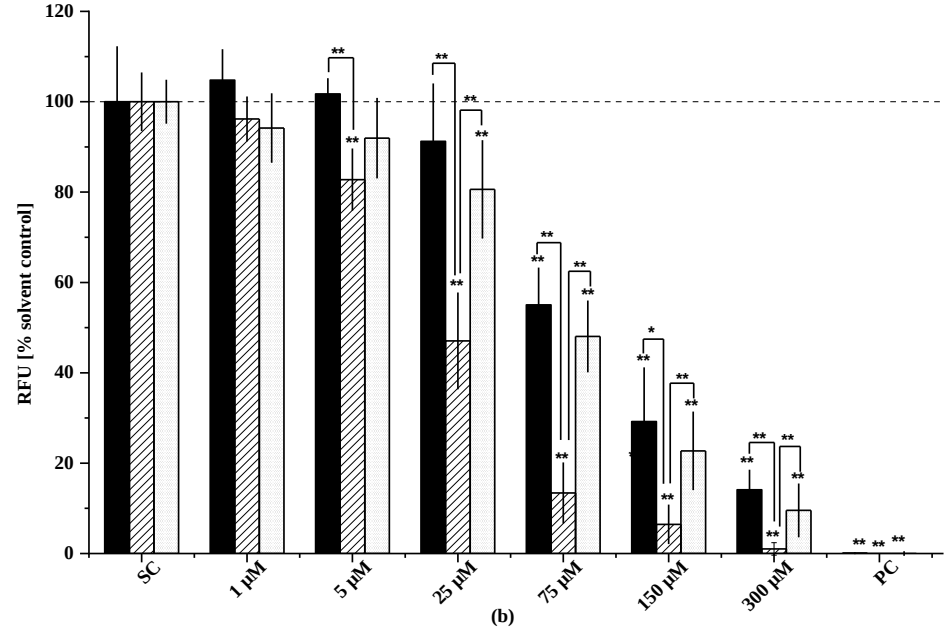

Figure 17: Cytotoxicity (Alamar blue assay) of retrorsine in the culture of primary rat hepatocytes, expressed as relative resorufin units (RFU). (a) Incubation with alkaloid for 24 hours. (b) Incubation with alkaloid for 48 hours. The cells were incubated with lasiocarpine at different concentrations after 24 h of pre-incubation (filled bars), or after 3 h of pre-incubation (scattered bars), or after 3 h of pretreatment with 5 µM of ketoconazole (dotted bars) for 2 h. Data are shown the mean ± SD of three different experiments. Each measurement was detected triplicate in independent culture wells. Resorufin reduction levels were significantly different from the solvent control at *p<0.05 or **p<0.01 or from each other, as indicated, at *p<0.05 or **p<0.01.

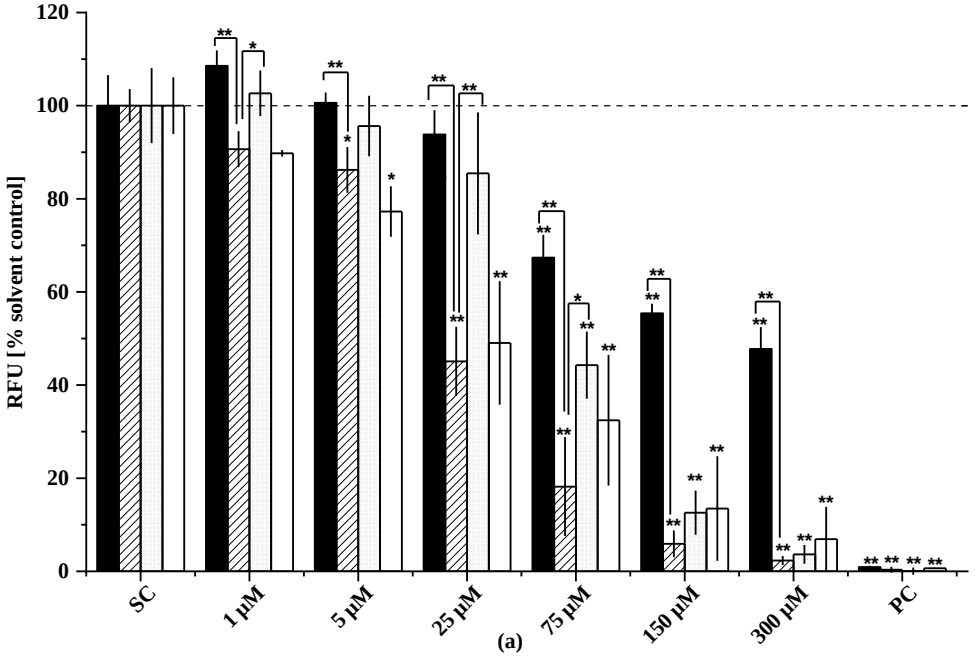

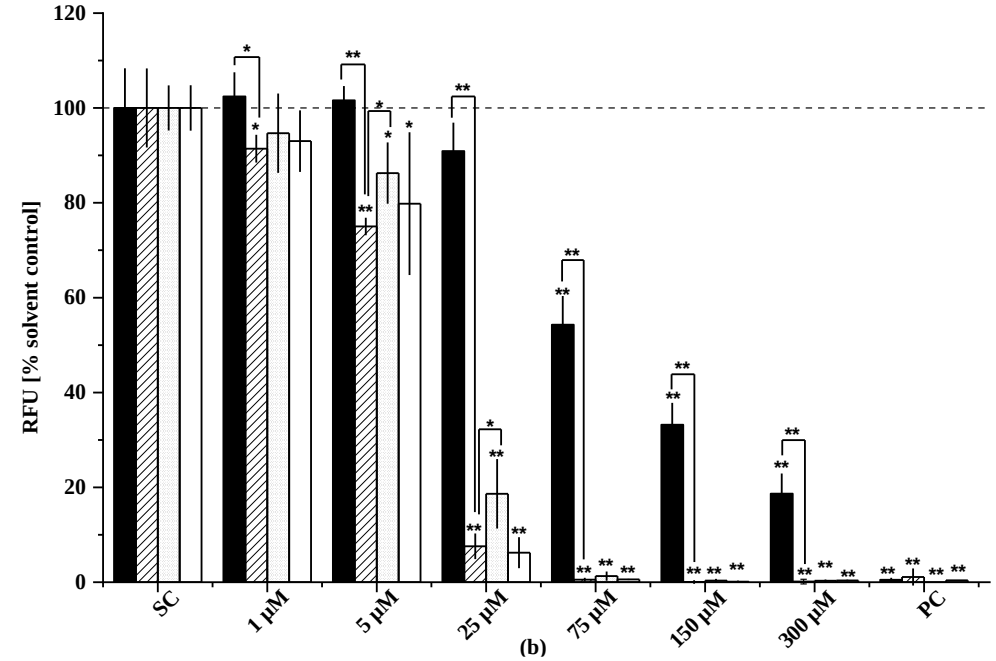

Figure 18: Cytotoxicity (Alamar blue assay) of senecionine in the culture of primary rat hepatocytes, expressed as relative resorufin units (RFU). (a) Incubation with alkaloid for 24 hours. (b) Incubation with alkaloid for 48 hours. The cells were incubated with lasiocarpine at different concentrations after 24 h of pre-incubation (filled bars), or after 3 h of pre-incubation (scattered bars), or after 3 h of pretreatment with 5 µM of ketoconazole (dotted bars) or with 1 mM BSO (open bars) for 2 h. Data are shown the mean ± SD of three different experiments. Each measurement was detected triplicate in independent culture wells. Resorufin reduction levels were significantly different from the solvent control at *p<0.05 or **p<0.01 or from each other, as indicated, at *p<0.05 or **p<0.01.

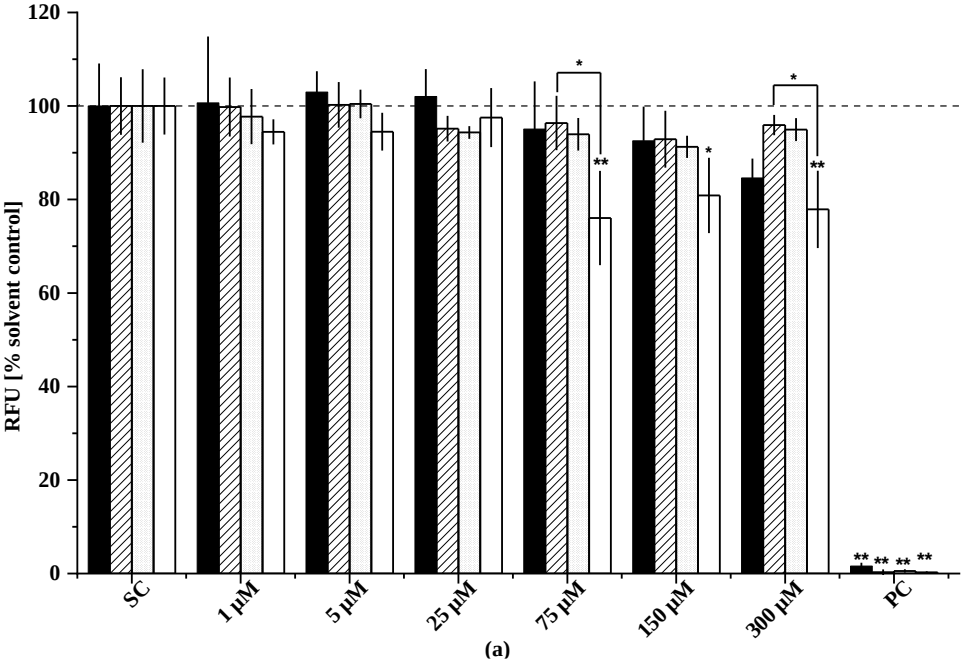

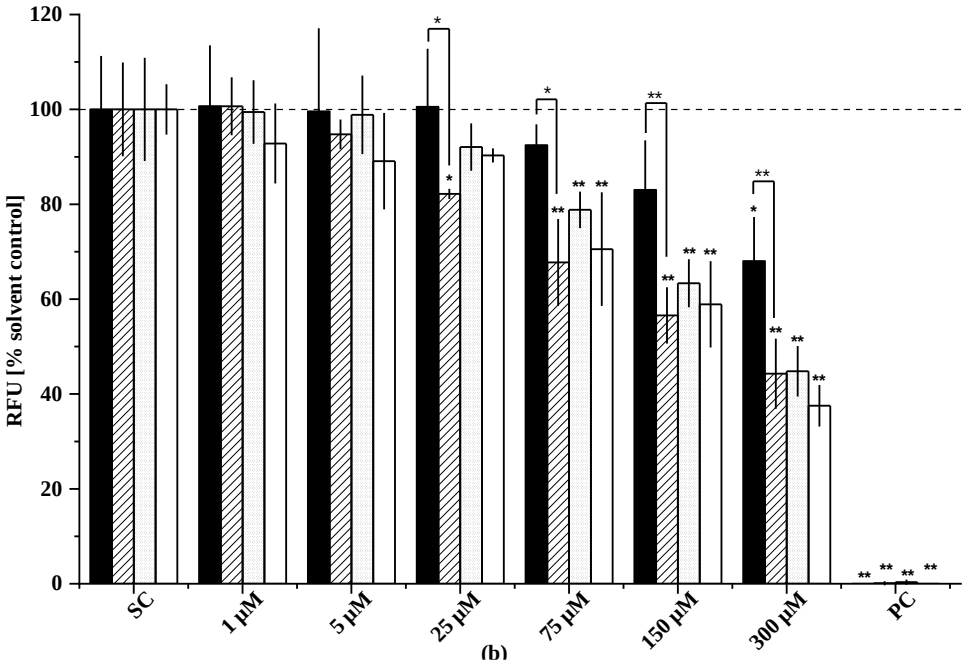

Figure 19: Cytotoxicity (Alamar blue assay) of indicine in the culture of primary rat hepatocytes, expressed as relative resorufin units (RFU). (a) Incubation with alkaloid for 24 hours. (b) Incubation with alkaloid for 48 hours. The cells were incubated with lasiocarpine at different concentrations after 24 h of pre-incubation (filled bars), or after 3 h of pre-incubation (scattered bars), or after 3 h of pretreatment with 5 µM of ketoconazole (dotted bars) or with 1 mM BSO (open bars) for 2 h. Data are shown the mean ± SD of three different experiments. Each measurement was detected triplicate in independent culture wells. Resorufin reduction levels were significantly different from the solvent control at *p<0.05 or **p<0.01 or from each other, as indicated, at *p<0.05 or **p<0.01.

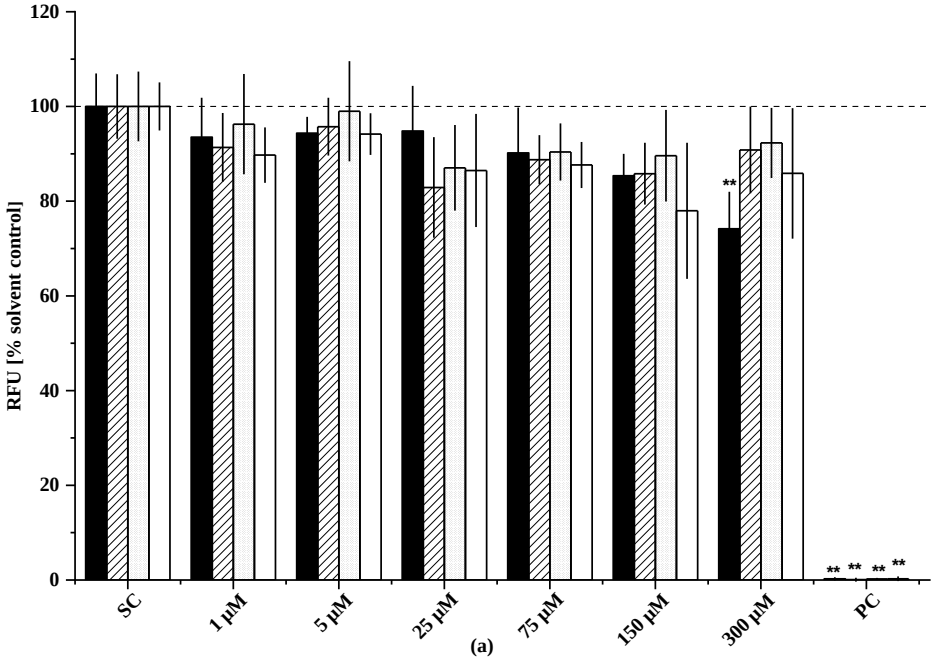

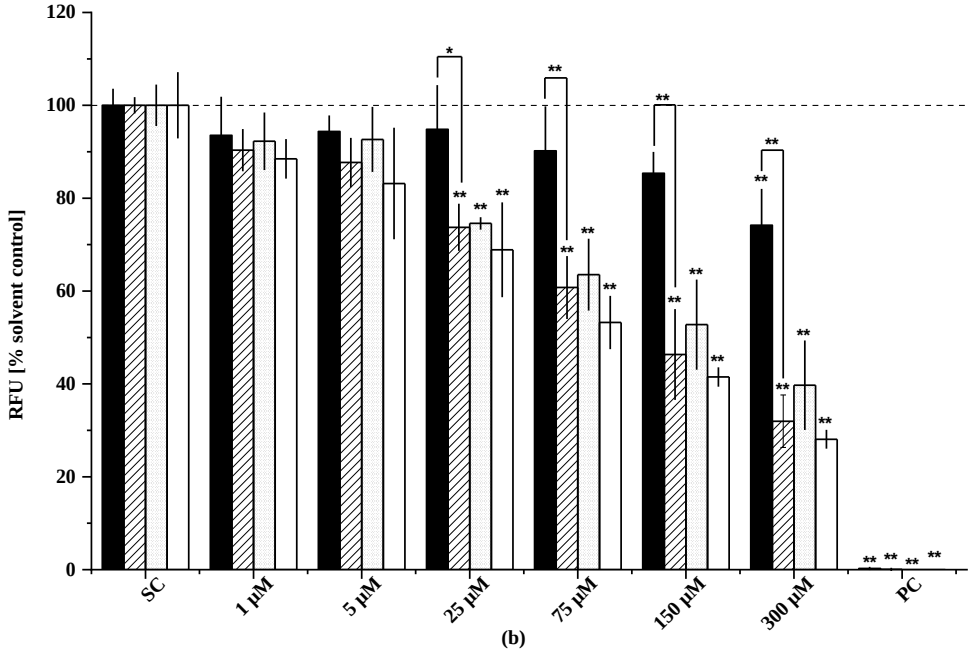

Figure 20: Cytotoxicity (Alamar blue assay) of lycopsamine in the culture of primary rat hepatocytes, expressed as relative resorufin units (RFU). (a) Incubation with alkaloid for 24 hours. (b) Incubation with alkaloid for 48 hours. The cells were incubated with lasiocarpine at different concentrations after 24 h of pre-incubation (filled bars), or after 3 h of pre-incubation (scattered bars), or after 3 h of pretreatment with 5 µM of ketoconazole (dotted bars) or with 1 mM BSO (open bars) for 2 h. Data are shown the mean ± SD of three different experiments. Each measurement was detected triplicate in independent culture wells. Resorufin reduction levels were significantly different from the solvent control at *p<0.05 or **p<0.01 or from each other, as indicated, at *p<0.05 or **p<0.01.

The cytotoxicity data obtained for five PA congeners after incubation 24 and 48 h were modeled using sigmoidal curve fitting. Half-maximal cytotoxic concentrations, i.e., EC_{50}, and their standard deviations were calculated in Tab. 3. It was shown that the cytotoxicity of PA congeners in primary rat hepatocytes with a pre-incubation time of 3 h was generally higher compared to that with 24 h pre-incubation. For some congeners such as senecionine, the effect of the shorter pre-incubation time was dramatic. But for retrorsine, shorter pre-incubation time combined with incubation for 24 h led to reduced cytotoxicity. All di-esters, including open-chained and cyclic congeners, were highly cytotoxic with EC_{50} values between 4 and 20 µM after 3 h pre-incubation then 48 h incubation with the PA congeners. Indicine and lycopsamine did not reach EC_{50}-concentrations even for 300 µM , the highest concentration tested. With 3 h pre-incubation and combined treatment of 48 h, they exhibited EC_{50} values below 300 µM, but still above 100 µM.

Table 3: Cytotoxicity (EC_{50}) of selected pyrrolizidine alkaloids in primary rat hepatocytes

PA (structural features)	EC_{50}: µM, 24 h/48 h 24 h after seeding	EC_{50}: µM, 24 h/48 h 3 h after seeding	iREP[a]
lasiocarpine (open, di, 7*S*)	91 ± 9 / 27 ± 2	86 ± 11 / 4 ± 1[c]	1.0
retrorsine (cyclic, di, 7*R*)	129 ± 9 / 90 ± 8	168 ± 30 / 19 ± 2[c]	1.0
senecionine (cyclic, di, 7*R*)	196 ± 31 / 95 ± 8	19 ± 3[c] / 8 ± 1[c]	1.0
indicine (mono, 7*R*)	>300 / >300	>300 / 210 ± 16	0.01
lycopsamine (mono, 7*R*)	>300 / >300	>300 / 114 ± 18	0.01

[a] Merz and Schrenk (2016);

[c] highly significantly different ($p \leq 0.01$) from the incubation with PA at 24 h after seeding.

In general, as shown in Tab. 4, the cytotoxicity of all five PA congeners was reduced significantly or highly significantly by the pre-treatment with ketoconazole. For an incubation time of 24 h, except for two mono-esters still with an EC_{50} value > 300 µM, lasiocarpine and senecionine were about 1.5-fold and 3-fold less toxic with ketoconazole, respectively. After an incubation time of 48 h, to all reported five PA congeners, ketoconazole led from a slight up to an about 3-fold reduction in cytotoxicity as estimated from the concentration-response curves. The EC_{50} value of retrorsine was 168 ± 30 µM with 24 h inhibition, whereas, with a CYP inhibition by ketoconazole, it even did not cause a reduction of 50% on viability at 300 µM.

Concomitantly, the GSH depletion had no significant effect for senecionine and indicine, but for lasiocarpine with a treatment of 24 h and lycopsamine with 48 h leading to an about 1.5 to 2-fold increase in cytotoxicity based on the estimated EC_{50} values.

Table 4: Effect of CYP inhibition with ketoconazole and GSH depletion with BSO on cytotoxicity (EC_{50}) of selected pyrrolizidine alkaloids in primary rat hepatocytes

PA (structural features)	EC_{50}: µM, 24 h/48 h 3 h after seeding	EC_{50}: µM, 24 h/48 h Pre-incubation with ketoconazole (5 µM)	EC_{50}: µM, 24 h/48 h Pre-incubation with BSO (1 mM)
lasiocarpine (open, di, 7*S*)	86 ± 11 / 4 ± 1	120 ± 10[b] / 11 ± 1[c]	55 ± 14[b] / 4 ± 1
retrorsine (cyclic, di, 7*R*)	168 ± 30 / 19 ± 2	>300 / 67 ± 6[c]	n.t.
senecionine (cyclic, di, 7*R*)	19 ± 3 / 8 ± 1	65 ± 4[c] / 12 ± 1[c]	19 ± 3 / 8 ± 2
indicine (mono, 7*R*)	>300 / 210 ± 16	>300 / 248 ± 2[b]	>300 / 191 ± 15
lycopsamine (mono, 7*R*)	>300 / 114 ± 18	>300 / 166 ± 26[b]	>300 / 77 ± 11[b]

n.t.: not tested;

[b] significantly different ($p \leq 0.05$) from the incubation with PA at 3 h after seeding;

[c] highly significantly different ($p \leq 0.01$) from the incubation with PA at 3 h after seeding.

3.3.2 HepG2 cells and HepG2 C9 (CYP3A4)

Furthermore, naïve HepG2 cells and the HepG2 C9 clone over-expressing the CYP3A4 gene were incubated with various concentrations of PAs for 24 and 48 h. The cytotoxicity was measured by Alamar blue assay and the data are shown in Fig. 21 to 25.

In the naïve HepG2 cells, none of the selected PA congeners exhibited significantly cytotoxic effects up to the highest tested concentration of 300 µM even after incubation for 48 h (s. Fig. 21 to 25, open bars).

Cytotoxic effects of most of the tested PA congeners in the HepG2 (CYP3A4) C9 cells turned out to be significantly higher than in naïve HepG2 cells but be less compared to the cytotoxicity in primary rat hepatocytes. For all three di-esters, treatment over 48 h exerted higher cytotoxicity than the treatment of 24 h. Lasiocarpine was non-toxic in naïve HepG2 cells up to a concentration of 300 µM while showing highly significant cytotoxicity at 5 µM in HepG2 (CYP3A4) C9 cells (s. Fig. 21, scattered bars). Moreover, the cyclic di-esters senecionine and retrorsine showed significant cytotoxicity at 25 µM and 75 µM, respectively (s. Fig. 19 and 20, scattered bars). The mono-esters indicine and lycopsamine with low cytotoxicity in primary rat hepatocytes were almost non-cytotoxic in HepG2 C9 (CYP3A4) clone, lycopsamine only decreased minorly in viability after 48 h at the highest concentration of 300 µM tested (s. Fig. 24 and 25, scattered bars).

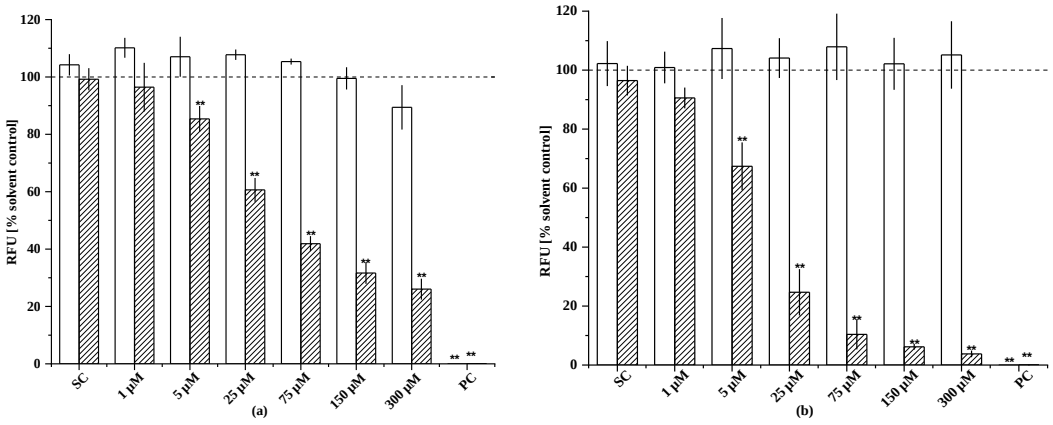

Figure 21:Cytotoxicity (Alamar blue assay) of lasiocarpine in the culture of HepG2 cells (open bars) and HepG2 C9 (CYP3A4) cells (scattered bars), expressed as relative resorufin units (RFU). (a) Incubation with alkaloid for 24 hours. (b) Incubation with alkaloid for 48 hours. Data are shown the mean ± SD of three different experiments. Each measurement was detected triplicate in independent culture wells. Resorufin reduction levels differed significantly from the solvent control at *p<0.05 or **p<0.01.

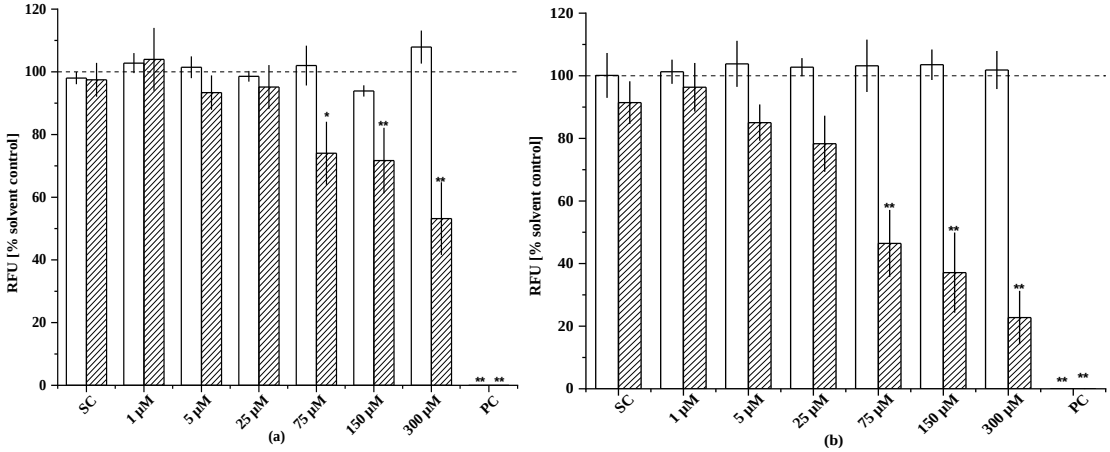

Figure 22: Cytotoxicity (Alamar blue assay) of retrorsine in the culture of HepG2 cells (open bars) and HepG2 C9 (CYP3A4) cells (scattered bars), expressed as relative resorufin units (RFU). (a) Incubation with alkaloid for 24 hours. (b) Incubation with alkaloid for 48 hours. Data are shown the mean ± SD of three different experiments. Each measurement was detected triplicate in independent culture wells. Resorufin reduction levels differed significantly from the solvent control at *p<0.05 or **p<0.01.

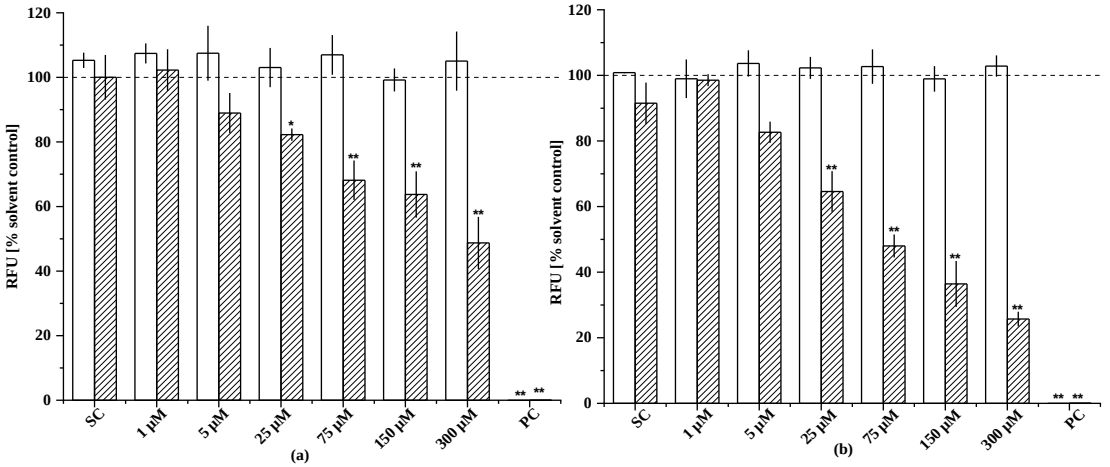

Figure 23: Cytotoxicity (Alamar blue assay) of senecionine in the culture of HepG2 cells (open bars) and HepG2 C9 (CYP3A4) cells (scattered bars), expressed as relative resorufin units (RFU). (a) Incubation with alkaloid for 24 hours. (b) Incubation with alkaloid for 48 hours. Data are shown the mean ± SD of three different experiments. Each measurement was detected triplicate in independent culture wells. Resorufin reduction levels differed significantly from the solvent control at *p<0.05 or **p<0.01.

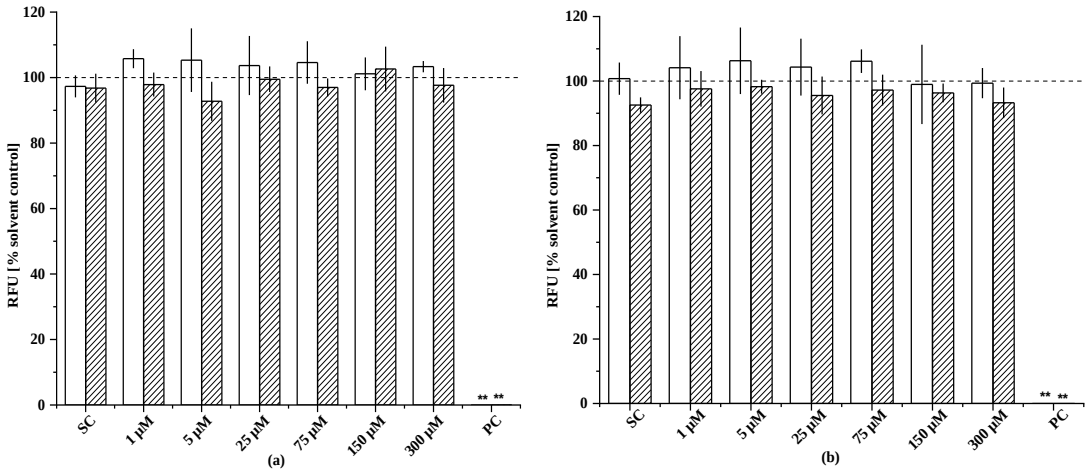

Figure 24: Cytotoxicity (Alamar blue assay) of indicine in the culture of HepG2 cells (open bars) and HepG2 C9 (CYP3A4) cells (scattered bars), expressed as relative resorufin units (RFU). (a) Incubation with alkaloid for 24 hours. (b) Incubation with alkaloid for 48 hours. Data are shown the mean ± SD of three different experiments. Each measurement was detected triplicate in independent culture wells. Resorufin reduction levels differed significantly from the solvent control at **p<0.01.

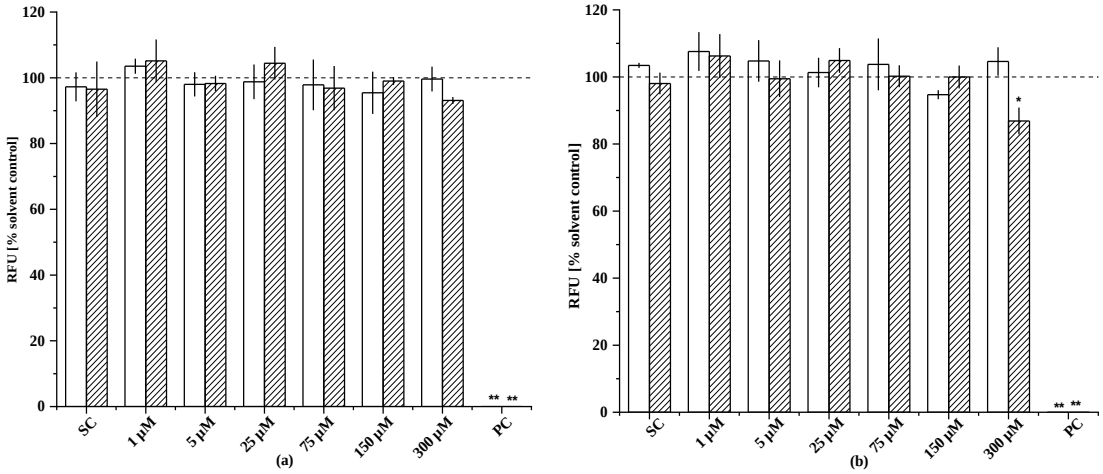

Figure 25: Cytotoxicity (Alamar blue assay) of lycopsamine in the culture of HepG2 cells (open bars) and HepG2 C9 (CYP3A4) cells (scattered bars), expressed as relative resorufin units (RFU). (a) Incubation with alkaloid for 24 hours. (b) Incubation with alkaloid for 48 hours. Data are shown the mean ± SD of three different experiments. Each measurement was detected triplicate in independent culture wells. Resorufin reduction levels differed significantly from the solvent control at *p<0.05 or **p<0.01.

The half-maximal cytotoxic concentrations in HepG2 C9 (CYP3A4) clone were also calculated (s. Tab. 5). For the incubation time of 24 h, only the EC_{50} value of lasiocarpine was lower than 300 µM. After 48 h incubation, similar to that in primary rat hepatocytes, lasiocarpine was the most cytotoxic PA and had an EC_{50} value of 10 ± 1 µM, the EC_{50} values of other di-ester compounds ranged between 60 and 80 µM. In contrast, the values of mono-esters indicine and lycopsamine were higher than the maximal tested concentration.

Table 5: Cytotoxicity (EC_{50}) of selected pyrrolizidine alkaloids in HepG2 (CYP3A4) C9 clone

PA (structural features)	EC_{50}: µM, 24 h/48 h	iREP[a]
lasiocarpine (open, di, 7*S*)	50 ± 4 / 10 ± 1	1.0
retrorsine (cyclic, di, 7*R*)	>300 / 73 ± 12	1.0
senecionine (cyclic, di, 7*R*)	>300 / 67 ± 8	1.0
indicine (mono, 7*R*)	>300 / >300	0.01
lycopsamine (mono, 7*R*)	>300 / >300	0.01

[a] Merz and Schrenk (2016)

3.4 Micronucleus assay

Because of the time required for micronuclei formation, the micronuclei counts were determined after treatment with different pyrrolizidine alkaloids for 24 h with an additional incubation in fresh medium over 72 h. In order to avoid false-negative results induced by the severe cytotoxic effects caused by alkaloids in HepG2 (CYP3A4) C9 cell culture, cytotoxicity was also measured in parallel (s. Fig. 26 to 30, square). After incubation with lasiocarpine, retrorsine, or senecionine, it exhibited an over 50% cytotoxic effect when incubated with a concentration higher than 25 µM, and there were even not enough cells (<1000) that could be counted. Therefore, the micronucleus assay for these di-esters was only tested up to the concentration of 25 µM. To obtain more information on the dose-response relationship, a lower concentration range from 0.01 µM to 25 µM of these three PA congeners was tested. The mono-esters, indicine and lycopsamine, were measured with the same concentrations as used in the Alamar blue assay to compare the relative potencies between different assays. Following the recommendation in the OECD 487 (2016) guideline of micronucleus test *in vitro* mammalian cell, the highest concentration tested should aim to achieve at least 50% in cell growth for further modeling.

All five PA congeners significantly increased micronuclei counts, but the induced toxic effect was toxic to some extent. A statistically significant increase in micronuclei counts compared to the solvent control was determined for lasiocarpine at 1µM, followed by 2.5 µM for retrorsine and senecionine, while indicine and lycopsamine induced significant increases in micronuclei counts starting from 150 µM (s. Fig. 26 to 30). The effect of open chain di-ester lasiocarpine is shown in Fig. 26: Micronuclei counts increased at low concentrations, reaching a maximum at about 1 – 5 µM. In all concentrations tested, the micronuclei counts of (24 ± 9)/1000 were mostly induced at dose 2.5 µM. The other cyclic diesters retrorsine and senecionine formed most micronuclei at concentrations between 2.5 and 25 µM (s. Fig. 27 and 28). At a concentration of 5 µM, both led to the highest level of micronuclei of (21 ± 2)/1000 and (23 ± 7)/1000, respectively. Consequently, the number of micronuclei counts

decreased at higher concentrations. The amount of micronuclei after treatment with mono-esters was increased concentration-dependently (s. Fig. 29 and 30). Indicine and lycopsamine at a concentration of 300 µM induced most micronuclei of (35 ± 4)/1000 and (26 ± 7)/1000. In general, with di-esters tested in my work, micronuclei counts commonly increased with increasing concentrations reaching a maximum at about 2.5 or 5 µM. In comparison, mono-esters led to a sustained increase in micronuclei counts up to 300 µM. This finding was in accordance with the assumption that severe cytotoxicity attenuated the formation of micronucleus.

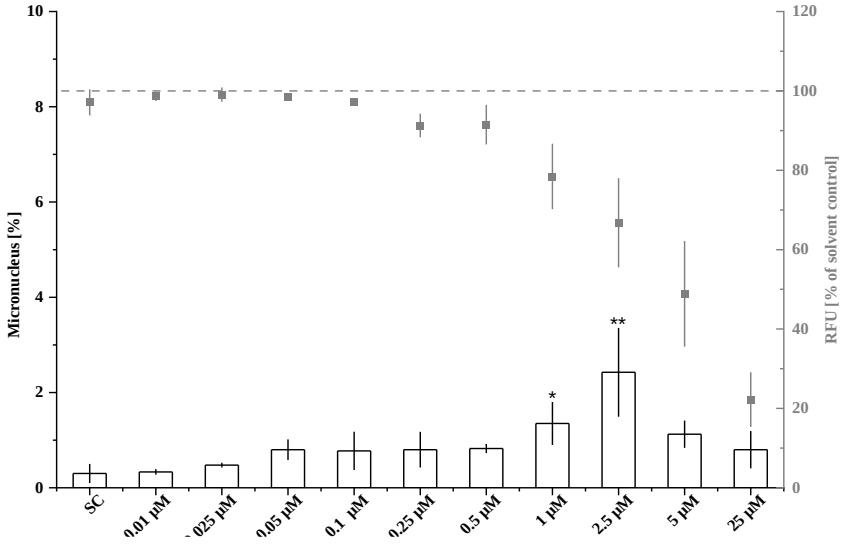

Figure 26: Micronuclei formation in HepG2 C9 (CYP3A4) clone (open bars) treated with lasiocarpine and cytotoxicity under the conditions of the micronucleus assay with recovery (square). Data are represented as means ± S.D. from n = 3 independent experiments. Micronuclei counts differed significantly from the solvent control at *p<0.05 or **p<0.01.

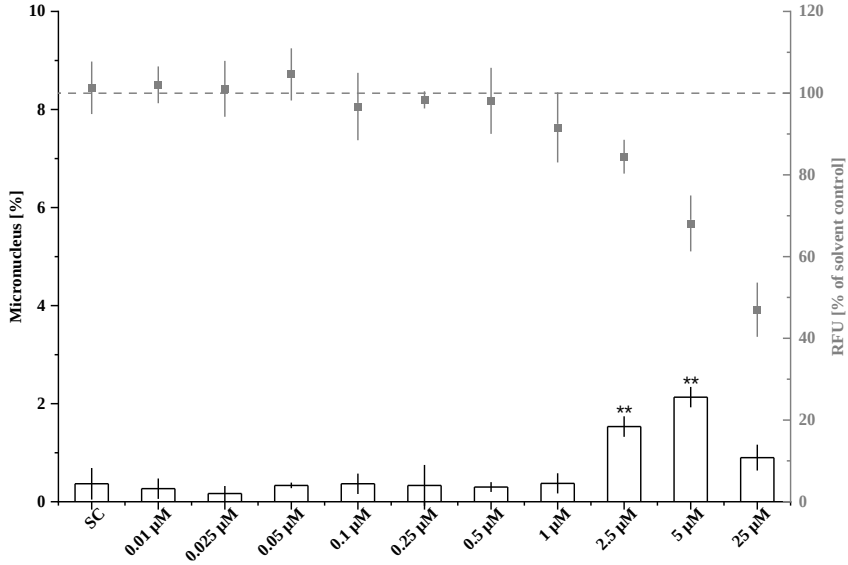

Figure 27: Micronuclei formation in HepG2 C9 (CYP3A4) clone (open bars) treated with retrorsine and cytotoxicity under the conditions of the micronucleus assay with recovery (square).

Data are represented as means ± S.D. from n = 3 independent experiments. Micronuclei counts differed significantly from the solvent control at **p<0.01.

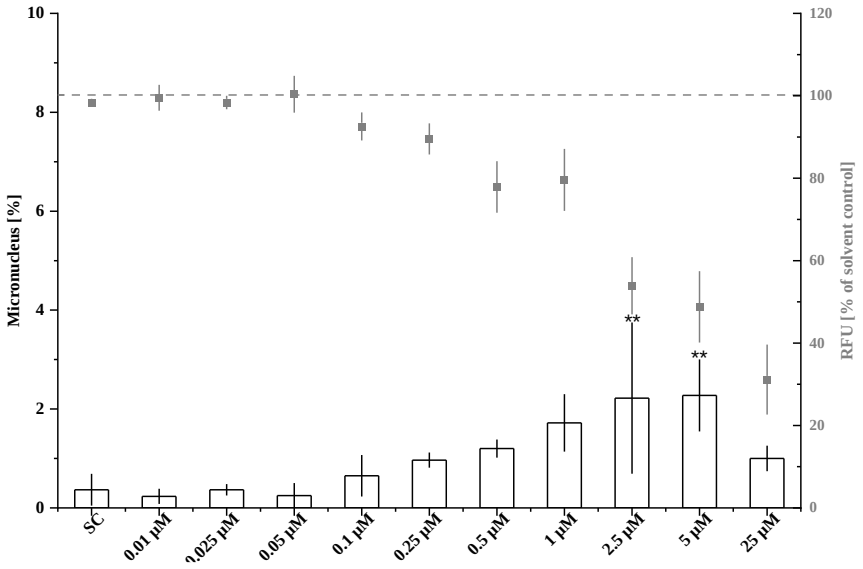

Figure 28:Micronuclei formation in HepG2 C9 (CYP3A4) clone (open bars) treated with senecionine and cytotoxicity under the conditions of the micronucleus assay with recovery (square). Data are represented as means ± S.D. from n = 3 independent experiments. Micronuclei counts differed significantly from the solvent control at **p<0.01.

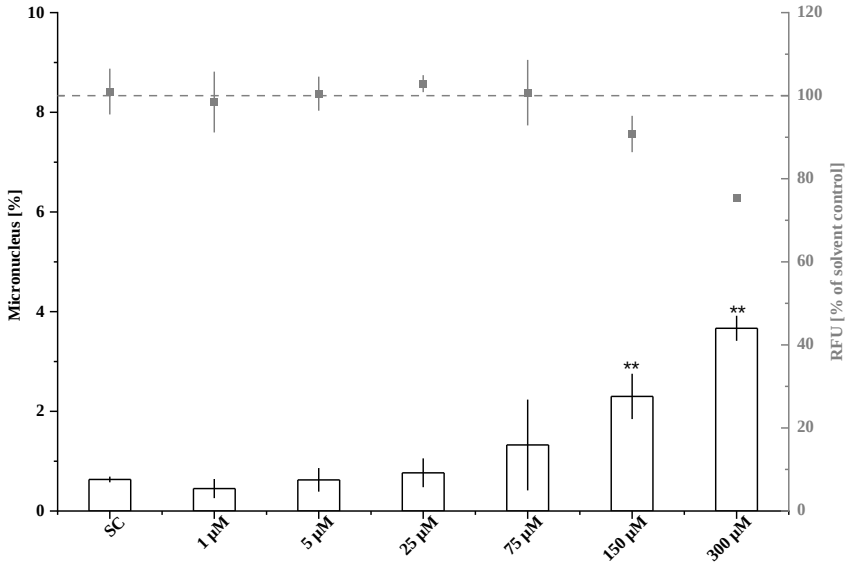

Figure 29: Micronuclei formation in HepG2 C9 (CYP3A4) clone (open bars) treated with indicine and cytotoxicity under the conditions of the micronucleus assay with recovery (square). Data are represented as means ± S.D. from n = 3 independent experiments. Micronuclei counts differed significantly from the solvent control at **p<0.01.

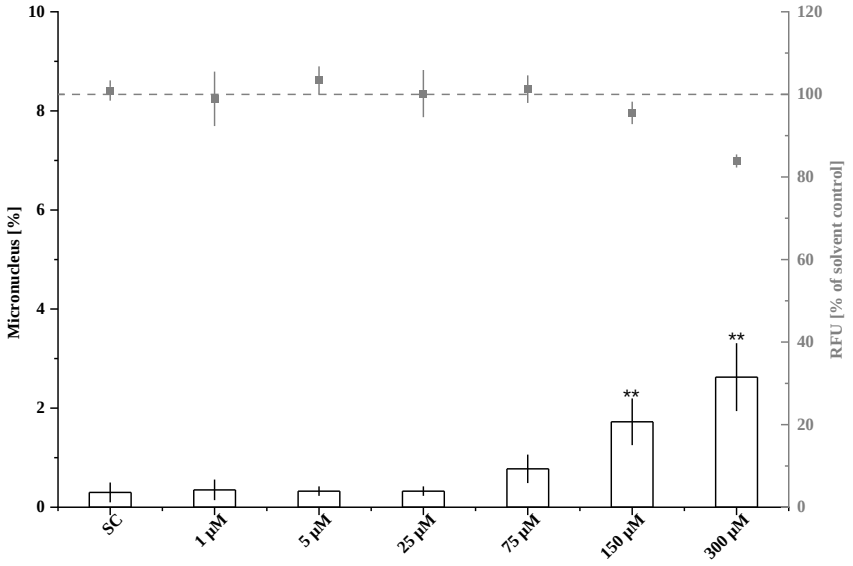

Figure 30: Micronuclei formation in HepG2 C9 (CYP3A4) clone (open bars) treated with lycopsamine and cytotoxicity under the conditions of the micronucleus assay with recovery (square). Data are represented as means ± S.D. from n = 3 independent experiments. Micronuclei counts differed significantly from the solvent control at **p<0.01.

In order to calculate and compare the relative genotoxic potencies of different PA congeners, the data from the micronucleus test were modeled according to the benchmark calculation model using software PROAST (EFSA). Fig. 31 to 35 showed the best-fit algorithms of dose-response modeling obtained for different PA congeners. For lasiocarpine, as shown in Fig. 31, no practical threshold could be seen. But for the other di-esters, no dose-response relationship was exhibited in the low concentration range below 1 µM for retrorsine and 0.1 µM for senecionine (s. Fig. 32 and 33). With indicine (s. Fig. 34), the no-effect threshold was higher at about 5 µM, and for lycopsamine (s. Fig. 35), in the range below 25 µM, no increase in micronuclei counts was found.

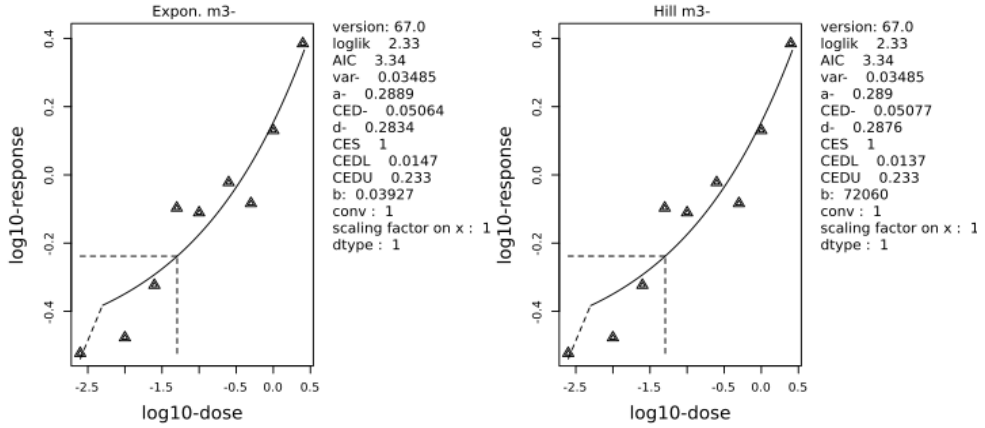

Figure 31: Benchmark-Dose modeling of micronuclei data in HepG2 C9 (CYP3A4) clone treated with various concentrations of lasiocarpine. The panel shows the four best fits using PROAST (EFSA) software and the concentration estimate for a Benchmark effect of doubling in the micronuclei counts.

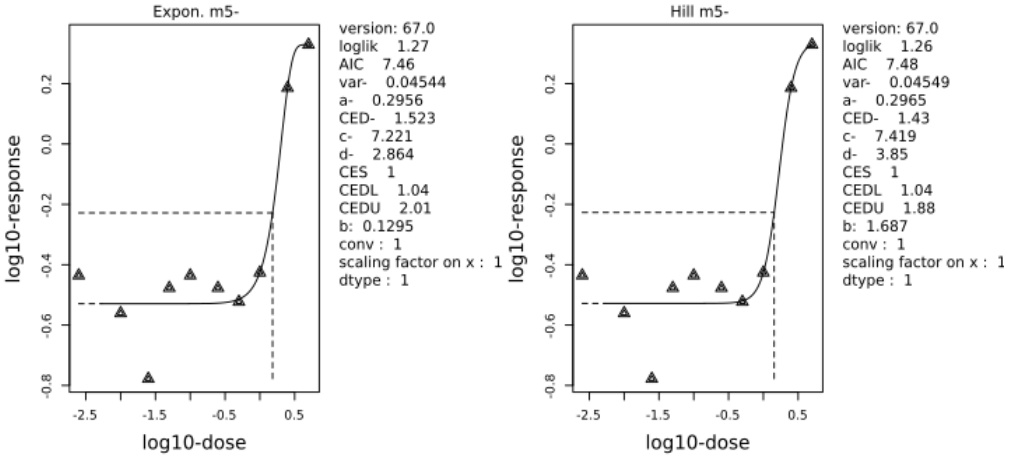

Figure 32: Benchmark-Dose modeling of micronuclei data in HepG2 C9 (CYP3A4) clone treated with various concentrations of retrorsine. The panel shows the four best fits using PROAST (EFSA) software and the concentration estimate for a Benchmark effect of doubling in the micronuclei counts.

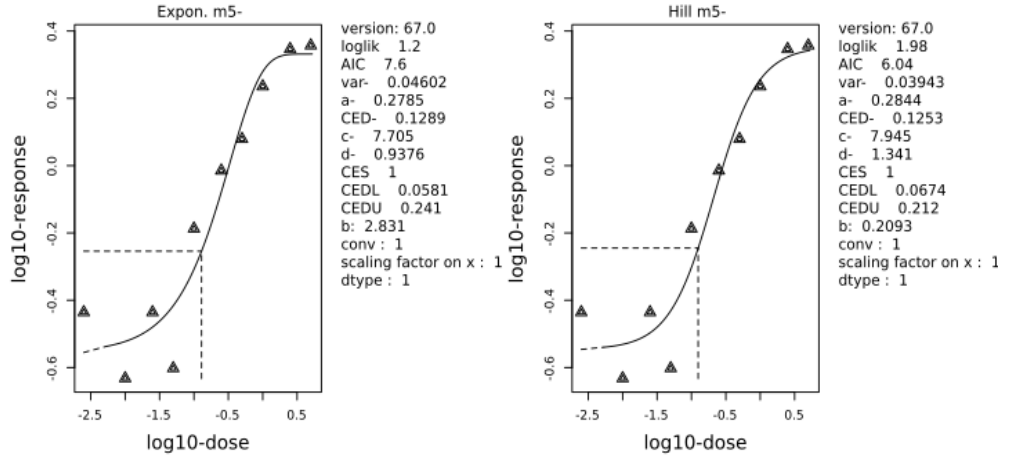

Figure 33: Benchmark-Dose modeling of micronuclei data in HepG2 C9 (CYP3A4) clone treated with various concentrations of senecionine. The panel shows the four best fits using PROAST (EFSA) software and the concentration estimate for a Benchmark effect of doubling in the micronuclei counts.

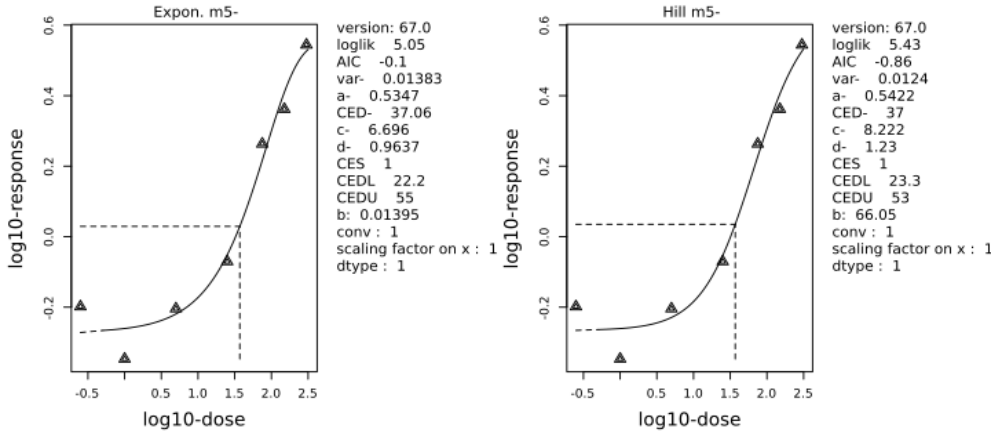

Figure 34: Benchmark-Dose modeling of micronuclei data in HepG2 C9 (CYP3A4) clone treated with various concentrations of indicine. The panel shows the four best fits using PROAST (EFSA) software and the concentration estimate for a Benchmark effect of doubling in the micronuclei counts.

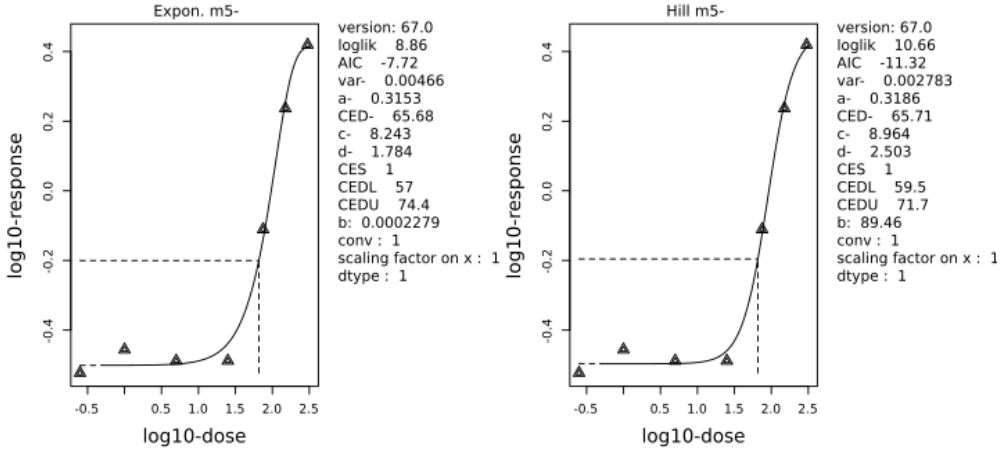

Figure 35: Benchmark-Dose modeling of micronuclei data in HepG2 C9 (CYP3A4) clone treated with various concentrations of lycopsamine. The panel shows the four best fits using PROAST (EFSA) software and the concentration estimate for a Benchmark effect of doubling in the micronuclei counts.

Based on the fittings, the benchmark dose (BMD) that led to a doubling of micronuclei counts over the background was calculated (s. Tab. 6), indicating an upper (BMDU) and lower (BMDL) confidence limit. Lasiocarpine and senecionine were most potent PAs with BMDLs both below 0.1 µM and with BMDUs of 0.28 µM and 0.26 µM (final BMD values reported in PROAST). The remaining cyclic di-ester retrorsine revealed distinctly less potency with BMDL and BMDU of 0.97 and 1.98 µM, respectively. The genotoxic effects of mono-esters indicine and lycopsamine were the least potent, with BMDL-BMDU in the range of 19.1 – 62.3 µM and 59.5 – 73.3µM. The benchmark dose approach was divided between the most toxic lasiocarpine, and the least potent lycopsamine spanned more than 5000-fold.

Table 6:Benckmark doses with lower and upper confidence limits calculated from exponential and Hill model of selected PA congeners

PA (structural features)	BMD: µM		BMDL: µM		BMDU: µM		iREP[a]
	Exp.	Hill	Exp.	Hill	Exp.	Hill	
lasiocarpine (open, di, 7*S*)	0.05	0.05	0.01	0.01	0.23	0.23	1.0
retrorsine (cyclic, di, 7*R*)	1.52	1.43	1.04	1.04	2.01	1.88	1.0
senecionine (cyclic, di, 7*R*)	0.13	0.13	0.06	0.07	0.24	0.21	1.0
indicine (mono, 7*R*)	37.1	37.0	22.2	23.3	55.0	53.0	0.01
lycopsamine (mono, 7*R*)	65.7	65.7	57.0	59.5	74.4	71.7	0.01

[a] Merz and Schrenk (2016);

3.5 Ames fluctuation assay

3.5.1 Checking of genotype

The strains were tested with three different antibiotics (ampicillin, neomycin, and tetracycline) (s. Fig. 36). Since the R-factor plasmid (pKM101), which contains an ampicillin gene, is presented in all strains, there was no inhibition around filter paper. On the contrary, incubation with neomycin led to an inhibited growth in all strains. For tetracycline, only TA102, which carries the multicopy plasmid pAQ1 besides the hisG428 mutation, showed an absence of an inhibitory zone indicating the resistance.

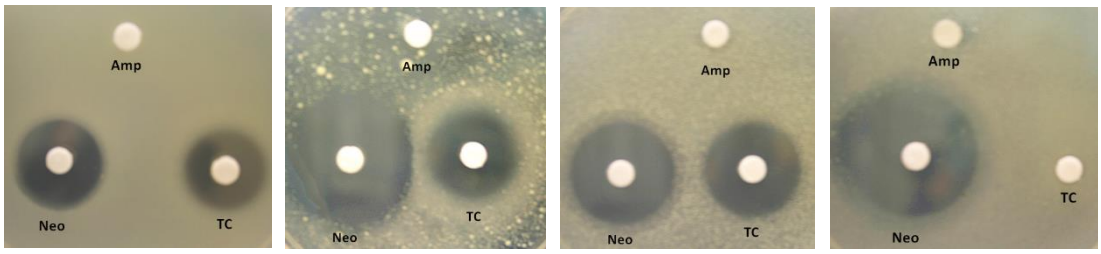

TA97a **TA98** **TA100** **TA102**

Figure 36: Genotype testing of bacterial strains for antibiotic resistance. 10 µl of the corresponding antibiotics solution (Amp: ampicillin, 8 mg/ml; Neo: neomycin, 8 mg/ml; TC: tetracycline, 0.8 mg/ml) was added to the filter paper.

For checking the crystal-violet resistance, which is evidence of the *rfa*-mutation that causes a partial defect of the lipopolysaccharide barrier, a filter paper disc was wetted with 10 µL of 1 mg/ml crystal violet solution was placed to the plates that seeded with different *Salmonella typhimurium* strains. After incubation, a clear zone of inhibition appeared around the disc for all strains (s. Fig. 37).

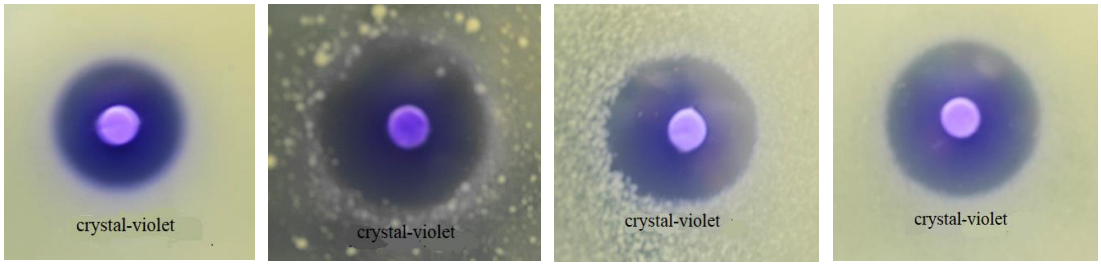

TA97a **TA98** **TA100** **TA102**

Figure 37: Genotype testing of bacterial strains for crystal-violet sensitivity. 10 µl of the crystal-violet solution (1 mg/ml; Neo: neomycin, 8 mg/ml; TC: tetracycline, 0.8 mg/ml) was added to the filter papier.

In order to confirm the *uvrB*-mutation, half of each bacterial streak was irradiated with UV-C light (2 x 15 W, distance 30 cm) for 8 s. After incubation for 24 hours at 37 °C, TA97a, TA98, and TA100 were all sensitive to the UV-C, only TA102 could still grow in the irradiated area since it is the only strain without *uvrB*-mutation (s. Fig. 38).

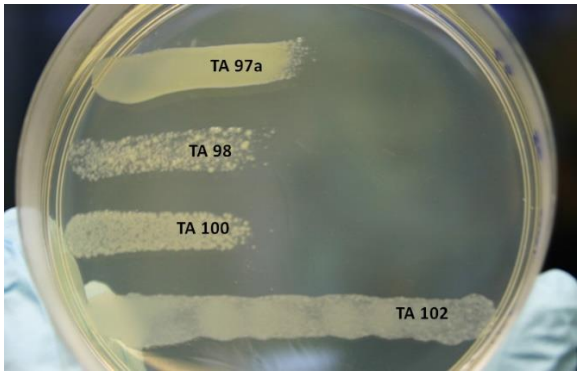

Figure 38: Genotype testing of bacterial strains for UV sensitivity (*uvrB*). Half of each bacterial streak was covered by an aluminum paper then irradiated with UV-C light (2 x 15 W, distance 30 cm) for 8 s.

It could be stated that all these four *Salmonella typhimurium* strains fulfilled the criteria of the genotype testing and could be subsequently used to determine the mutagenicity of PA congeners.

3.5.2 Testing of pyrrolizidine alkaloids

Because there was a loss of sensitivity to standard positive controls of TA97a and TA102, the mutagenicity of PAs was only tested in strain TA98 sensitive to a frameshift mutation and TA100 that detected base pair substitution. It was tested with and without metabolic activation using the S9 mix. The negative control values with the S9 mix were low in all cases, indicating that the S9 mix does not enhance the spontaneous mutation. In addition, the protein concentration of the S9 mix was 17.5 ± 2.5 mg/ml as determined by the procedure of Bradford (Bradford, 1976), and 11.0 ± 1.3 mg/ml as determined based on Lowry et al. (Lowry et al., 1951).

To confirm no false-negative results induced by cytotoxic effects, the viability of the bacterial strains was determined using Alamar blue assay. However, the viability could only be measured without exogenous metabolic activation by the S9 mix since resazurin would be immediately reduced to resorufin by the regenerated NADPH in S9 mix. The seeded density of the bacteria, the incubation time, and the tested concentration range of the PA congeners were the same as in the Ames fluctuations assay. After incubation with various PAs, the viability of both strains remained between 90 and 110%, even with 300 µM.

As shown in Fig 39 to 43 (open and scattered bars), in Ames fluctuation assay, none of the PA congeners measured in my work caused detectable mutagenicity in TA98 and TA100. The addition of rat liver S9-mix did not affect the outcome of the assay. But the negative results do not mean that these PA congeners are not mutagenic.

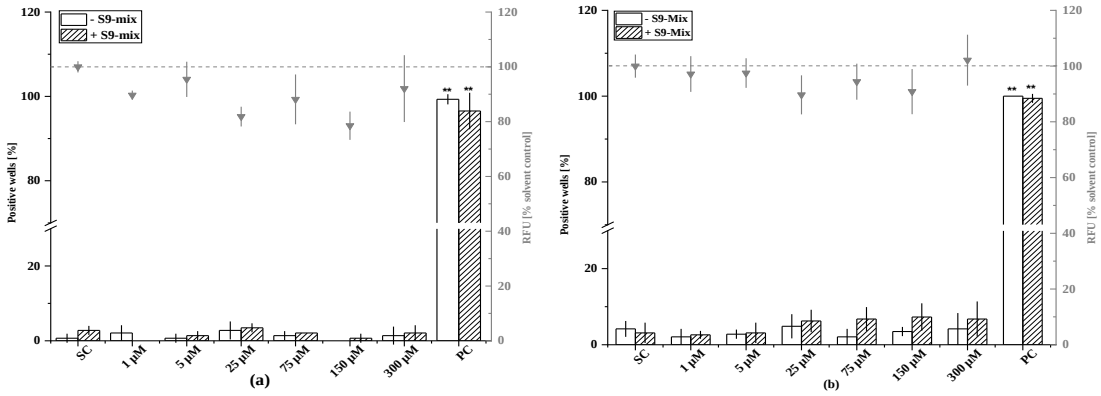

Figure 39: Ames fluctuation assay (open and scattered bars) in combination with Alamar blue assay (down triangle) with lasiocarpine in (a) TA98 and (b) TA100. Data are shown the mean ± SD of three different experiments. Each measurement was detected triplicate in independent culture wells. Resorufin reduction levels were significantly different from the solvent control at **p<0.01.

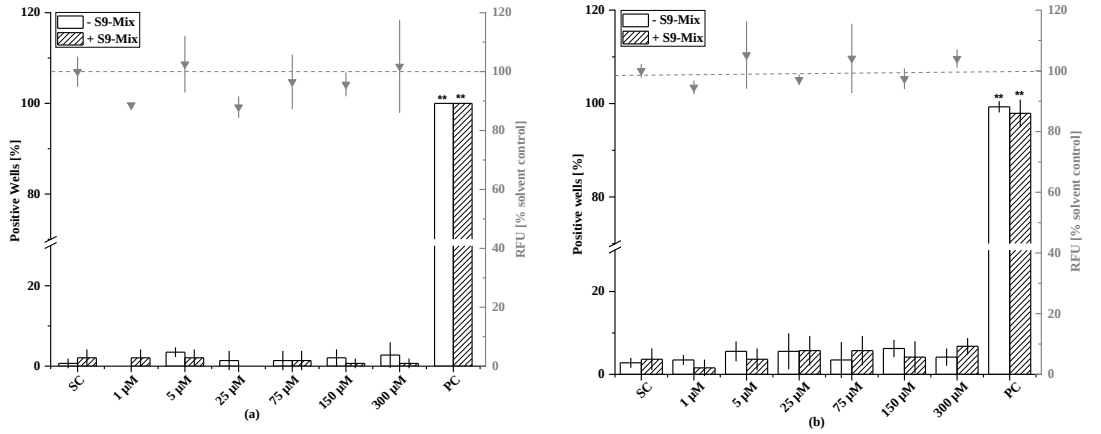

Figure 40: Ames fluctuation assay (open and scattered bars) in combination with Alamar blue assay (down triangle) with retrorsine in (a) TA98 and (b) TA100. Data are shown the mean ± SD of three different experiments. Each measurement was detected triplicate in independent culture wells. Resorufin reduction levels were significantly different from the solvent control at **p<0.01.

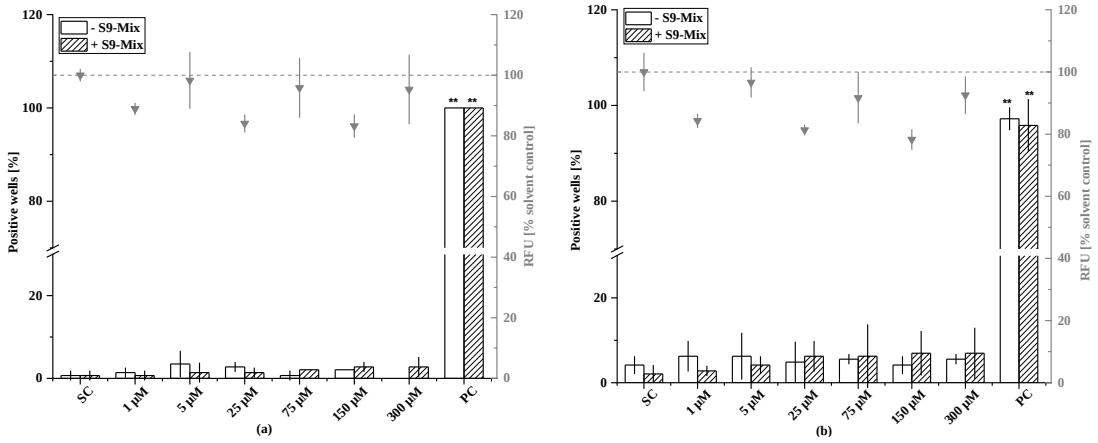

Figure 41: Ames fluctuation assay (open and scattered bars) in combination with Alamar blue assay (down triangle) with senecionine in (a) TA98 and (b) TA100. Data are shown the mean ± SD of three different experiments. Each measurement was detected triplicate in independent culture wells. Resorufin reduction levels were significantly different from the solvent control at **p<0.01.

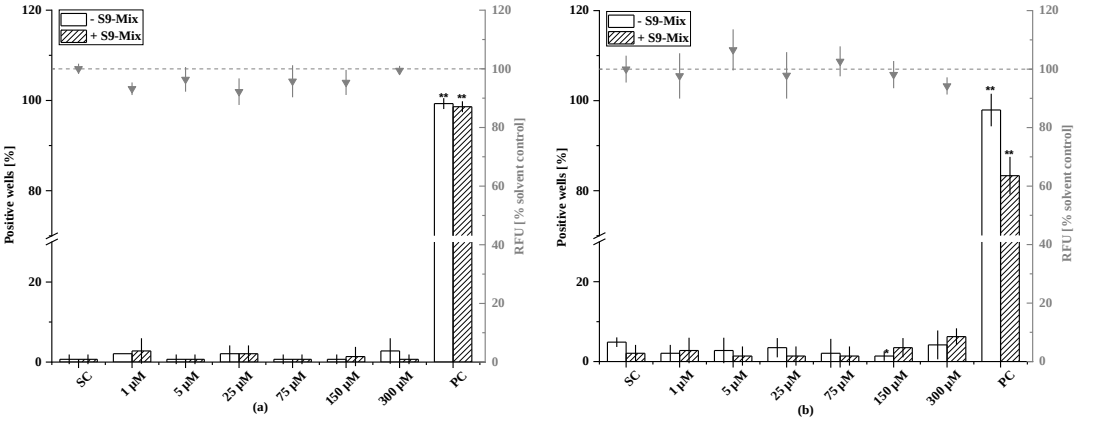

Figure 42: Ames fluctuation assay (open and scattered bars) in combination with Alamar blue assay (down triangle) with indicine in (a) TA98 and (b) TA100. Data are shown the mean ± SD of three different experiments. Each measurement was detected triplicate in independent culture wells. Resorufin reduction levels were significantly different from the solvent control at **p<0.01.

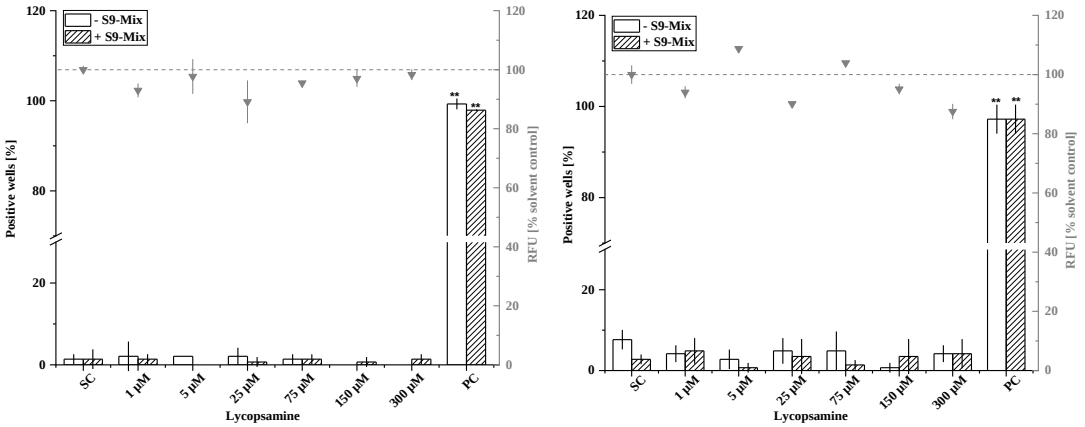

Figure 43: Ames fluctuation assay (open and scattered bars) in combination with Alamar blue assay (down triangle) with lycopsamine in (a) TA98 and (b) TA100. Data are shown is the mean ± SD of three different experiments. Each measurement was detected triplicate in independent culture wells. Resorufin reduction levels were significantly different from the solvent control at **p<0.01.

4 DISCUSSION

4.1 7-Benzyloxyresorufin-*O*-dealkylase (BROD) assay

PAs require metabolic activation to exert their toxic effect. Cytochrome P450 monooxygenases are involved in both *C*- and *N*-oxidation of the necine bases of PAs to form the reactive pyrrolic derivatives and the corresponding *N*-oxides. Many metabolic studies have determined the formation of reactive pyrrolic esters mainly catalyzed via CYP3A and CYP2B subfamilies (Buhler and Kedzierski, 1986; Chung et al., 1995; Huan et al., 1998; Li et al., 2011; Miranda et al., 1991). It is well known that the distribution of CYP450 enzymes is species- also tissue-dependent and substrate-specific, making it challenging to use only one assay to measure all CYP450 isoforms in different cell lines. Moreover, the individual PA congeners are possibly catalyzed by different isoforms. On the other hand, even the same congener in other species also could be catalyzed by different isoforms (Chung et al., 1995; Huan et al., 1998).

The *O*-dealkylations of methoxyresorufin, ethoxyresorufin, benzyloxyresorufin, and pentoxyresorufin to highly fluorescent resorufin were widely used for investigating the cytochrome P450 isoforms (Burke et al., 1994). This work used cultured primary rat hepatocytes and human hepatocellular carcinoma cells as an *in vitro* model to investigate PAs' potentially toxic effects. According to the previous reports, the benzyloxyresorufin *O*-dealkylation activity, i.e., BROD activity, has been considered an indicator mainly for CYP2B and CYP3C (Chen and Eaton, 1991; Meehan et al., 1988; Nerurkar et al., 1993). Based on the antibody inhibition study of Burke et al. (Burke et al., 1994), BROD could be catalyzed by several CYP450 isoforms in liver microsomes of untreated rats and humans. The 7-benzyloxyresorufin-*O*-debenzylase activity was determined more likely as the CYP activity of broad-spectrum than a specific isoform. Therefore, the general CYP450 activity was measured here using a simplified BROD microassay based on the metabolism of 7-benzyloxyresorufin (5 µM) by cell cultures. After incubation, the formed dealkylated resorufin was released into the culture and fluorometrically quantified.

The initial amount of CYP450s varied from each species, eventually individual animals. In my study, a BROD activity in naïve HepG2 cells of 0.09 ± 0.01 pmol resorufin/mg protein per minute was determined. In consideration of the individual diversity, these results related to the data presented in the study of Donato et al. (2015) where after 16-24 hours of adherence and incubation of next 48 hours, BROD activity was expressed as 0.26 ± 0.11 pmol/mg protein per minute.

A mean BROD activity of 0.44 ± 0.18 pmol resorufin/mg protein per minute in human HepG2 (CYP3A4) C9 cell line determined in my work was remarkably lower than the activity of 600 pmol/mg protein per minute demonstrated using testosterone as substrate by Herzog et al. (2015). This considerable difference possibly resulted from

the insufficient sensitivity of benzyloxyresorufin against CYP3A4 compared to testosterone.

Donato et al. (2008) demonstrated that the specific mRNA transcription levels of most CYP450 isoforms determined in HepG2 cells were for 2-3 orders of magnitude lower than in primary cultured human hepatocytes, and except for 7-ethoxyresorufin-*O*-demethylase (EROD), i.e., CYP1A1, a non-hepatic isoform. Basal biotransformation activities of 7-ethoxycoumarin-*O*-deethylase (ECOD), 7-methoxyresorufin-*O*-demethylase (MROD), 7-benzoxyresorufin-*O*-debenzylase (BROD), and 7-penthoxyresorufin-*O*-dependentylase (PROD) in HepG2 cells were less than a tenth of levels in primary hepatocytes.

Nevertheless, my results were comparable to the data in other studies that also confirmed a loss of CYP450 activity. The amount of microsomal CYP450 in freshly isolated hepatocytes about 0.140 ± 0.047 nmol per mg protein (n = 10) reported by Guzelian et al. did not differ significantly from the levels *in vivo*. Cellular concentration was spontaneously reduced after plating and cultivating in L-15 medium containing 100 U/ml penicillin and 1 mM succinate. The most rapid decline of rat hepatocytes after isolation in culture was demonstrated during the initial 24 hours (Guzelian et al., 1977; Maslansky and Williams, 1982), after which the amount of CYP450 enzymes decreased progressively to 10 – 20% of the level in freshly isolated hepatocytes (Bissell et al., 1973; Bissell and Guzelian, 1979; Guzelian et al., 1977). Similar results have also been reported by Evarts et al. (1984). When freshly isolated hepatocytes were cultivated in Waymouth´s MB752/1 medium supplemented with several vitamins, hormones, antibiotics, and δ-aminolevulinic acid, during the first 24 hours, there was a 60 – 70% loss of CYP450s of the isolated cells from untreated rats. If the hepatocytes were obtained from the female rats treated with phenobarbital, the CYP450s decreased rapidly and retained only 40% of the original level after 2 hours. More than 80% vanished in 2 days. The spontaneous loss of CYP activity during the culture was also confirmed by the study of Maslansky and Williams (1982) that the CYP450 activity maintained less than 41% after 24 hours. (n = 3). Accordingly, the decrease in sensitivity of the rat hepatocytes in primary culture towards certain PA congeners with longer pre-incubation is probably because of the loss of CYP activity. The different influences caused by the pre-incubation time varied among the congeners may be due to the different CYP isoforms responsible for the metabolic activation of each congener.

Inhibition or induction of cytochrome P450 enzymes is the most used method to determine whether a chemical evokes its toxic effects through metabolic activation and formation of an active metabolite or to investigate which isoforms of CYP450s play the most critical role in the metabolism of the toxin. The inhibition study in this work was investigated with ketoconazole, a relatively broad-spectrum and non-competitive inhibitor in the human liver microsome (Fayer et al., 2001). At the concentration of

5 µM after incubation for 2 hours, BROD activity was inhibited by about 80% without being cytotoxic.

Since resorufin in contact with cell culture could conjugate with endogenous glucuronic acid and sulfate, which are more low fluorescent, Donato et al. (1993) reported that even only about 50% of the total formed resorufin were not conjugated. The enzyme activity possibly might be critically underestimated. Therefore, this method could be further improved by adding β-glucuronidase and arylsulfatase into the BROD incubation medium to avoid the conjugate binding.

4.2 Glutathione reductase-DTNB recycling assay

Metabolites of numerous toxic chemicals covalently bind to glutathione to form a readily excreted mercapturic acid. This is considered one of the most important detoxification pathways. Once GSH is expended, the reactive metabolites could no longer be eliminated by this pathway, then might bind covalently more preferably to cytosolic or mitochondrial macromolecular components such as DNA and proteins, consequently increasing the cytotoxicity or genotoxicity of the compounds feasibly (Hinson et al., 2010). The role of glutathione in the toxicity of PA congeners is unclear. In this study, the cytotoxicity between hepatocytes with glutathione depletion and untreated hepatocytes were compared to investigate whether glutathione played a critical role in the metabolism or detoxification of PAs.

L-Buthionine sulfoximine (BSO), a specific and irreversible inhibitor of γ-glutamylcysteine synthetase, thereby blocking glutathione synthesis in various experimental systems, was chosen to deplete intracellular glutathione stores in my work (Drew and Miners, 1984; Griffith and Meister, 1979). In primary rat hepatocytes with a 2-hour incubation time, the BSO (40, 100, 200, 500, 1000 µM) -induced reduction on intracellular GSH statuses and at the concentration induced corresponding cytotoxic effects have been investigated. The intracellular reduced GSH declined approx. 50% at concentrations of 500 and 1000 µM compared to the solvent control, while it had no significant toxicity on primary human hepatocytes.

Similar experiments on BSO-induced GSH depletion have also been reported previously. It was found that intracellular GSH content could be decreased by 1 mM BSO to 5.3% after treating the primary rat hepatocytes for 24 h without demonstrating the cytotoxicity on BSO (Shi et al., 2015). In another study using primary human hepatocytes, Jiang et al. (2018) have shown a loss of intracellular GSH after treatment with 1 mM BSO for 24 h. At the same time, BSO itself had no significant toxicity on cells. In some studies with the exact duration of 2 hours for pre-treatment using rat hepatocytes, Tong et al. (2005) found that the intracellular GSH levels were decreased to a maximum of 50% firstly with 8 mM BSO, and to gain an approx. 20% depletion combined the 2 mM BSO with 0.5 mM diethyl maleate. Hammond and Fry (1996) have

revealed which ineffective or a slight depletion induced by BSO at a concentration of 0.5 mM after pre-treatment of two hours, whereas 70% loss of glutathione could be generated if the exposure period extended to 18 hours. On the contrary, 2 mM BSO was also identified to cause a decrease in intracellular GSH concentration to 56% by only 1 h of incubation compared to the untreated cultures. The GSH levels progressively decreased to about 20% after 3 h (Jurima-romet et al., 1996).

Similar to the CYP enzymes, the intracellular level of reduced GSH levels declined spontaneously to approx. 50% of that in freshly isolated hepatocytes with 1 h culture probably due to its regulatory function of thiol/disulfide groups in protein and/or its involvement in the synthesis of essential cytosol proteins, although the GSH content could be recovered between 4 and 24 h in the presence of amino acids in culturing medium. In addition, the attaching of the hepatocytes to collagen in the plate would be attenuated by inhibition of GSH synthesis, which possibly led to a non-cytotoxic loss on the viability (Morrison et al., 1985). Therefore, BSO was perhaps not optimal for the depletion of GSH based on the inconsistent results from various studies.

4.3 Alamar blue (Resazurin) assay

Many previous publications concerning the metabolic activation and the active uptake of PAs suggested that the liver or the hepatocyte is the primary target after PA exposure. To determine the hepatotoxicity, selected PA congeners were tested using Alamar blue assay with primary rat hepatocytes, naïve HepG2 cells and HepG2 C9 (CYP3A4) cells. To better understand the relationship between structure and cytotoxicity, besides the five congeners determined in my work, the same protocol was also applied to five other PA congeners in our project, including echimidine[‡], europine[‡], heliotrine[‡], monocrotaline[‡], and seneciphylline[‡].

All these ten PA congeners belonging to different structural classes generally showed concentration-response characteristics. EC_{50} values calculated by modeling sigmoidal concentration-response curves of all these PA congeners measured in primary rat hepatocytes were summarized in Tab. 8, together with standard deviations. It was observed considerably structure-differentiated cytotoxicity that di-esters were generally more toxic than mono-esters. Except for monocrotaline, all di-esters, including cyclic and open-chained congeners, were with EC_{50} values between 4 to 25 µM when primary rat hepatocytes were pre-incubated for 3 h followed with a treatment of 48 h with these congeners. It is consistent with the findings reported by Moore et al. (1989). Under the same conditions, lasiocarpine presented a concentration- and time-dependent leakage of lactate dehydrogenase, while monocrotaline and heliotrine showed no cytotoxic effect.

In our project, for the exposure duration of 24 h, the EC_{50} value of the most potent congener lasiocarpine was 86 ± 11 µM, also in primary culture of rat hepatocytes,

lasiocarpine was found by Chen et al. (2018) to be even more cytotoxic with an EC_{50} value of 10.9 ± 1.6 µM. Also using MTT assay Field et al. (2015) reported that cell viability dropped below 10% of control at 150 µM after an incubation time of 48 h, it was confirmed here. In my work, lasiocarpine with an EC_{50} value of 4 ± 1 µM was at least about 70-fold more toxic than monocrotaline and europine, which were least potent with EC_{50} values over 300 µM. The high potency of lasiocarpine, eventually distinctively more cytotoxic than other cyclic di-esters, was also reported in other studies (Field et al., 2015; Tamta et al., 2012). Echimidine, an open-chain di-ester with 7*R*-configuration, showed an EC_{50} value of 143 ± 7 µM after 24 h of exposure. This is generally comparable to the results with the MTT and DAPI assays by Waizenegger et al. (2018) in HepaRG cells, where after an incubation time of 24 h with an exposure of 250 µM, echimidine was cytotoxic with a decrease in viability to 68 and 74%. Using primary rat hepatocytes in my work echimidine with the same concentration led to a higher decrease in viability, possibly caused by the disparate sensitivity towards the congeners among different cell lines. Nevertheless, echimidine turned out to be more cytotoxic than its toxicity suggested with an iREP factor only of 0.1.

Next, various concentrations of selected PA congeners were also incubated with the HepG2 (CYP3A4) C9 clone cells. A similar pattern was observed, although this cell line was less sensitive towards PA congeners than rat hepatocytes in primary culture. As presented in Tab. 7, When the HepG2 (CYP3A4) C9 cells were incubated with PA congeners for 48 h, EC_{50} values of all other di-esters were found to be between 10 – 180 µM except for monocrotaline with an EC_{50} value above 300 µM. This PA exhibited much less cytotoxic effect than expected from the structural features as cyclic di-ester. Concomitantly, mono-esters showed relatively low cytotoxicity with EC_{50} levels over 300 µM except for heliotrine. Such similar findings were observed in a study by Field et al. (2015), which investigated the cytotoxicity of selected PA congeners and their *N*-oxides in chicken hepatocellular carcinoma cells using MTT- and LDH-assay. According to PA-induced viability decreases in MTT assay and lactate dehydrogenase release, PA congeners were then identified into three groups. Lasiocarpine, seneciphylline, senecionine, and heliotrine belonged to the group with the highest potency. Among them, lasiocarpine consistently was the most cytotoxic and distinguished from other congeners in this group. The intermediate group included riddelliine and monocrotaline. Lycopsamine and *N*-oxides were the least potent.

The unexpected low potency of monocrotaline was also confirmed by Müller et al. (1992), using V79 cells. No cytotoxic effect was observed despite addition of the S9 mix as an external metabolization system. Even after cocultivation with primary rat hepatocytes cytotoxic effects were only evident at the highest concentration of 1000 µM tested.

Furthermore, the shorter duration of pre-incubation considerably induced the cytotoxicity of most PA congeners, especially after 48 h. For some congeners such as lasiocarpine, senecionine and retrorsine, the effect was dramatic. It was observed that the shorter pre-incubation led to an over 5-fold increase in cytotoxic effects for lasiocarpine and retrorsine with an incubation time of 48 h, eventually induced cytotoxicity over 10-fold for senecionine no matter with incubation of 24 or 48 h (s. Tab. 8). The suppression of cytotoxicity with long pre-incubation might be due to a loss of enzyme activity during the culture for its metabolic activation.

This finding was supported by the results from the BROD assay and confirmed the notion that certain CYP enzymes are critical for PA-induced cytotoxicity. In order to investigate the effects of BROD-inhibition on the cytotoxicity of PAs, CYPs were inhibited by ketoconazole. In humans, ketoconazole at low concentration demonstrated a respective selective inhibitory effect of CYP3A, whereas the inhibition of the other CYP450 activities was significantly less. On the contrary, it acts as a far less specific inhibitor in rats, especially here at a concentration of 5 µM, inhibiting many different isoforms (Baldwin et al., 1995; Eagling et al., 1998; Novotná et al., 2014). After pre-treatment with ketoconazole, most PA congeners measured here led to a slight to about 3-fold reduction in cytotoxicity (s. Tab. 8). The fact is that the toxicity was affected by the pre-incubation duration or pre-treatment with a CYP450 inhibitor could be due to the impact of cytochrome P450 enzymes on their metabolic activation. The different effects on the cytotoxicity among congeners suggested that PAs might be activated by different CYP isoforms.

When combined with an incubation time of 24 h, the effects of shorter pre-incubation on most PA congeners were slightly enhanced or less pronounced. In addition, neither with a shorter pre-incubation time nor pre-treatment of ketoconazole before adding test compounds significantly altered the cytotoxic effects induced by monocrotaline or europine at least up to 300 µM. However, a shorter pre-incubation unexpectedly reduced their cytotoxicity for retrorsine, seneciphylline, and echimidine. It might be that the metabolic activation of these PAs depends on CYP isoforms which could not be revealed by BROD activity or the enzymes not belonging to the CYP family (Huan et al., 1998).

Cytochrome P450 enzymes play an important role was also confirmed by comparing PA-induced cytotoxic effects in non-transfected HepG2 cells and a HepG2 C9 clone, which was over-expressed CYP3A4 gene.

In näive HepG2 cells, neither the di-esters nor the mono-esters exhibited detectable cytotoxic effects up to a concentration of 300 µM. The two mono-esters, indicine and lycopsamine, were also almost non-cytotoxic. Even using HepG2 (CYP3A4) C9 cells expressing the human CYP3A4 gene, lycopsamine induced a minor but significant

decrease in viability after the incubation of 48 h at the highest concentration of 300 µM. Lasiocarpine was still the most potent congener in HepG2 C9 cells. Treatment of 24 h even exhibited a somewhat more cytotoxic effect than that observed in primary rat hepatocytes (s. Tab. 4 and 5). When compared to the EC_{50} values of cytotoxicity from the treatment of 48 h (s. Tab. 7) in rat hepatocytes in primary culture, all ten PA congeners selected in our project exerted generally lower cytotoxicity in HepG2 C9 cells suggesting a less sensitivity towards most PA congeners. Concomitantly, heliotrine was equally cytotoxic in both cell types. This finding supported the BROD assay that cytochrome P450 activity in HepG2 (CYP3A4) cell line was determined about several folds more minor than that in primary rat hepatocytes and a deficient expression and activity in the naïve HepG2 cell. The cytotoxicity of lasiocarpine and heliotrine, which were found more or equally potent in HepG2 (CYP3A4) C9 cells, possibly attributed to their relatively higher specificity towards CYP3A4 isoform. As reported by Ruan et al. (2014b), predominantly CYP3A4 and then following CYP3A5 mediated the formation of pyrrole-protein adducts of lasiocarpine in the individual human recombinant CYP supersomes. In comparison, CYP2A6 exhibited the greatest activity in the metabolic activation of monocrotaline, while CYP2A6, CYP3A4/5 were all mainly involved in mediating the metabolic activation of retrorsine and senecionine. In previous studies, CYP3A and CYP2B subfamilies were proved as important enzymes mediated metabolism to exert toxicity of many PA congeners with different *in vivo* or *in vitro* measuring systems (Fu et al., 2004; Ruan et al., 2014b), such as lasiocarpine in microsomes from various species (Fashe et al., 2015), retrorsine in cultured MDCK (Madin-Darby canine kidney)-CYP3A4 cells (Tu et al., 2014), and senecionine in human liver microsomes (Miranda et al., 1991).

On the other hand, no cytotoxic effect confirmed in HepG2 cells might be also due to the poor expression of the transporters. It is known that some transporters play a critical role in the toxicokinetics of numerous chemicals in the main organs such as the liver, kidney, intestine, and other organs (Hilgendorf et al., 2007; Shitara et al., 2005; Sun et al., 2001; Treiber et al., 2004; van Montfoort et al., 2003). The solute carrier (SLC) family, including organic anion transporters (OATs), organic anion-transporting polypeptides (OATPs), organic cation transporters (OCTs), and ATP-binding cassette (ABC) family, comprising such as multidrug resistance (MDR) proteins, multidrug resistance-associated proteins (MRP), and many others, have been identified. Hilgendorf et al. (2007) suggested that OCT1, expressed most highly in the liver but at deficient levels in the other organs, seemed to be a potentially important transporter involved in the uptake or excretion of chemicals that undergo hepatic metabolism in the liver.

The cytotoxicity of PAs was related to CYP-mediated bioactivation, the efficiency of *N*-oxidation or carboxylesterase-mediated hydrolysis, as well as the detoxification,

such as the amount of cellular GSH, which plays an essential role in the detoxification of a great number of chemicals. Wang et al. (2000) revealed that intraportal infusion of GSH could protect against the monocrotaline-induced hepatotoxicity using sinusoidal endothelial cells. However, the mechanism of the PA-induced hepatotoxic effect is not completely clear. To investigate whether glutathione plays a crucial role in detoxification, GSH was first depleted to approx. 50% via pretreatment with 1 mM BSO leading to no significant cytotoxic effect by 2 hours, at which time PA congeners with different concentrations were added. However, compared to the untreated cells, only the cytotoxicity of indicine was slightly enhanced at the concentrations of 75 and 300 µM after 24 h incubation. For other congeners, there was almost no effect with GSH depletion (s. Tab. 8). It suggested GSH might not play a critical role in PA-induced cytotoxicity. This finding was supported by *in vitro* semiquantitative analysis of main metabolites of lasiocarpine in liver microsomes from different species. The formation of the demethylation product (s. Fig. 44.a) as the prominent and detoxification metabolite was not affected by reduced glutathione. The highest rate of reactive metabolite (3*H*-pyrrolizin-7-yl) methanol (s. Fig. 44.b) and the GSH conjugate was also observed in the most susceptible human HL22 microsomes (Fashe et al., 2015).

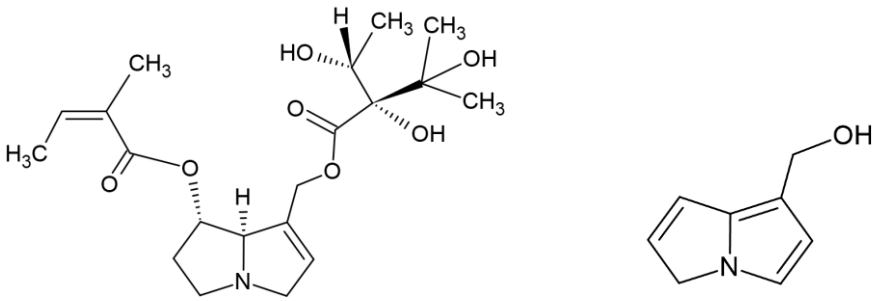

(a) (b)

Figure 44: Structure of two metabolites from lasiocarpine. (a) the demethylation product; (b) 3*H*-pyrrolizin-7-yl) methanol

Table 7: Comparision of the PA-induced cytotoxicity (EC_{50}) in primary rat hepatocytes and HepG2 (CYP3A4) C9 cells

PA (structural features)	**EC_{50}: µM, 48 h 3 h after seeding Primary rat hepatocytes**	**EC_{50}: µM, 48 h HepG2 (CYP3A4) C9**
lasiocarpine (open, di, 7*S*)	4 ± 1	10 ± 1[f]
[‡]monocrotaline (cyclic, di, 7*R*)	>300	>300
retrorsine (cyclic, di, 7*R*)	19 ± 2	73 ± 12[f]
senecionine (cyclic, di, 7*R*)	8 ± 1	67 ± 8[f]
[‡]seneciphylline (cyclic, di, 7*R*)	19 ± 6	73 ± 7[f]
[‡]echimidine (open, di, 7*R*)	25 ± 1	179 ± 1[f]
[‡]europine (mono, 7*S*)	>300	>300
[‡]heliotrine (mono, 7*S*)	193 ± 17	176 ± 31
indicine (mono, 7*R*)	210 ± 16	>300
lycopsamine (mono, 7*R*)	114 ± 18	>300

[‡] congeners tested by Mr. Rutz;

[f] highly significantly different ($p \leq 0.01$) from the incubation with PA at 3 h after seeding.

Table 8: Summary of all ten selected PA congeners induced cytotoxicity (EC_{50}) in primary rat hepatocytes

PA (structural features)	EC_{50}: µM, 24 h/48 h 24 h after seeding	EC_{50}: µM, 24 h/48 h 3 h after seeding	EC_{50}: µM, 24 h/48 h pre-incubation with ketoconazole (5 µM)	EC_{50}: µM, 24 h/48 h pre-incubation with BSO (1 mM)	iREP[a]
lasiocarpine (open, di, 7*S*)	91 ± 9 / 27 ± 2	86 ± 11 / 4 ± 1[c]	120 ± 10[d] / 11 ± 1[e]	55 ± 14[d] / 4 ± 1	1.0
[‡]monocrotaline (cyclic, di, 7*R*)	>300 / >300	>300 / >300	>300 / >300	n.t.	1.0
retrorsine (cyclic, di, 7*R*)	129 ± 9 / 90 ± 8	168 ± 30 / 19 ± 2[c]	>300 / 67 ± 6[e]	n.t.	1.0
senecionine (cyclic, di, 7*R*)	196 ± 31 / 95 ± 8	19 ± 3[c] / 8 ± 1[c]	65 ± 4[e] / 12 ± 1[e]	19 ± 3 / 8 ± 2	1.0
[‡]seneciphylline (cyclic, di, 7*R*)	109 ± 10 / 31 ± 4	178 ± 16[c] / 19 ± 6[b]	>300 / 54 ± 11[e]	n.t.	1.0
[‡]echimidine (open, di, 7*R*)	120 ± 18 / 48 ± 3	143 ± 7 / 25 ± 1[c]	>300 / 51 ± 10[d]	n.t.	0.1
[‡]europine (mono, 7*S*)	>300 / >300	>300 / >300	>300 / >300	n.t.	0.3
[‡]heliotrine (mono, 7*S*)	>300 / 294 ± 27	>300 / 193 ± 17[c]	>300 / >300	n.t.	0.3
indicine (mono, 7*R*)	>300 / >300	>300 / 210 ± 16	>300 / 248 ± 2[d]	>300 / 191 ± 15	0.01
lycopsamine (mono, 7*R*)	>300 / >300	>300 / 114 ± 18	>300 / 166 ± 26[d]	>300 / 77 ± 11[d]	0.01

[‡] congeners tested by Mr. Rutz;

[a] Merz and Schrenk (2016);

[b] significantly different ($p \leq 0.05$) from the incubation with PA at 24 h after seeding;

[c] highly significantly different ($p \leq 0.01$) from the incubation with PA at 24 h after seeding,.

[d] significantly different ($p \leq 0.05$) from the incubation with PA at 3 h after seeding;

[e] highly significantly different ($p \leq 0.01$) from the incubation with PA at 3 h after seeding, n.t.: not tested.

4.4 Ames fluctuation assay

Ames fluctuation assay used histidine requiring strains of *Salmonella typhimurium* to provide information on the types of mutations induced by genotoxic agents. The principle is that the revertant bacteria restored the ability to synthesize the essential amino acid histidine and were capable of growing in the culture without histidine required by the parent test strains.

Clark reported in 1976 that PAs did not signal mutagenicity in the classic Ames test with *S. typhimurium* even if in the presence of a liver microsomal preparation and declared the bacterial systems were failing to provide optimal conditions for determining these mutagens (Clark, 1976). In different *Salmonella* strains, a series of PA congeners, such as heliotrine, lasiocarpine, monocrotaline, and seneciphylline were afterward found to be mutagenic (s. Tab. 9). The mutagenicity of some PAs to *Drosophila*, *Aspergillus*, and E.coli has also been reported (Acosta et al., 1979; Alderson and Clark, 1966; Brink, 1969, 1966; Clark, 1959; Green and Muriel, 1975).

However, as one of the most frequently investigated congeners, retrorsine was not mutagenic with strain TA100 via standard Ames test despite metabolic activation (Wehner et al., 1979). On the other hand, it was shown weakly mutagenic at the extremely high concentration of 2000 µg/plate if with a pre-incubation (Rubiolo et al., 1992). The mutagenicity of retrorsine was also demonstrated with strains TA1535 and TA1537 at optimal concentrations of only 0.25 and 25 µg/plate, respectively, with metabolic activation (Wehner et al., 1979). However, in Rubiolo´s research also using TA1535, it was shown no mutagenic activity with doses ranging from 0.25 to 2000 µg/plate in the presence of S9 mix using a modified Ames test involving pre-incubation (Rubiolo et al., 1992). Similar inconsistencies also occurred with monocrotaline and seneciphylline, using the modified Ames test. Yamanaka et al. in 1979 reported that up to a concentration of 2000 µg/plate, no mutagenic effects was observed with the *Salmonella* strains of TA92, TA98, TA100, TA1535, TA1537, and hisG46 either with or without S9 mix, whereas, slightly to weakly mutagenic activity of monocrotaline and seneciphylline was exhibited at a dose of 2000 µg/plate in Rubiolo´s study (Rubiolo et al., 1992; Yamanaka et al., 1979). The mutagenicity of lasiocarpine, one of the most toxic PAs, could be demonstrated to strain TA100 with doses of 50 – 500 µg/plate in the presence of hamster liver S9, however, with rat liver S9, at a dose of 500 µg/plate, a bactericidal action was unfolded. Yamanaka et al. (1979) also reported the mutagenicity of heliotrine, with likewise the strain TA100 after metabolic activation and pre-incubation.

Table 9: Summary of the previous results from other Ames tests

PA congener	Test strain/ S9 mix / pre-incubation	Results	Concentration
Heliotrine	TA92, TA98, TA1535, TA1537, hisG46 + S9 mix + pre-incubation	negative	200 – 2000 µg/plate (Yamanaka et al., 1979)
	TA100 + S9 mix + pre-incubation	positive	200 – 2000 µg/plate (Yamanaka et al., 1979)
Lasiocarpine	TA92, TA98, TA1535, TA1537, hisG46 + S9 mix + pre-incubation	negative	200 – 2000 µg/plate (Yamanaka et al., 1979)
	TA100 + S9 mix + pre-incubation	positive	50 – 500 µg/plate (Yamanaka et al., 1979)
Lycopsamine	TA92, TA98, TA100 TA1535, TA1537, hisG46 + S9 mix + pre-incubation	negative	200 – 2000 µg/plate (Yamanaka et al., 1979)
Monocrotaline	TA92, TA98, TA100 TA1535, TA1537, hisG46 + S9 mix + pre-incubation	negative	200 – 2000 µg/plate (Yamanaka et al., 1979)
	TA100 + S9 mix + pre-incubation	slightly positive	250 – 2000 µg/plate (Rubiolo et al., 1992)
Retrorsine	TA97a, TA98, TA1535, TA1538 + S9 mix +/- pre-incubation	negative /negative	0.25 – 2000 µg/plate (Rubiolo et al., 1992)
	TA98 +/- S9 mix	negative /negative	0.25 – 500 µg/plate (Wehner et al., 1979)
	TA100 +/- S9 mix	negative /negative	0.25 – 500 µg/plate (Wehner et al., 1979)

	TA100 + S9 mix +/- pre-incubation	weakly positive /negative	2000 µg/plate /0.25 – 2000 µg/plate (Rubiolo et al., 1992)
	TA1535, TA1537 +/- S9 mix	positive /negative	0.25, 25 µg/plate /0.25 – 500 µg/plate (Wehner et al., 1979)
Senecionine	TA92, TA98, TA100, TA1535, TA1537, hisG46 + S9 mix + pre-incubation	negative	200 – 2000 µg/plate (Yamanaka et al., 1979)
	TA100 + S9 mix + pre-incubation	negative	0.25 – 2000 µg/plate (Rubiolo et al., 1992)
Seneciphylline	TA92, TA98, TA100, TA1535, TA1537, hisG46 + S9 mix + pre-incubation	negative	200 – 2000 µg/plate (Yamanaka et al., 1979)
	TA100 + S9 mix + pre-incubation	weakly positive	2000 µg/plate (Rubiolo et al., 1992)

Counting the other five congeners determined by my colleague Mr. Rutz, in total, ten PAs belonging to different structural classes have been investigated with Ames fluctuation assay, an initial scan for mutagenic potency of selected PA congeners. In order to provide more information on the types of mutations, more different strains have been considered to be used, but of strain TA97a for detection of frameshift mutation and TA102 relating a mutation at the A/T site in the hisG428 gene, there was a critical loss of sensitivity to the standard positive controls. Therefore, PA congeners from different structural classes have only been measured with strain TA98 and TA100, respectively sensitive to a frameshift mutation and base-pair substitution. *S. typhimurium* differed from mammalian cells in factors such as uptake, transport, or metabolism. The test needed thus generally an exogenous metabolic activation, here a supplemented post-mitochondrial fraction, i.e., S9 mix, prepared from the liver of rodents treated with Aroclor 1254 was used. Up to a concentration of 300 µM, causing a less than 50% loss of bacterial viability, no mutagenic activity of any PA congener could be demonstrated even after adding the S9 mix as exogenous metabolic activation. It does not mean the selected PA congeners are not mutagenic. In addition, the viability

of the bacteria could only be measured in the absence of the S9 mix since resazurin would be immediately reduced to resorufin when the S9 mix is containing an NADPH-regenerating system. The results obtained in this work indicated the Ames *S. typhimurium* with rat liver S9-mix metabolic activation system appears not to be sensitive enough to PAs.

Compared to the previous studies, extremely high concentrations were not used in this work. The back-calculated highest concentration of lasiocarpine was determined to be 123.5 µg/ml. It might well be that higher doses could provide better conditions to induce mutagenic action. Nevertheless, there is no doubt that some toxic congeners may exhibit their bactericidal or cytotoxic effects, leading to more false-negative results. Furthermore, based on the relatively limited studies for investigating the mutagenicity of PAs using the Ames test or modified Ames test, it could not be assured which PA congeners were mutagenic. Under similar conditions in other studies, they also exhibited no mutagenic effects, or conversely.

It is well known that the organic cation transporter OCT1 (SLC22A1) probably plays a critical role in mediating the uptake of cationic drugs and xenobiotics into hepatocytes. Tu et al. successively confirmed that OCT1s also participate in the hepatic influx of monocrotaline and retrorsine related to PA-induced hepatotoxicity. Thus lacking a mechanism for taking up PAs in bacterial cells might be another cause for the entirely negative results in this work (Tu et al., 2014; Tu et al., 2013).

In brief, active metabolites of PAs congeners need to enter the bacterial cells then be capable of exerting their mutagenicities. Due to the limited sensitivity, insufficient repetitiveness, and possible absence of active influx mechanism in bacteria *Salmonella typhimurium*, either standard Ames test or Ames fluctuation assay using this bacteria is inappropriate for investigating the mutagenicity of PA congeners. Therefore, this assay was not further worked with, and even it has been successfully used to determine a massive number of chemical compounds.

4.5 Micronucleus assay

Micronuclei counts were determined after treatment over 72 h with various concentrations of selected PA congeners. For some PAs, the maximal determined concentration was up to 300 µM. In comparison, a lower concentration range of up to 25 µM was applied for others such as lasiocarpine, senecionine, and retrorsine which were more toxic observed in the cytotoxicity testing. To obtain more information on the concentration-response relationship at low-effect concentrations, another range of lower concentrations (0.01, 0.025, 0.05, 0.1, 0.25, and 0.5 µM) was determined for these more potent congeners. A more extended treatment of 72 h was required to form micronuclei after 1.5 – 2 cell cycles as recommended in OECD (2016).

There was evidence that the specific enzyme systems, especially the cytochrome P450 enzymes, are essential to generate toxic metabolites for PAs. The data of Müller et al. (1992) indicated that genotoxicity was shown at lower concentrations when a highly metabolically competent *in vitro* test system was employed. Compared to naïve HepG2 cells deficient in CYP enzymes, HepG2 (CYP3A4) cells were transformed with virus genes or oncogenes to express CYP450 enzymes. When considering the metabolic competency, HepG2 (CYP3A4) cells or the pre-differentiated HepaRG cells, initially expressed CYP450 enzymes, would be more suitable for investigating genotoxicity *in vitro* for pyrrolizidine alkaloids, even though the enzyme activity was not at similar levels to primary human hepatocytes.

The observed relative genotoxic potencies of the 10 PA congeners in our project (s. Tab: 10) span a factor of 5950 (BMDL) and 665 (BMDU). The number of micronuclei was concentration-dependent. The potency varied from individual to individual PA congener, but all selected congeners significantly increased micronuclei counts. However, probably due to the severe cytotoxic effects, the formed micronuclei became less at the relatively high concentration range of some potent PA congeners. Similar situations with some chemicals at higher concentrations exhibited notably less pronounced increases in micronuclei have also been reported in other studies using micronucleus assay (Dorn et al., 2008; Schuler et al., 2010). This observation was also consistent and supported the OECD guideline's recommendation that micronuclei counts need to process at the concentration range, leading to a loss of less than 50% viability, otherwise not considered for further modeling.

It was sufficient to induce a doubling of micronuclei counts over the background in the concentration range tested. When the benchmark doses (BMDs) and their lower and upper 10% confidence limits were used to represent the relative genotoxic potencies and rank the PA congeners, the differences on the Lower and Upper Bounds of BMDs among the congeners spanned over more than two orders of magnitude. Lasiocarpine and senecionine were the most potent and distinct from other PAs tested, followed by seneciphylline and retrorsine. Similar to the findings from cytotoxic assays, in the group of cyclic di-ester with 7*R*-configuration, monocrotaline was also an exception that exhibited remarkably lower genotoxic potency. Except for monocrotaline, all the other most potent genotoxicants attributed with an iREP factor of 1.0 (Merz and Schrenk, 2016) were within the range of 0.01 – 1.04 µM (BMDL) and 0.23 – 2.01 µM (BMDU). Although europine and heliotrine both are mono-esters with 7*S*-configuration, their genotoxic potencies differed notably from each other, heliotrine being 4- to 8-fold more potent than europine, while the potency of echimidine, a 7*R* di-ester, was between them. The mono-esters with 7*R*-configuration were the least potent with a BMDL range of 19.1 - 59.5 µM and a BMDU range of 62.3 – 73.3 µM.

The genotoxicity of PA congeners was demonstrated in many different *in vitro* assays exhibiting generally similar patterns. In the study of Allemang et al. (2018), lasiocarpine, retrorsine, monocrotaline, echimidine, europine, heliotrine, indicine, and lycopsamine have also been investigated. The pre-differentiated HepaRG human liver cells were treated over 24 h with increasing concentrations then the micronucleus induction was analyzed using flow cytometric micronucleus assessment. The following rank order of genotoxic potency was found: lasiocarpine > echimidine ≥ retrorsine ≥ heliotrine > europine > indicine > lycopsamine ≥ monocrotaline. To induce a doubling increase in micronucleus frequencies was observed for lasiocarpine at 0.98 µM, i.e., BMD from Hill model, retrorsine, echimidine, and heliotrine belonging to the next potent group, required concentration about 10-folds higher than lasiocarpine. It was found that echimidine was more genotoxic in HepaRG cells than expected, and heliotrine was 3-fold more potent than europine, even though they own similar structural features. The least potent group included the mono-esters, indicine and lycopsamine, and the di-ester, monocrotaline, which was predicted to be one of the most potent congeners. The findings were in excellent agreement with my work. Only the BMDL and BMDU levels were somewhat lower with HepG2 C9 cells than with HepaRG cells, possibly due to the long incubation time or higher metabolic competency in HepG2 C9 cells.

The basal cytochrome P450 mRNA levels in HepaRG cells were comparable to primary human hepatocytes (Westerink and Schoonen, 2007). Indeed, the gene expression levels could not directly well correlate to the enzyme activity. The work of Yokoyama et al. (2018) suggested that the CYP3A4 activity in the differentiated HepaRG cells was almost 200-fold higher than that in naïve HepG2 cells. Gerets et al. (2012) found that the sensitivity for detecting the reference hepatotoxic compounds in HepaRG cells was much lower than primary human hepatocytes, but based on current studies, HepaRG cells still seem to be a suitable model to investigate PAs metabolism and toxic behavior than many other cell lines as an alternative to primary hepatocytes.

Also using HepaRG cells, Louisse et al. (2019) determined the genotoxic potencies of 37 different PAs using γH2AX histone phosphorylation as endpoint measured by In Cell Western (ICW) assay. The 10 PA congeners selected for our project were also tested in this study. Interestingly, based on the BMDL and BMDU values calculated from the ICW assay, lasiocarpine exhibited almost the same genotoxic potency as retrorsine, senecionine, and seneciphylline. They owned BMDs between 4.6 – 6.4 µM, BMDLs between 3.4 – 4.4 µM, and BMDUs between 5.6 – 8.5 µM. This finding was different from what was found in our project or the results published by Allemang et al. that the lasiocarpine-induced genotoxic effect was distinct from other PAs congeners. Europine and heliotrine showed nearly equal potencies with the same BMD value of 62 µM, respectively, with BMDL values of 49 and 45 µM, BMDU values of 75 and

80 µM. As expected, lycopsamine and indicine were found to be the least potent. Generally, the genotoxic manners showed in this study were more close to the proposed iREP concept (Merz and Schrenk, 2016). On the other hand, similar in this study, echimidine was found to be more potent than supposed, and monocrotaline was due to a relatively low potency placed into the same category with lycopsamine and indicine.

Nearly the same potency ranking of lasiocarpine, echimidine, heliotrine, europine, monocrotaline, lycopsamine, and indicine represented as DNA adducts were also reported by Lester et al. (2019). Still, the linearity of the concentration-response was for several PA congeners at higher concentrations than that was found in the micronucleus assay of our project. It might be due to an essential cellular defense mechanism like DNA repair at low concentrations. DNA adducts of lasiocarpine, retrorsine, senecionine, seneciphylline, heliotrine, and lycopsamine formed *in vitro* or *in vivo* have also been identified (Eastman et al., 1982; Wang et al., 2005c; Xia et al., 2013, 2013; Xia et al., 2008; Xia et al., 2006). At the same time, studies of unscheduled DNA synthesis (UDS) induced by lasiocarpine, senecionine, seneciphylline, and monocrotaline in hepatocytes from different species were also reported (Mori et al., 1985; Williams et al., 1980).

Monocrotaline also exhibited markedly unexpected low potency in other studies (Lester et al., 2019). Concomitantly, it was evident by Müller et al. (1992) that monocrotaline yields a much higher chromosomal aberration rate if using primary rat hepatocytes as an external metabolizing system at a much lower concentration of 31.6 µM. This finding was supported by another *in vitro* rat hepatocyte micronucleus assay, whereby monocrotaline enhanced micronucleus formation with active concentrations of 3 – 30 µM (Müller-Tegethoff et al., 1997). Heliotrine showed similar circumstances in V79 cells inducing no sister chromatid exchange (SCE) even in the presence of the S9 mix. However, when the cells were co-cultivated with chick embryo hepatocytes, heliotrine presented a positive effect (Bruggeman and van der Hoeven, 1985). These results revealed the limitations of *in vitro* measuring systems to determine the toxicity of individual PA congeners, which are probably mediated by different enzyme systems, and therefore not substantially represent the actual metabolism in the organism.

The toxic potencies of some PA congeners *in vitro* were not consistent with those exhibited in *in vivo* assays. For instance, monocrotaline led to a significant increase in micronuclei in the bone marrow and fetal liver of mice (Sanderson and Clark, 1993). Micronucleus inducibility of monocrotaline in rat liver has also been revealed in a repeat-dose assay (once daily for 14 or 28 days) at a dose range between 0.15 and 15 mg/kg bw by Takashima et al. (Takashima et al., 2015). In a study with mice, riddelliine could not induce micronuclei (Mirsalis et al., 1993). In the work of Xia et al. (2013), the genotoxic potencies associated with formation of nucleotide-adducts after orally gavaged female rats were found following the potency rank order: lasiocarpine

(25.2) > riddelliine (13.2) ≥ monocrotaline (12.6) > heliotrine (4.1) > lycopsamine (0.3) adducts/10^8 nucleotides (dA + dG). Obviously, monocrotaline exhibited generally higher potency *in vivo* than that in *in vitro* assays. The much lower genotoxicity demonstrated *in vitro* assays of monocrotaline might be due to its unique properties in the transport, eventually the uptake (Chen et al., 2019a; Tu et al., 2013).

Although belonging to cyclic di-esters, the most potent toxic group, monocrotaline with an EC_{50} value above 300 µM, was much less cytotoxic than other congeners bearing similar structural features, even less cytotoxic than some mono-esters. This finding was consistent with the results obtained by Allemang et al. (2018), where monocrotaline showed no cytotoxic effect up to 1000 µM in HepaRG cells. A similar outcome was found by Yang et al. (2017) that monocrotaline was less cytotoxic than retrorsine in rat liver microsomes. Using human recombinant CYP supersomes, Ruan et al. (2014b) confirmed that CYP2A6 and followed by CYP2E1 exhibited the greatest activity in mediating the formation of pyrrole-protein adducts, whereas for retrorsine, not only CYP2A6 but also CYP3A4/5 showed similar high activity. Allemang et al. (2018) also discussed that the low levels of CYP2A6 and CYP2E1 in HepaRG cells were a possible explanation of the lower cytotoxicity of monocrotaline. In addition, it was found that in comparison to senecionine, monocrotaline could be much more effectively hydrolyzed by carboxylesterase using Guinea pigs (Dueker et al., 1992). Echimidine, another exception, which turned out to be more potent than expected from the previously assigned REP factor of 0.1, also showed a similar picture in HepaRG cells (Allemang et al., 2018; Waizenegger et al., 2018). Allemang et al. discussed that the involvement of ABCB1-driven efflux of echimidine from the gastrointestinal epithelium into the gastrointestinal lumen for noncyclic PA congeners as a possible reason would lead to the decreased bioavailability and the deviation of the intrinsic toxic potency.

Generally, all *in vitro* models exhibit advantages and disadvantages. A “perfect” cell model is not yet available. Primary hepatocytes express a high level of metabolizing enzymes but are also limited by their short life span, complex availability, and high variability. In addition, the activity of human CYP2A, CYP2B, and CYP3A isoforms was almost not detectable in rat liver microsomes (Turpeinen et al., 2007) and not fully quantified in primary rat hepatocytes, making it difficult to compare to those in human hepatocytes directly. From this point, rat cells might not be the most appropriate model to imitate human CYP patterns. On the other hand, due to the discrepancies in essential CYPs of individual PA biotransformation, rats that display the most divergent CYP isoforms were probably more suitable for determining the CYP-related metabolism of different PA congeners. Permanent cell lines show easier handling, lower costs, and higher reproducibility but are probably deficient with essential metabolizing enzymes. There is no doubt that the permanent cell lines can never act as primary hepatocytes, especially human hepatocytes, concerning realistic metabolism.

Except for metabolism factors, several critical kinetic factors such as uptake, transport, and deposition should also be taken into account. For instance, membrane transporter OCT1 playing a crucial role in the uptake of retrorsine and monocrotaline was confirmed (Tu et al., 2014; Tu et al., 2013). *In vitro* transport study using Caco-2 and MDCKII/ABCB1 cells, Hessel et al. (2014) demonstrated that the gastrointestinal translocation rate of heliotrine and echimidine was substantially lower than the passage rate of senecionine and senkirkine due to the active P-glycoprotein (ABCB1)-mediated excretion from the intestinal epithelium back into the gut lumen.

Anyhow, the *in vitro* results cannot directly represent the PA-induced response in humans. Physiologically based kinetic (PBK) modeling is an important approach to convert the facilitated reverse dosimetry *in vitro* concentration-response data to *in vivo* concentration-response curves while at the same time taking toxicokinetics into account (Chen et al., 2019b; Chen et al., 2018; Ning et al., 2019).

Table 10: Summary on cytotoxicity (EC_{50}) and genotoxicity (BMDs) of all ten PA congeners in HepG2 (CYP3A4) C9 cells

PA (structural features)	Cytotoxicity EC_{50}: µM, 24 h/48 h HepG2 (CYP3A4) C9	Doubling of Micronuclei			iREP[a]
		BMD: µM	BMD Lower Bound: µM	BMD Upper Bound: µM	
lasiocarpine (open, di, 7*S*)	50 ± 4 / 10 ± 1	0.05	0.01	0.23	1.0
‡monocrotaline (cyclic, di, 7*R*)	>300 / >300	79.9	23.7	153	1.0
retrorsine (cyclic, di, 7*R*)	>300 / 73 ± 12	1.52	0.97	1.98	1.0
senecionine (cyclic, di, 7*R*)	>300 / 67 ± 8	0.13	0.06	0.26	1.0
‡seneciphylline (cyclic, di, 7*R*)	>300 / 73 ± 7	0.96	0.66	1.34	1.0
‡echimidine (open, di, 7*R*)	>300 / 179 ± 17	12.3	7.85	17.3	0.1
‡europine (mono, 7*S*)	>300 / >300	38.0	34.1	45.5	0.3
‡heliotrine (mono, 7*S*)	>300 / 176 ± 31	6.53	4.42	10.4	0.3
indicine (mono, 7*R*)	>300 / >300	37.1	19.1	62.3	0.01
lycopsamine (mono, 7*R*)	>300 / >300	65.7	59.5	73.3	0.01

‡ congeners tested by Mr. Rutz; [a] Merz and Schrenk (2016); BMD (µM) values from Expon. modeling.

4.6 Relative potency factors

The risk assessment of PAs still uses the most potent congener lasiocarpine or riddelliine, and all PAs are supposed to be equally potent. Adequate information indicates that the toxic potencies of individual PA congeners could be extraordinarily different. However, a great number of PAs, including their corresponding *N*-oxides occurring in nature, make it impossible to generate massive data on all of them. Therefore, the concept of relative potency (REP) factors has been proposed (Merz and Schrenk, 2016). Based on the available *in vivo* and *in vitro* data from literature of congener-specific acute toxicity, genotoxicity, and cytotoxicity, the interim relative potency (iREP) factors were suggested to classify the PAs into four groups hints for the different structural features (s. Tab.11). An iREP factor of 1.0 describing the toxicity of 100% was assigned to the most toxic congeners with cyclic di-esters with 7*R* configuration and open-chain di-ester with 7*S*configuration, including lasiocarpine, monocrotaline, retrorsine, senecionine, and seneciphylline in our project. For mono-esters with 7*S* configuration, europine and heliotrine were assigned a factor of 0.3, followed by echimidine, the only open-chain di-ester congener with 7*S* configuration, suggesting a factor of 0.1. As the least potent group, mono-esters with 7*R* configuration, indicine, and lycopsamine implied an iREP factor of 0.01.

The concept of relative potency factors of PAs was once discussed in an earlier year. Frei et al. (1992) investigated the genotoxic potency of PA congeners using the *in vivo* wing spot test in *Drosophila melanogaster* following oral application. The senkirkine-induced genotoxic effect was automatically set as 100%, then the relative potencies in percent were monocrotaline 90.0, seneciphylline 54.5, senecionine 39.1, heliotrine 13.4, retrorsine 8.3, indicine 0.27, and lycopsamine 0.19 (Frei et al., 1992).

In our project, lasiocarpine exhibited extremely high potency in micronucleus assay and distinctly from other PAs tested. When suggested the relative potency, i.e., BMD value determined upon PROAST modeling, of lasiocarpine as 1.0, almost half of PA congeners tested here would obtain an iREP ≤ 0.01. Therefore, riddelliine, a congener considered one of the most potent PA congeners, was then investigated in our project. It had a more appropriate BMD value of 1.76 µM upon exponential modeling (BMDL = 1.29 µM, BMDU = 2.29 µM) to access the relative potencies of other PAs. Additionally, BMD values from the exponential model were similar to the values obtained using the Hill model. When REPs (s.Tab.11) were determined by calculating the ratio of the BMD value of PA riddelliine and the BMD value of individual PA congeners, the most potent congeners were lasiocarpine and senecionine with REPs > 10.0. The second group consisted of PAs for which the REP was between 1.0 and 10.0, including seneciphylline and retrorsine. Heliotrine and echimidine belonged to the third group (REPs between 0.1 and 1.0). The rest of the PA congeners, europine, indicine, lycopsamine, and monocrotaline with REPs ≤ 0.1, were divided into the fourth category

of least potent. Similar to the findings in Alamar blue assay, monocrotaline as the exception exhibited remarkably lower genotoxic potency.

Studies to estimate the structure-related relative potencies of individual PA congeners have also been published by Allemang et al. (2018), which were developed to determine formed micronuclei in HepaRG cells via flow cytometry. Lester et al. (2019) also reported the structure dependence using DNA adducts in rat sandwich culture hepatocytes as an endpoint (s. Tab.11). Our results compare favorably with the data from all the *in vitro* studies mentioned above, whose studies indicated that the open-chain 7*S*-configurated di-ester lasiocarpine and 7*R* cyclic di-esters were very potent and generally more potent than mono-esters. The previously assigned interim relative potency factors roughly reflect the relative toxic potencies except for monocrotaline and echimidine.

The deviated findings of monocrotaline between *in vitro* and *in vivo* assays and the unexpected high potency of echimidine hint that particular metabolic activation or toxicokinetics of individual PA congeners should be considered when the relative toxic potencies are defined. The factor that most PA congeners were activated predominantly by CYP3A4, while the metabolic activation of monocrotaline was associated with CYP2A6 rather than CYP3A4 (Ruan et al., 2014a). In the liver, the expression of the CYP3A subfamily was well known to be the most abundant (Lamba et al., 2002). Uptaking of monocrotaline and retrorsine into cells required the organic cation transporter 1 (OCT1) (Tu et al., 2014; Tu et al., 2013). P-glycoprotein (ABCB1) was related to the transport of echimidine and heliotrine through the gastrointestinal barrier, but senecionine and senkirkine seemed to be no substrates of ABCB1 (Hessel et al., 2014).

Data from recent studies indicate that not all PA congeners with cyclic di-ester structures should be directly assigned an iREP factor of 1.0. Besides, the configuration at position 7 was considered probably to affect the pre-hepatic absorbance. However, it did not seem to have a strong influence on the relative toxicity. For the mono-esters, no consistent toxic potency could be well summarized. The provisional values of relative toxic potency factors suggested a classification based on structural features. Still, it could not perfectly represent the true toxic potency or explain the departure of intrinsic toxic potency differences in *in vitro* studies from the previously proposed REP factors. A better understanding of toxicokinetics is needed to predict *in vivo* toxicity via the PBK modeling based on *in vitro* data, thereby refining the concept of relative toxic potency.

Table 11: Comparison of relative potency factors estimated from different assays

PA (structural features)	**Micronucleus assay** ($HepG_2$ C9, *in vitro*) Riddelliine[a] = 1.0	**Wing spot test** (Drosophila, *in vivo*) Frei et al., 1992 Senkrikine = 1.0	**DNA adducts** (SCH, *in vitro*) Lester et al., 2019 Lasiocarpine = 1.0	**γH2AX assay** (HepaRG, *in vitro*) Louisse et al., 2019 Riddelliine = 1.0	**iREP** (*in vivo + in vitro*) Merz and Schrenk, 2016	**REP** (*in vivo*) Chen et al., 2017
lasiocarpine (open, di, 7*S*)	35.2	--	1.0	1.08	1.0	1.0
ǂmonocrotaline (cyclic, di, 7*R*)	0.02	0.90	0.09	0.06	1.0	0.39
retrorsine (cyclic, di, 7*R*)	1.15	0.08	--	0.90	1.0	--
senecionine (cyclic, di, 7*R*)	13.5	0.39	--	1.24	1.0	--
ǂseneciphylline (cyclic, di, 7*R*)	1.83	0.55	--	1.20	1.0	--
ǂechimidine (open, di, 7*R*)	0.14	--	0.7	0.61	0.1	--
ǂeuropine (mono, 7*S*)	0.05	--	0.1	0.09	0.3	--
ǂheliotrine (mono, 7*S*)	0.27	0.13	0.3	0.09	0.3	--
indicine (mono, 7*R*)	0.05	≤ 0.01	0.04	≤ 0.01	0.01	--
lycopsamine (mono, 7*R*)	0.03	≤ 0.01	0.08	0.02	0.01	--

ǂ congeners tested by Mr. Rutz;

[a] Riddelliine was also tested in micronucleus assay, and BMDs were determined upon PROAST modeling, BMD = 1.76, BMDL = 1.29, and BMDU = 2.29.

4.7 Structure-toxicity relationship

Attempting to predict the potential toxicity of chemicals based on the structural characteristics began in very early years (Goldberg, 1983; McKinney, 2000; Wang et al., 1999). The general structures of PAs include necine base and necine acids. Necine base has been the most discussed. It is well known that a double bond between C1 and C2 position, i.e., unsaturated necine base, enables PAs to undergo metabolic activation to exert their toxicity. Therefore, platynecine-type containing a saturated necine base was considered to be irrelevant to safety assessment. In addition, the C7 *R/S*-configuration was also regarded as related to the toxicity.

Culvenor et al. (1976) concluded in their *in vivo* study that the di-esters of heliotridine- and retronecine-type were more toxic than respective mono-esters, heliotridine necine based congeners were about 2- to 4-fold toxic as that retronecine based, and cyclic di-esters were possibly more toxic than the open-chain di-esters (Culvenor et al., 1976). The heliotridine-associated higher cytotoxicity has also been demonstrated *in vitro* by Field et al. (2015). In addition, it suggested the necine base, ester configuration, and saturation contribute to the cytotoxicity. But if reviewed the results from *in vivo* studies, heliotrine was much less toxic than from *in vitro* assays. In our project, di-esters were generally more potent than mono-esters except for monocrotaline. Lasiocarpine, as only heliotridine-type di-ester, exhibited distinctively higher potency than other retronecine-type cyclic di-esters, especially in HepG2 (CYP3A4) C9 cells. In contrast, the effect of *R/S*-configuration at C7 on the toxicity of mono-esters could not be demonstrated. Briefly, the structural differences between the PA congeners to classify the toxic potency lack absolute predictability, whether cyclic di-ester or mono-ester occurred with more or less potency belonging to another potency group.

In this present study, it seems that some chemical structures or groups (s.Tab.12) in side-chains also possibly affected the toxic potency:

A: the chain consists of 5 or 6 C-atoms that link two hydroxyl-groups at position C7 and C9 of the necine base (e.g., monocrotaline vs. other cyclic PA congeners);

B: methoxy-group (e.g., lasiocarpine vs echimidine)

C: hydroxyl-group (e.g., europine vs. heliotrine)

D: allyl-group (e.g., monocrotaline vs. other di-esters)

After analyzing the *in vitro* data cytotoxicity (Alamar blue assay) and genotoxicity (micronucleus assay), as well as using two different cell types, including primary rat hepatocytes and HepG2 (CYP3A4) C9 cells in terms of structure differences, it might be suggested as follows: (1) the steric hindrance of the side-chains could inhibit the enzymatic hydrolysis, the allylic ester group of mono-esters could be easily hydrolyzed

due to the less steric hindrance (+) (Mattocks, 1982); (2) the cyclic side-chain consisting of 5 C-atoms might be more unstable than a side chain with 6 C-atoms due to the enhanced ring strain facilitating hydrolysis (-); (3) methoxy-group (-OCH_3) instead of hydroxy-group (-OH) at the exact position of the side-chains is reducing hydrophilicity (+); (4) more hydroxy-groups in side-chains raise the hydrophilicity possibly increasing the excretion (-) (Okuno et al., 1988); (5) the allyl-group at the side-chain connected to position 7 applied an electronic enhancement for Michael-Addition whether lending to detoxification or intoxification could not be confirmed (+/-).

Nevertheless, all these based on structural features and the *in vitro* findings in our project summarized outlines are only an assumption. To develop a better understanding of what structural features are related to PA-induced toxicity, more specific cases should be summarized to analyze their similarity and diversity, then establish the mathematical association between the properties and the toxicity.

Table 12: Summary of metabolite-relevant CYP450 isoforms and possible toxic potency related structure features on side-chains of all ten PA congeners

	Species	**Rat liver**	**Human liver**		
	Mainly isoforms	CYP1A1/2, CYP2A1/2, CYP2B1/2, CYP2C6/11/12, CYP2E1, CYP3A1/2/9/18	CYP1A1/2, CYP2A6, CYP2B6, CYP2C8/9/19, CYP2D6, CYP2E1, CYP3A4/5		
PA (structural features)	**Metabolic activation**	**Primary rat hepatocytes Alamar blue assay 48 h, 3 h after seeding**	**HepG2 (CYP3A4) C9 cells**		**Structure**
			Alamar blue assay, 48 h	**Micronucleus assay**	
Riddelliine (cyclic, di, 7*R*)	**CYP3A4/5, (CYP2A6, CYP2D6)**	**1.0**	**1.0**	**1.0**	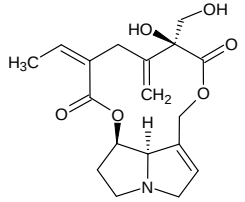
Lasiocarpine (open, di, 7*S*) iREP = 1.0	CYP3A4/5, (CYP1A1, CYP2D6)	2.0	9.7	35. 2	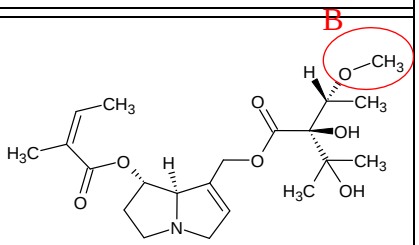

ǂmonocrotaline (cyclic, di, 7*R*) iREP = 1.0	CYP2A6, CYP2E1	<0.03	<0.32	0.02	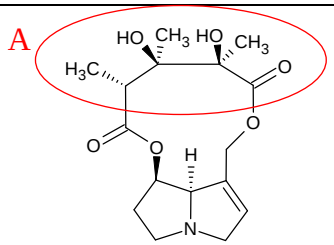
retrorsine (cyclic, di, 7*R*) iREP = 1.0	CYP2A6, CYP3A4/5	0.42	1.33	1.15	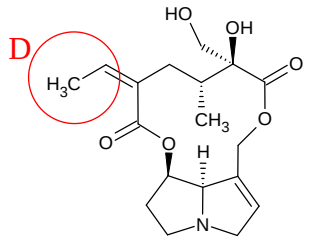
senecionine (cyclic, di, 7*R*) iREP = 1.0	CYP3A4/5, CYP2A6, CYP2D6	1.0	1.45	13.5	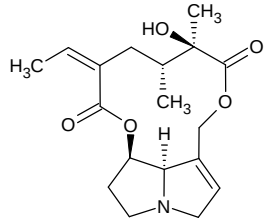
ǂseneciphylline (cyclic, di, 7*R*) iREP = 1.0	CYP3A4/5, CYP2A6	0.42	1.33	1.83	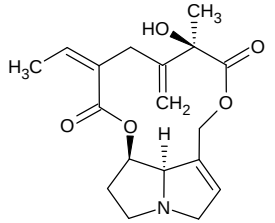

ǂechimidine (open, di, 7*R*) iREP = 0.1	n.c.	0.32	0.54	0.14	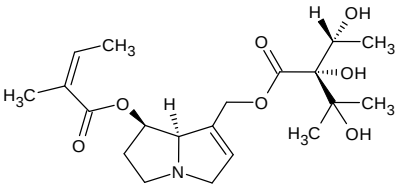
ǂeuropine (mono, 7*S*) iREP = 0.3	n.c.	<0.03	<0.32	0.05	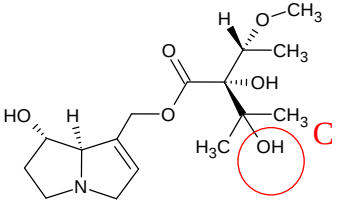
ǂheliotrine (mono, 7*S*) iREP = 0.3	n.c.	0.04	0.55	0.27	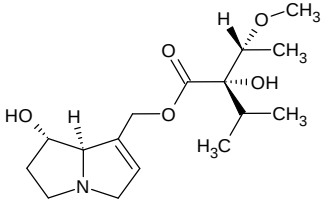
indicine (mono, 7*R*) iREP = 0.01	n.c.	0.04	<0.32	0.05	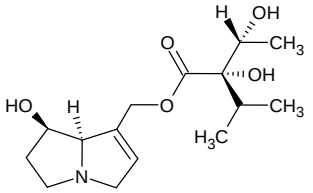

lycopsamine (mono, 7*R*) iREP = 0.01	n.c.	0.07	<0.32	0.03	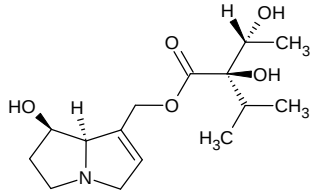

A, B, C, D: structural features possibly accountable for different toxicity

n.c.: not clear

(Martignoni et al., 2006; Ruan et al., 2014b)

5 CONCLUSION AND FUTURE WORK

PAs as constituents, i.e., secondary metabolites, distributed in a broad spectrum of plant species mainly belong to three families *Asteraceae, Boraginaceae, and Fabaceae*. More than 660 different PAs and corresponding *N*-oxides have been identified so far (Mattocks, 1986; Roeder, 2000; Smith and Culvenor, 1981; Stegelmeier et al., 1999). They are not only found in foodstuffs prepared from PA-containing plants, such as herbal tea and herbal remedies but may also occur as potential contamination in a variety of foods via cross-effect with plants containing PAs or be brought through a carry-over effect from feed containing toxic PAs into animal products. During the last years, a broad determination of food products revealed the possible exposure pathways, including wheat, honey, eggs, milk or milk products, meat products, herbal teas, and herbal medicines. Incidents of human and livestock poisoning with PAs have been reported in different countries (Creeper et al., 1999; Edgar et al., 2015; Hill et al., 1997; Mohabbat et al., 1976; Molyneux et al., 2011; Tandon et al., 1978; Tandon et al., 1976). Due to the widespread distribution and the carcinogenicity, the presence of PA in market products would be a concern for public health (BfR, 2015; Crews et al., 1997a; Edgar et al., 2002; Edgar and Smith, 2000; Kempf et al., 2010; Kowalczyk and Kwiatek, 2018; Mohabbat et al., 1976; Mulder et al., 2016; Tandon et al., 1978; Tandon et al., 1976; Wang et al., 2019).

Currently, the risk assessment of PAs is generally on account of the two most potent congeners, lasiocarpine and riddelliine. Numerous *in vivo* and *in vitro* studies on their hepatotoxicity, genotoxicity, and carcinogenicity demonstrated that the toxic potencies of individual PA congeners differentiated widely with each other. Several PAs mainly contributed to the dietary exposure were considerably lower potent than lasiocarpine and riddelliine. According to the data on the toxicity of the most potent PA congeners, the risk assessment results in overestimating the risk leading to excessively restricted limitations for the market products. To better estimate the risk of PA-containing products, a concept of (interim) relative toxic potency (REP) to represent the possibly structure-related diversely toxic potencies of individual PAs was proposed. PA congeners were classified into four groups assigned with factors of 1.0, 0.3, 0.1, and 0.01 (Merz and Schrenk, 2016). Since this concept was derived from an inadequate database, it was found that the relative toxicity of individual congeners cannot be entirely reliably evaluated. Our project aimed to achieve more comprehensive congener-specific *in vitro* toxicological data and estimate the structure-related characteristics for refining this concept.

Ten PA congeners with different structural features belonging to four groups were selected for our investigation: (1) open-chain di-ester with 7*S*-configuration, or cyclic di-ester with 7*R*-configuration (iREP = 1.0): lasiocarpine, monocrotaline, retrorsine,

senecionine, seneciphylline; (2) mono-esters with 7*S*-configuration (iREP = 0.3): europine, heliotrine; (3) open-chain di-ester (iREP = 0.1): echimidine; (4) mono-ester with 7*R*-configuration (iREP = 0.01): indicine, and lycopsamine. They were determined in a series of *in vitro* test systems with different endpoints to quantify their hepatotoxicity, genotoxicity, and mutagenicity. Among them, lasiocarpine, retrorsine, senecionine, indicine and lycopsamine have been investigated on my part. Meanwhile, monocrotaline, seneciphylline, europine, heliotrine and echimidine have been measured by Mr. Rutz. Therefore, the data from Mr. Rutz were not reported in the results of this work. Only the values already published, such as EC_{50}s or BMDs, were cited for discussing the probable relationship between the structural features and the relative toxic potencies.

Cytotoxicity was investigated using Alamar blue assay in primary rat hepatocytes, naïve HepG2 cells, and HepG2 C9 (CYP3A4) cells transformed with virus genes or oncogenes enable to express CYP450 enzymes. Except for naïve HepG2 cells, all congeners generally showed a dose-dependent cytotoxic effect. A longer incubation time of 48 h led to higher toxicity suggesting cumulative damage related to the pyrrole-protein adducts as reported (Ma et al., 2018). When comparing the results in primary rat hepatocytes to those in HepG2 (CYP3A4) cells with an incubation time of 48 h, the relative potencies of the congeners tested exhibited in the same manner as follows: lasiocarpine > senecionine > retrorsine ≈ seneciphylline > echimidine ≥ heliotrine ≥ europine ≈ lycopsamine ≈ indicine ≈ monocrotaline (s.Tab.12).

In addition, it was found that a shorter pre-incubation period from adherence to the exposure could also increase the cytotoxic effect. Using a BROD assay, a considerable spontaneous loss of CYP450 enzyme activity was determined during the culture, particularly in the first 24 hours. Nevertheless, similar to most other toxicants, PAs require metabolic activation to exert toxicity, where the cytochrome P450s play an essential role. No detectable cytotoxic effect found in the naïve HepG2 cell line due to its insufficient expression of crucial metabolism enzymes has exactly supported this inference. That the CYP450 enzymes are critical metabolizing enzymes for PAs was further ascertained in an inhibition study. In primary rat hepatocytes, pre-treatment with ketoconazole led to a slight to several times reduction in PA-induced cytotoxicity.

The effect of a short pre-incubation or CYP-inhibition diversity among the individual congeners also suggested that different CYP450 isoforms or the enzymes even not belonging to the cytochrome P450 family are responsible for the PA-specific metabolic activation. On the other hand, the role of intracellular reduced glutathione in the toxicity of PA congeners was investigated. Comparing the cytotoxicity between glutathione depletion with BSO in primary rat hepatocytes and untreated cells suggested that the GSH depletion was not improved or only slightly enhanced the cytotoxic effects of most PA congeners tested.

Ames fluctuation assay modified from classic Ames test was used to determine the mutagenicity. No detectable mutagenicity could be demonstrated of any PA congener in *Salmonella typhimurium* strains TA98 or TA100 despite an extern metabolism system of rat liver S9-mix. However, the negative results suggested more likely the unavoidable limitations of the mutagenicity test in bacteria, especially the need to transport the chemicals into the cells or an ineffective extern metabolic activation, rather than non-mutagenicity of all PA congeners.

For the micronucleus assay to investigate the PA-induced clastogenic genotoxicity, the HepG2 (CYP3A4) C9 clone was selected due to its metabolic competency of CYP3A4, which is well known that involved in the metabolism of specific PA congeners. All selected PA congeners observed a dose-dependent increase in micronuclei counts. Only several more potent PAs exhibited a less pronounced increase at the higher concentration range, possibly due to the severe cytotoxic effect. The data were analyzed according to the different benchmark calculation models using the software PROAST online provided. If using the benchmark dose (BMD) calculated by PROAST to estimate and compare the relative potencies, the PA congener followed the ranking: lasiocarpine > senecionine > seneciphylline > retrorsine > heliotrine > echimidine > europine ≈ indicine ≈ lycopsamine ≈ monocrotaline (s. Tab.12)

The relative potency rankings estimated by Alamar blue assay (i.e., cytotoxicity) and micronucleus assay (i.e., genotoxicity) are generally consistent. Notably, if the relative potency factors from assays with primary rat hepatocytes or HepG2 (CYP3A4) C9 cells were all estimated using the toxicity of riddelliine as 1.0, lasiocarpine owned a remarkedly higher value in HepG2 (CYP3A4) C9 cells than in primary rat hepatocytes. It was not only the most potent congener but also distinctly from other di-esters. (s. Tab.12). It is possible due to an overexpression of CYP3A4 enzyme in the transfected C9 cell line, and CYP3A4 and CYP3A5 isoforms predominantly mediated the metabolism of lasiocarpine (Ruan et al., 2014b).

On the other hand, this study revealed, although CYP3A4 and CYP3A5 were also mainly responsible for the metabolic activation of some other PA congeners, different CYP450 isoforms could almost equally metabolize them. Heliotrine showed similar behavior, which was found least potent as other mono-esters in primary rat hepatocytes, exhibited notably higher toxic potency with HepG2 (CYP3A4) C9 cells. This finding could be traced back to what CYP3A4 isoform could also be the most crucial metabolism enzyme for heliotrine, comparable to lasiocarpine. However, this assumption needs more testings to confirm.

The relative potency factor calculated based on our findings was not completely consistent with the iREP classification previously inferred by Merz and Schrenk (2016). Monocrotaline in both assays exhibited considerably lower toxic potency, echimidine

as the other inconsistent case, by contrary, was more toxic than expected. CYP2A6 and CYP2E1 were indicated as the most critical isoforms for the bioactivation of monocrotaline, whereas for the other retronecine-type di-esters, CYP3A4 and CYP3A5 exhibited the most significant activity in mediating the metabolism (Ruan et al., 2014b). Besides the most discussed cause of PA-specific metabolic profile, several other toxicokinetic factors were also demonstrated. OCT1 (SLC22A1), an organic cation transporter highly expressed in the liver, was confirmed to participate in the influx-transport of monocrotaline and retrorsine. It seems to be a potentially critical transporter involved in the uptaking of PAs into the cells (Tu et al., 2014; Tu et al., 2013). The involvement of ABCB1-driven efflux of echimidine from gastrointestinal epithelium into the gastrointestinal lumen was also a possible reason that would result in a decreased bioavailability and lead to a deviation of the intrinsic toxic potency. (Allemang et al., 2018; Hessel et al., 2014). Therefore, more specific toxicokinetic factors not expressed in the simple *in vitro* cell models should be considered, preventing reliable estimations in risk assessment. It is necessary to improve the understanding of congener-specific toxicokinetics, such as metabolic activation, transport mechanism, or efficient clearance.

The general structure of PAs consists of necine base and necine acid(s). It is well known that a double bond between C1 and C2 position was essential for undergoing a metabolic activation to exert their toxicity. Thus, only the PA congeners with an unsaturated necine base were considered a public health concern. My findings supported the notion of the influence of structural features on their toxicity. The di-esters were generally much more toxic than the mono-esters since steric hindrance of side-chains at di-esters, particularly with long and branched acid, prevent the allylic ester groups from enzymatic hydrolysis. (Fu et al., 2001; Mattocks, 1982). The conjugated double bond or the allyl-group in lasiocarpine, retrorsine, senecionine, seneciphylline, and echimidine, whether influenced the toxic potency, could not be concluded. Based on the relative potencies estimated from the data of both assays, it suggested the cyclic side-chain of monocrotaline consisting 5 C-atoms was possibly more unstable than the other cyclic PAs with 6 C-atoms. If a methoxy-group (-OCH_3) instead of hydroxyl-group (-OH) at the exact position of the side-chains reduced hydrophilicity, by contrary, more hydroxyl-groups in side-chains raised the hydrophilicity increased the excretion (Okuno et al., 1988). The influence of (*R/S*) stereochemistry configuration at the C7 position previously regarded as related to the toxicity could not be revealed in the present work. Overall, the structural differences between the PA congeners with respect to their cytotoxic or genotoxic potency were still inadequate and need more evidence.

Our project evaluated PAs with diverse structural features in three different *in vitro* cell models: primary rat hepatocytes, HepG2, and HepG2 (CYP3A4) C9 cell lines. The

primary hepatocyte culture system, which presents the most metabolic and differentiated functions similar to those observed *in vivo*, can efficiently delineate PA-induced cellular cytotoxic effects (Bissell et al., 1973; Jeejeebhoy and Phillips, 1976). Concomitantly, it is limited by a short life span, individual differences, and complex availability. Additionally, cytochrome P450 isoforms mainly expressed in humans, such as CYP3A4, was almost not detectable in rats (Turpeinen et al., 2007). HepG2, a hepatoma cell line, due to the deficient expression of many important CYP450 enzymes responsible for the metabolic activation, is not appropriate for determining the toxic potency of PA congeners. Afterward, a transformed HepG2 with Lentivirus, which overexpressed CYP3A4, was used to test the cytotoxicity and the genotoxicity. Since CYP3A4 is involved in mediating the metabolic activation of many PA congeners, HepG2 (CYP3A4) C9 cell line seems more suitable than naïve HepG2 cells or the rat hepatocytes. However, it might not be ideal for specific congeners, such as monocrotaline, predominantly metabolized by CYP2A6 (Ruan et al., 2014b).

On the other hand, due to the species-specific distribution of enzymes, the corresponding metabolic pathways and toxic response (Mitchell and Jollows, 1975; Williams, 1978, 1974), as well as the species-differentiated metabolic degradation observed in different species microsomes (Geburek et al., 2020b; Geburek et al., 2020a), the results of primary rat hepatocytes cannot be directly transmitted to humans. Generally, all *in vitro* models reported here exhibit design limitations and indicate the need for additional human cell models for a more reliable estimation of PA toxicity. There is no doubt that the permanent cell lines can never indeed extent as primary hepatocytes. Hence, primary human hepatocytes are possibly the best option. HepaRG, a human hepatocellular carcinoma cell line that expressed various CYP450 enzymes at levels even comparable to those in primary human hepatocytes, can be a great alternative (Guillouzo et al., 2007).

Refining the relative toxic potencies concept requires a great number of concentration-dependent data. *In vivo* studies, i.e., animal experiments, could more accurately estimate the potency in humans adjusted to the more reliable risk assessment. In order to reduce the use of animals, the alternative testing strategy is attempted to establish a model, that can translate the data obtained from *in vitro* assays via modeling to predict an *in vivo* situation, particularly for the PAs which *in vivo* data are lacking. Chen et al. suggested that physiologically based kinetic (PBK) modeling facilitated reverse dosimetry can be possibly afterward used to deduce *in vivo* dose-response of PAs based on their *in vitro* cell testing (Chen et al., 2019b; Chen et al., 2018). By far, the performance of the PBK model was only evaluated and integrated with riddelliine and lasiocarpine due to the limited *in vivo* data.

Overall, there is space to gain a more appropriate approach of PAs in the risk assessment. Even available data are inadequate. At the moment, the dose-response studies on their

cytotoxicity and genotoxicity are primarily *in vitro* applied. It is necessary to establish a model assuming PAs with similar structural features share the comparable mode of action and taking the toxicokinetic factors, including metabolic biotransformation, clearance, transport, etc., into account for extrapolating the *in vitro* cell-based data to *in vivo* situation. In addition, major types of PA congeners that contribute to the toxicity and their amount in the products should also be identified. An improved understanding of the structure-dependent relative toxic potency could help to predict the toxic effect of different PA congeners. In addition, the corresponding *N*-oxides usually balanced with parent PA in nature which has not yet been considered as noticeable as their parent compounds, need more attention due to their various metabolism routes after application. Yang et al. (2017) demonstrated the remarkable differences in toxicokinetics between the *N*-oxides and their parent PAs leading to varied internal concentrations. The exposure to PA *N*-oxides should also be included in the further risk assessment of PAs or establish the toxic dose threshold of daily intake.

6 MATERIALS AND RESEARCH METHODS

6.1 Animals, hepatocyte preparation, and cell culture

Rat hepatocytes were isolated from Sprague-Dawley male rats from Janvier (Le Genest-Saint-Isle, France), weighing about 200 g by a two-step *in situ* perfusions of the liver with collagenase modified from the method described by Seglen (1976). Maintenance of animals and isolation of hepatocytes followed the 2010/63/EU guidelines on protecting animals used for scientific research. After the cell harvests, the number of parenchymal cells in the preparations was estimated by microscopic inspection > 95%. The viability as measured by trypan blue dye exclusion test exhibited more than 90% routinely. The isolated hepatocytes were suspended in DMEM-LG supplemented with 10% FCS and 1% P/S , then seeded on collagen-coated 24-well plates at a final density of 0.2 x 10^6 cells in 1 ml medium per well. Cells were maintained at 37 °C in 95% air/5% CO_2 and aggregated and attached to form cluster after about 3 hours. The medium was then once changed to remove unattached hepatocytes. After that, the culture medium was renewed before incubation with test compounds.

Naïve HepG2 cells obtained from German collection of microorganisms and cell culture GmbH (DSMZ) were cultivated after thawing in DMEM-HG (with *L*-glutamine 4 mM, with Na-pyruvat) supplemented with 10% FBS and 1% P/S. Cytochrome P450 3A4-overexpressing HepG2 cell clones were obtained from BTU Cottbus-Senftenberg and routinely cultivated in DMEM-HG (with *L*-glutamine 4 mM; without Na-pyruvat) supplemented with 10% FBS and 3 µg/ml blasticidin-*S*-hydrochloride. Both cell lines were also maintained at 37°C in an incubator with 5% CO_2. The cellular viability of both HepG2 cell lines was also assessed by the trypan blue dye exclusion test.

Afterward, for Alamar blue assay or BROD assay, naïve HepG2 cells and HepG2 (CYP3A4) C9 cells were seeded into 48-well plates about 65,000 cells per well in 500 µl culture medium. In comparison, about 700,000 cells were seeded in 60 mm Petri dishes with 2 ml culture medium for the micronucleus test. By 24 h, fresh medium was shifted, and culture was incubated with different PAs.

6.2 Pyrrolizidine alkaloids

All five PAs, i.e., lasiocarpine, retrorsine, senecionine, indicine, and lycopsamine were purchased from PhytoLab GmbH & Co, KG. (Vesternbergsgreuth, Germany). Stock solutions of various pyrrolizidine alkaloids were prepared in solvent as shown in Tab. 13 and 14 then stored in the dark at -20 °C. Because of the different solubility, PAs were dissolved in different suitable solvents with appropriate concentrations.

Table 13: Stock solutions of pyrrolizidine alkaloids for Ames fluctuation assay

Stock solution	Substance and CAS#	Quantity
Lasiocarpine (15 mM)	Lasiocarpine (303-34-4)	10 mg
	DMSO	1620 µl
Retrorsine (15 mM)	Retrorsine (480-54-6)	10 mg
	DMSO	1897 µl
Senecionine (15 mM)	Senecionine (130-01-8)	10 mg
	DMSO	1988 µl
Indicine (15 mM)	Indicine hydrochloride (1195140-94-3)	10 mg
	H_2O_{dd}	1985 µl
Lycopsamine (15 mM)	Lycopsamine (10285-07-1)	10 mg
	DMSO	2227 µl

The stock solutions with corresponding solvents produce a dilution series of concentrations 7.5, 3.75, 1.25, 0.25, and 0.05 mM.

Table 14: Stock solutions of pyrrolizidine alkaloids for assays (except for Ames fluctuation assay)

Stock solution	Substance and CAS#	Quantity
Lasiocarpine (300 mM)	Lasiocarpine (303-34-4)	20 mg
	DMSO	162 µl
Retrorsine (50 mM)	Retrorsine (480-54-6)	20 mg
	ACN (0.3%-F_3CCOOH)	1138 µl
Senecionine (50 mM)	Senecionine (130-01-8)	20 mg
	ACN (0.3%-F_3CCOOH)	1193 µl
Indicine (300 mM)	Indicine hydrochloride (1195140-94-3)	20 mg
	H_2O_{dd}	199 µl
Lycopsamine (300 mM)	Lycopsamine (10285-07-1)	20 mg
	DMSO	223 µl

Afterward, using the stock solutions of lasiocarpine, indicine, and lycopsamine with corresponding solvents to produce a dilution series of concentrations 150, 75, 25, 5, and 1 mM, of retrorsine and senecionine thus to 25, 12.5, 4.17, 0.83, and 0.17 mM due to their limited solubility.

6.3 7-Benzyloxyresorufin-*O*-dealkylase (BROD) assay

BROD enzyme activity was determined in primary rat hepatocytes and both HepG2 cell lines. The primary rat hepatocytes (0.2 Mio./ml) and HepG2 cells (0.13 Mio/ml) were prepared and seeded in 24-well plates. After incubation, the monolayers were rinsed twice with PBS (phosphate-buffered saline, pH 7.4) to remove detached cells. The measurement was started by the addition of 1 ml/well assay mixture, i.e., 1 ml PBS containing $MgCl_2$ (5 mM), dicumarol (10 µM), and 7-benzyloxyresorufin (5 µM). Dicumarol was added to prevent further metabolism of the resorufin formed by the cytosolic enzymes that shared many characteristics with chemotherapeutic quinone diaphorase (Lubet et al., 1985).

In contrast with the microsomes assays, adding the NADPH-regenerating system was unnecessary since primary rat hepatocytes and hepatoma cell lines could generate their own NADPH. The amount of resorufin formed by *O*-dealkylation of 7-benzyloxyresorufin was determined every 90 seconds up to 30 minutes fluorometrically using Thermo Scientific Fluoroskan Ascent FL with 544 nm excitation and 590 nm emission wavelengths. The determination time was set at 30 minutes because it ensured that BROD enzymatic reaction progressed linearly.

The status of CYP3A activity in primary rat hepatocytes was determined to start after attachment for about 3 hours then at different time points over up to 72 hours after seeding. For HepG2 cells, instead of 3 hours, the cells were attached to the plate for 24 hours. The BROD activity in HepG2 cells was measured firstly after 24 hours. For the inhibition study, rat hepatocytes in primary culture were incubated after attachment in the absence and presence of ketoconazole with different concentrations (1, 5, 10, and 40 µM) for 2 hours before adding the assay mixture.

The BROD activities were estimated by comparison of the results with a standard curve. Resorufin standards within the range of 0.5 nM – 500 nM were prepared in PBS, processed as described for samples, and normalized to protein content. Thus, the plate was washed with PBS again and then frozen for protein determination after the measurement. Since the initial concentration and activity of CYP450s in primary rat hepatocytes varied from individual animals, in order to more clearly present the change of the CYP450s-status, the BROD-activity after attachment for 3 h was defined as 100%. For the inhibition study, the same amount of the solvent, i.e., in the absence of ketoconazole only with DMSO (0.1%), was added in the medium as control. The BROD activity was set as 100%. Each enzyme activity measured was calculated as a percentage.

Table 15: Solutions for the BRDO assay

Solution	Substance	Quantity
7-Benzyloxyresorufin (0.9 mM) aliquot, stored at -20 °C, protected from light	7-Benzyloxyresorufin DMSO	5 mg 18.32 ml
Magnesium chloride (1 M) stored at room temperature	$MgCl_2$ $(H_2O)_6$ H_2O_{dd}	20.33 g 100 ml
Sodium hydroxide (0.2 M) stored at room temperature	NaOH H_2O_{dd}	0.8 g 100 ml
Dicumarol (10 mM) aliquot, stored at 4 °C	Dicumarol NaOH (0.2 M)	33.63 mg 10 ml
Resorufin stock solution (10 mM) stored at 4 °C for 4 weeks, protected from light	Resorufin sodium salt DMSO	23.5 mg 10 ml
Resorufin working solution (1 mM) prepared immediately before use, protected from light	Resorufin-stock solution DMSO	50 µl 450 µl

Table 16: Composition of BROD medium

Solution	Volume
$PBS^{-/-}$ (pH 7.4)	25 ml
Magnesium chloride (1 M)	125 µl
Dicumarol (10 mM)	25 µl
7-Benzyloxyresorufin (0.9 mM)	140 µl

Table 17: Pipetting scheme for the preparation of resorufin calibration standards

Calibration standard [Cal Nr.]	Resorufin concentration [nM]	Volume of working solution [100 µM] [µl]	Volume of $PBS^{-/-}$ [µl]
0	1000	50	4950
1	250	2000 from Cal 0	6000
2	100	2000 from Cal 1	3000
3	50	2500 from Cal 2	2500
4	20	2000 from Cal 3	3000
5	10	2500 from Cal 4	2500
6	5	2000 from Cal 5	2000
7	1	1000 from Cal 6	4000
8	0.5	2000 from Cal 7	2000

6.4 Glutathione-reductase-DTNB recycling assay

To estimate an appropriate concentration inducing GSH depletion in primary rat hepatocytes, the cells were incubated with BSO (40, 100, 200, 500 µM, and 1mM) dissolved in dd.H_2O. The pre-treatment duration was chosen for 2 hours, the same period as that selected in the cytochrome P450 inhibition study.

For sample preparation, the cultures of primary rat hepatocytes after the incubation period were rinsed with 0.9% NaCl solution, frozen overnight, thawed on ice, and lysed in 150 µl of 10 mM HCl. Then, 20 µl of the lysate was removed for protein determination and 120 µl for glutathione analysis. Therefore, 30 µl of 6.5% aqueous 5-sulfosalicylic acid solution was added for protein precipitation. After centrifugation at 13,000 g and 4°C for 15 min, 20 µl of protein-free supernatants and the standards (s. Tab. 19) were transferred to a 96-well plate, 20 µl of assay stock buffer (s. Tab. 18: 143 mM NaH_2PO_4, 6.3 mM EDTA) for neutralization, afterward 200 µl of Daily reagent (s. Tab. 18: 1 mM DTNB, 0.17 mM $NADP^+$, 0.34 mM G6P, 3 mM $MgCl_2$, 1 unit/ml G6P-DH) and 40 µl of glutathione reductase solution (s. Tab. 18) were added. Absorbance was measured in a microplate reader at the wavelength of 405 nm. For GSSG analysis, 80 µl of the protein-free supernatants were transferred into each well of a 96-well plate and readily derivatized by adding 5 µl of 2-vinyl pyridine per well. After 1 h, 40 µl of the sample and each GSSG calibration standard (s. Tab. 20) per well were transferred into another 96-well plate for determination. The glutathione content as GSx and GSSG was analyzed by comparison to a standard curve generated with known glutathione concentrations. The reduced form of glutathione, i.e., GSH, was calculated as the difference between GSx and GSSG.

Table 18: Solutions for the Glutathione-reductase-DTNB recycling assay

Solution	Substance	Quantity
Hydrochloric acid (1 M)	HCl (37%)	5 ml
stored at room temperature	H_2O_{dd}	ad. to 50 ml
Hydrochloric acid (10 mM)	HCl (1 M)	1:100 (v/v)
stored at room temperature	H_2O_{dd}	
5-Sulfosalic acid (6.5% w/v)	5-sulfosalicylic acid (SSA)	13 g
stored at room temperature	HCl (10 mM)	200 ml
Standard buffer (SB)	5-sulfosalicylic acid (SSA)	2.6 g
stored at room temperature	HCl (10 mM)	200 ml
Assay stock buffer (ASB)	NaH_2PO_4 (H_2O)	19.73 g
pH 7.4	EDTA (0.5 M)	12.6 ml
stored at 4 °C for 4 weeks	H_2O_{dd}	ad. to 1 l
DTNB (10 mM)	DTNB	158.6 mg
stored at -20 °C for one week	ASB	40 ml

NADP (1.89 mM) prepared immediately before use	NADP sodium salt ASB	7.4 mg 5 ml
Glucose-6-phosphate (3.89 mM) prepared immediately before use	G6P ASB	6.9 mg 5 ml
Magnesium chloride (33.45 mM) stored at 4 °C	$MgCl_2 (H_2O)_6$ ASB	273 mg 40 ml
Daily reagent (for 1 x 96 well plate) prepared immediately before use	DTNB (10 mM) NADP (1.89 mM) G6P (3.89 mM) $MgCl_2$ (33.45 mM) G6P-DH (50 unit/ml) ASB	2 ml 1.8 ml 1.8 ml 1.8 ml 400 µl 12.6 ml
Glutathione reductase (8.5 Unit/ml) (for 1 x 96 well plate) prepared immediately before use	GR from yeast (600 U/ml) ASB	57 µl 4 ml
GSH stock solution (800 µM) stored at -80 °C for one week	GSH HCl (10 mM)	2.5 mg 10 ml
GSSG stock solution (400 µM) stored at -80 °C for one week	GSSG HCl (10 mM)	2.5 mg 10 ml

Table 19:Pipetting scheme for the preparation of GSH calibration standards

Calibration standard [Cal Nr.]	GSH concentration [µmol/ml]	Volume of GSH stock solution [800 µM] [µl]	Volume of SB [µl]
1	80	100	900
2	40	500 from Cal 1	500
3	20	500 from Cal 2	500
4	10	500 from Cal 3	500
5	6	600 from Cal 4	400
6	3	500 from Cal 5	500
7	1	333 from Cal 6	667
8	0.5	500 from Cal 7	500

Table 20: Pipetting scheme for the preparation of GSSG calibration standards

Calibration standard [Cal Nr.]	GSSG concentration [µmol/ml]	Volume of GSSG stock solution [400 µM] [µl]	Volume of SB [µl]
1	10	25	975
2	8	20	980
3	6	15	985
4	5	500 from Cal 1	500
5	4	500 from Cal 2	500
6	3	500 from Cal 3	500
7	2	500 from Cal 5	500
8	1	500 from Cal 7	500
9	0.5	500 from Cal 8	500

6.5 Alamar blue (Resazurin) assay

The viability of bacteria was also determined using Alamar blue assay in TA98 and TA100, both strains. 490 µl bacteria diluted in exposure medium with the same density as that in Ames fluctuation assay was incubated in 24-well plate, then 10 µl of different concentrations of the test compounds were added. At the same time, 500 µl of bacterial suspension was used as negative control (= 100%), DMSO (2%) as solvent control, and SDS (3.5 mM; s. Tab. 21) as a positive control. The plates were incubated at 37 °C and shaken at 125 rpm for 100 minutes. After that, 10 µl of resazurin working solution (s. Tab. 21) was added to each well. After further incubation of 10 min at 37 °C with shaking, the fluorescence was measured using Fluoroskan Ascent FL (Thermo Scientific).

An overview of the different treatment schedules for rat hepatocytes in primary culture is shown in Fig. 45. Rat hepatocytes (1 ml/well) were seeded into 24-well collagen-coated plates.

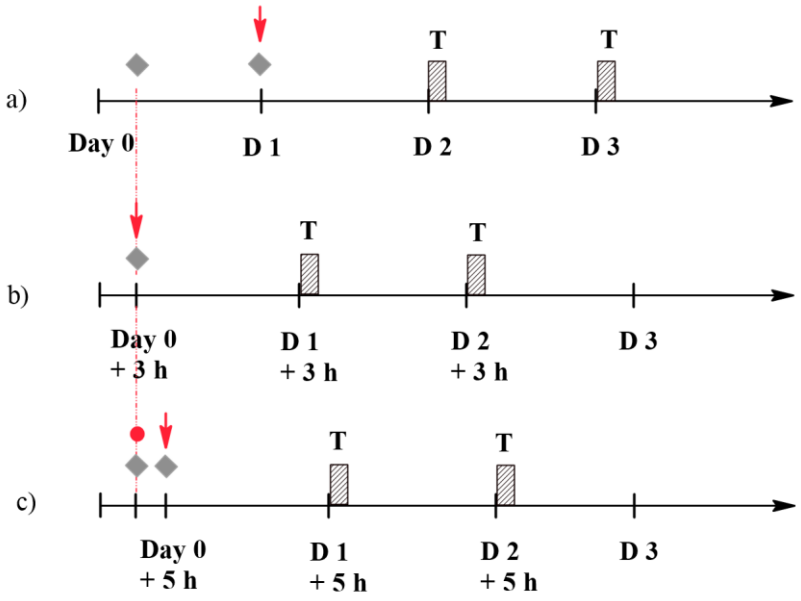

Figure 45: An overview of different incubation schedules in primary rat hepatocytes

a) Medium was replaced by fresh medium after a pre-incubation period of about 24 hours (D 1). The primary rat hepatocytes were treated for 24 h and 48 h in triplicate with six concentrations (1, 5, 25, 75, 150, and 300 µM) of each PA. The stock solutions (s. Tab. 21) were diluted in a cultured medium to a final concentration of 0.1%. After incubation, the viability of cells was measured respectively on D 2 and D 3 using Alamar blue assay.

b) Primary rat hepatocytes were directly treated with PAs after adherence for 3 hours and changing medium (D 0). After 24 h or 48 h, the viability of cells was measured respectively on D 1 and D 2.

c) For further confirmation of the role of CYP450-mediated metabolic activation and to investigate the influence of GSH depletion in the toxicity of PAs, after attachment and renewal of the medium (day 0), cells were firstly pre-treated with 5 µM ketoconazole or 1 mM BSO (s. Tab. 22, 1 µl stock solution in 1 ml culture medium) for 2 h. Afterward, the plates were also incubated with different PAs after the medium had been replaced. For an additional 24 h or 48 h, the cytotoxicity was then analyzed on D 1 and D 2.

Naïve HepG2 and HepG2 C9 (CYP3A4) cells were seeded on 48-well plates about 65,000 cells per well in 500 µl of culture medium. The medium was replaced after 24 h. Then the cultures were also incubated with six concentrations of each PA congener for a further 24 or 48 h.

For the primary rat hepatocytes or both HepG2 cell lines, the same amount of the solvent as the test compound solution was added to the culture as the vehicle control.

At the same time, the cells were also incubated only with medium, of which the viability would be defined to 100%, and with saponin (0.1%) as the positive control.

Resazurin stock solution (s. Tab. 21) was prepared in double-distilled water at the rate of 110 mg to 100 ml. The fresh solution was made once monthly and stored at 4°C. After incubation, the medium containing PAs was removed, and the resazurin reagent was added to cells at 1 ml/well. The plate(s) was then incubated at 37°C (5% CO_2) for 90 min, and the fluorescence was determined using Fluoroskan Ascent FL (Thermo Scientific) automated fluorescence plate reader. Results are presented in relative fluorescence units (RFU).

The viability of HepG2 (CYP3A4) C9 cells after incubation was also determined using the Alamar blue assay parallel to the micronucleus assay.

Table 21: Solutions for the Alamar blue assay

Solution	Substance	Quantity
$PBS^{-/-}$ (phosphate-buffered saline without calcium and magnesium pH 7.4 stored at room temperature	NaCl KCl Na_2HPO_4 KH_2PO_4 H_2O_{dd}	8.000 g 0.200 g 1.440 g 0.240 g ad. to 1 l
NaCl/P_i-buffer stored at 4 °C	NaCl Na_2HPO_4 KH_2PO_4 H_2O_{dd}	9.000 g 0.528 g 0.144 g ad. to 1 l
in *Salmonella typhimurium*		
Stock solution (440 mM) stored at 4 °C for one week, protected from light	Resazurin sodium salt Dimethylformamide	110.5 mg 1 ml
Working solution prepared immediately before use, protected from light	Stock solution NaCl/Pi-buffer	1:100 (v/v)
Positive control: **SDS (173 mM)** stored at -20 °C	Sodium dodecyl sulfate H_2O_{dd}	50 mg 1 ml
in mammalian cells		
Stock solution (440 µM) stored at 4 °C for 4 weeks, protected from light	Resazurin sodium salt Dimethylformamide NaCl/P_i-buffer	110.5 mg 1 ml ad. to 1 l

Working solution prepared immediately before use, protected from light	Stock solution NaCl/Pi-buffer	1:1000 (v/v)
Positive control: **Saponin (10%)** stored at -20 °C	Saponin H_2O_{dd}	100 mg 1 ml

Table 22: Stock solutions of ketoconazole and BSO inhibition assay

Stock solution	Substance	Quantity
Ketoconazole (40 mM)	Ketoconazole	212.6 mg
	DMSO	10 ml
BSO (1000 mM)	BSO	2.222 g
	H_2O_{dd}	10 ml

Afterward, using the stock solutions of ketoconazole with corresponding solvent DMSO to produce a dilution series of concentrations 1, 5, and 10 mM, of BSO thus to 40, 100, 200, and 500 mM.

6.6 Ames fluctuation assay

Preparation of liver homogenate S9 fraction: for the preparation of the S9 fraction, young male Wistar rats with a bodyweight of 200 ± 10 g obtained from Janvier labs were used. The animals were *i.p.* injected with Aroclor 1254 at a dosage of 500 mg/kg bodyweight (diluted in corn oil to a concentration of 200 mg/ml), a polychlorinated biphenyl mixture, to induce liver enzymes five days before they were killed. The rats were given sterile food and drinking water. The liver was removed aseptically and prepared based on the procedure of Maron and Ames (1983). All steps were preceded at 4°C with cold, sterile solution and glassware. The harvested liver was pre-weighted, washed with 0.15 M KCl, then placed in a beaker containing three volumes of this KCl solution (3 ml/g wet liver), and minced with a sterile scalpel homogenized with a Potter-Elvehjem apparatus. The homogenate was centrifuged at 9000 g for 10 min, and the supernatant (S9 fraction) was distributed in 1.5 ml centrifuge tubes and then stored at -80°C. Besides the liver enzymes, the metabolic activation of some substances also requires NADPH. In vitro, e.g., in Ames fluctuation assay, it is customary to add an NADPH-generating system containing $NADP^+$, G6P, (G6PDH), and $MgCl_2$, KCl, as well as phosphate buffer. The S9 mix (s. Tab. 26) should always be prepared freshly before use.

Confirming of genotypes: Nutrient agar plates (s. Tab. 24) were prepared and stored at 4°C. Before use, the plates were incubated at 37°C for about 15 minutes to equilibrate.

rfa mutation. 100 µl of the individual culture of each test strain added to the 2 ml top agar (s. Tab. 24) preheated at 45°C, vortex and then spread onto equilibrated nutrient agar plates. After the top agar was firmed, a filter paper disc wetted with 10 µl of 1 mg/ml crystal violet solution was placed on the surface of each seeded plate and using

sterile forceps slightly pressed. Subsequently, the plates were incubated at 37°C for 24 h. The crystal violet sensitivity could be indicated by a clear zone of inhibition around the disc.

uvrB mutation. Aliquots of the strain cultures were streaked with sterile swabs parallel across the nutrient agar plate. Then an aluminum paper was placed to cover that half of each bacterial streak and irradiated the plate with UV-C light (2 x 15 W, distance 30 cm) for 8 s. The plates were also cultivated at 37°C for 24 h. Strains with *uvrB*-mutation could only grow on the unirradiated side.

R-Plasimid. Various strain cultures were added to top agar and poured onto nutrient agar plates as described above to confirm the crystal violet sensitivity. Instead of crystal violet, 10 µl of solutions of three different antibiotics, ampicillin, neomycin, and tetracycline (s. Tab 25), pipetted to the filter paper discs, then placed on the firmed top agar. The Petri dishes were incubated as well at 37 °C for 24 h.

Table 23: Solutions for the Ames fluctuation assay

Solution	Substance	Quantity
Crystal-violet (1 mg/ml) stored at 4 °C, protected from light	Crystal-violet H_2O_{dd}	50 mg 50 ml
D-Biotin (0.122 mg/ml) sterilized by filtration (0.2 µm), aliquot, stored at -20 °C	D-Biotin H_2O_{dd}	12.2 mg 100 ml
Bromocresol purple (1.7 mg/ml) prepared immediately before use, protected from light	Bromocresol purple sodium salt NaCl/Pi-buffer	51 mg 30 ml
Formazine Standard (4000 FAU) stored at room temperature, protected from light	Hexamethylenetetramine Hydrazine sulfate H_2O_{dd}	5.0 g 0.5 g ad. to 100 ml
Glucose-6-phosphate (0.24 M) sterilized by filtration (0.2 µm), aliquot, stored at -20 °C	G6P H_2O_{dd}	0.68 g 10 ml
L-Histidine (1 mg/ml) sterilized by filtration (0.2 µm), aliquot, stored at -20 °C	L-Histidine H_2O_{dd}	50 mg 50 ml
Magnesium chloride (0.25 M) autoclaved, stored at room temperature	$MgCl_2 (H_2O)_6$ H_2O_{dd}	5.08 g 100 ml
NADP (0.04 M) sterilized by filtration (0.2 µm), aliquot, stored at -20 °C	NADP sodium salt H_2O_{dd}	0.31 g 10 ml

Potassium chloride (0.15 M) autoclaved, stored at room temperature	KCl H_2O_{dd}	7.46 g 100 ml
Sodium dihydrogen phosphate (0.2 M)	NaH_2PO_4 H_2O_{dd}	14.39 g 600 ml
Disodium hydrogen phosphate (0.2 M)	Na_2HPO_4 H_2O_{dd}	28.39 g 1000 ml
Phosphate buffer autoclaved, stored at room temperature	ad. NaH_2PO_4 (0.2 M) to Na_2HPO_4 (0.2 M) until pH value of 7.4 reached	
Reversion indicator solution I (RI solution I) pH 7.3 (± 0.1) autoclaved, stored at room temperature, protected from light	$MgSO_4$ $(H_2O)_7$ Citric acid (H_2O) K_2HPO_4 $NaNH_4HPO_4$ $(H_2O)_4$ H_2O_{dd} Bromocresol purple (1.7 mg/ml)	0.4 g 4.0 g 20 g 7.0 g Ad. to 1 l 30 ml
Reversion indicator solution II (RI solution II) pH 7.3 (± 0.1) autoclaved, stored at room temperature protected from light	D-glucose H_2O_{dd}	10 g ad. to 1 l

Table 24: Media and cultures in the Ames fluctuation assay

Medium	Substance	Quantity
Nutrient medium autoclaved, poured in the Petri plates (each 25 ml, d = 94 mm) stored at 4 °C for one week	Nutrient Broth No. 2 Bacto™ Agar H_2O_{dd}	25 g 15 g ad. to 1 l
Top agar autoclaved, stored at room temperature, protected from light	Bacto™ Agar NaCl H_2O_{dd}	0.6 g 0.5 g ad. to 100 ml
Stock culture pH 7.5 (± 0.1) sterilized by filtration (0.2 µm), stored at 4 °C	Nutrient Broth No. 2 NaCl Glycerol (87%) H_2O_{dd}	0.94 g 0.062 g 4.6 ml ad. to 25 ml
Growth medium pH 7.5 (± 0.1) autoclaved, stored at -20°C	Nutrient Broth No. 2 NaCl H_2O_{dd}	18.8 g 1.24 g ad. to 1 l

Exposure medium (EM, stock solution) pH 7.0 (± 0.2) sterilized by filtration (0.2 µm), stored at 4 °C	$MgSO_4$ $(H_2O)_7$	0.2 g
	Citric acid (H_2O)	2.0 g
	K_2HPO_4	10 g
	$NaNH_4HPO_4$ $(H_2O)_4$	3.5 g
	D-glucose	4.0 g
	H_2O_{dd}	ad. to 1 l
Exposure medium (EM, working solution) prepared immediately before use	EM- stock solution	100 ml
	L-Histidine (1 mg/ml)	0.1 ml
	D-Biotin (0.122 mg/ml)	0.6 ml
Reversion indicator medium prepared immediately before use	RI solution I	103 ml
	RI solution II	100 ml
	D-Biotin (0.122 mg/ml)	4.0 ml

Table 25: Antibiotics for the Ames fluctuation assay

Solution	Substance	Quantity
Ampicillin (8 mg/ml) sterilized by filtration (0.2 µm), stored at -20 °C	Ampicillin sodium salt	400 mg
	H_2O_{dd}	50 ml
Tetracycline (0.8 mg/ml) sterilized by filtration (0.2 µm), stored at -20 °C	Tetracycline hydrochloride	40 mg
	H_2O_{dd}	50 ml
Neomycin (8 mg/ml) sterilized by filtration (0.2 µm), stored at -20 °C	Neomycin sulfate	400 mg
	H_2O_{dd}	50 ml

Preparation of overnight culture: Under the sterile condition, 20 ml of growth medium supplemented with 125 µl of ampicillin solution was pipetted into a 100 ml Duran® baffled flask, and 20 µl of the respective test strain aliquot (TA98 and TA100) were added. The flasks were covered with aluminum paper and incubated in a 37°C shaking incubator at approximately 125 rpm to avoid foaming overnight but not exceeding 16 h. After the cultivation, the flasks were placed directly in an ice bath to stop the growth of the bacteria.

Storage of the test strains: the overnight culture of various strains was diluted at 1:2 in stock culture (s. Tab. 24) and aliquoted after snap freezing in liquid nitrogen then stored at -80°C.

Preparation of test strains: In the assay, a final cell density of 180 ± 10 Formazine Attenuation Units (FAU) for TA98 and 45 ± 5 FAU for TA100 is recommended. The density of bacteria in the overnight culture expressed as turbidity was determined

according to ISO 7027-1: 2016 by comparison to the standard curve of formazine solutions with a range between 25 FAU to 250 FAU (s. Fig. 46).

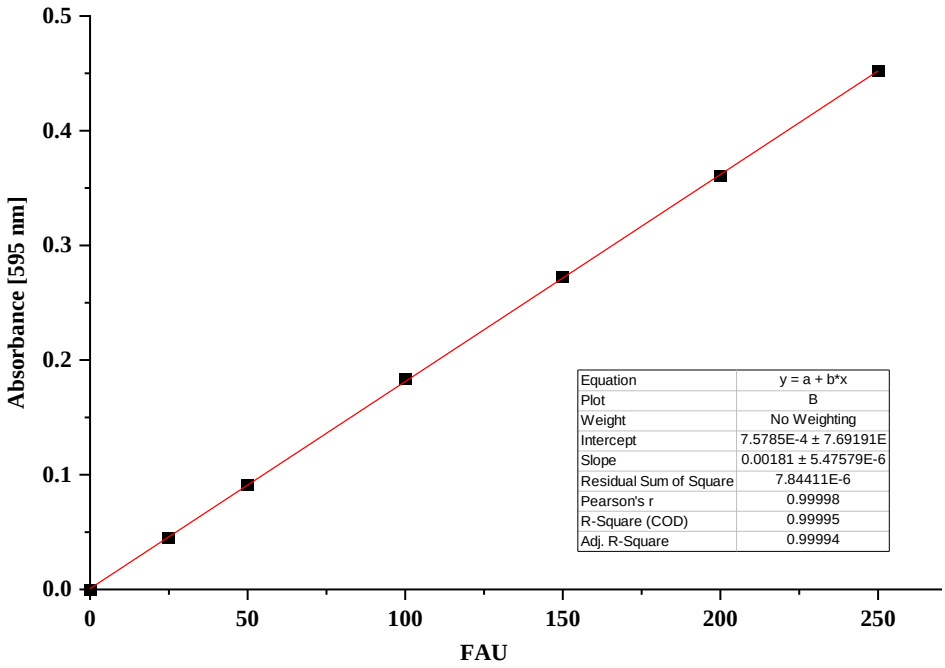

Figure 46: Formazine standard curve

The FAU values of overnight culture were calculated using the formazine calibration curve. In order to determine the density, the overnight culture was diluted at 1:10 in the growth medium (s. Tab. 24) and photometrically measured at the wavelength 595 nm against the growth medium. Then a dilution factor was calculated according to the following equations:

In the case of Strain TA98:

$$d = \frac{X_{595\,nm}\,[FAU]}{180}$$

In the case of strain TA100:

$$d = \frac{X_{595\,nm}\,[FAU]}{45}$$

with $X_{595\,nm}$: the FAU value of the 10-fold diluted overnight culture

using the dilution factor (d) and the calculated final volume (V_{final}, depending on how many 24 well plates to be tested) to determine the required volume of the overnight culture and the exposure medium (working solution; s. Tab. 24):

$$V_{culture} = \frac{V_{final}}{d}$$

$$V_{exp.medium} = V_{final} - V_{culture}$$

The FAU values of adjusted overnight culture were then measured again photometrically but against exposure medium. If the required FAU deviated, an appropriate volume of overnight culture or exposure medium (working solution) would be added until the value of FAU needed has been reached.

Preparation of S9-mix: The S9-mix was always prepared freshly on the day before testing and kept permanently on ice.

Table 26: Composition of S9 mix

Solution	Volume
Phosphate buffer solution (pH 7.4)	500 µl
S9 fraction	300 µl
NADP (40 mM)	100 µl
KCl (0.15 M)	33 µl
$MgCl_2$ (0.25 M)	32 µl
Glucose-6-phosphate (0.24 M)	25 µl
H_2O_{dd}	10 µl

Test for pyrrolizidine alkaloids: The PA congeners with six different concentrations were incubated using a sterile 24-well plate. Vehicle solution (2%) was used as a negative control to establish the spontaneous mutation, and the positive controls varied depending on the tested strain. The positive controls with a single dose to demonstrate the effective performance of the assay selected based on the type of bacterial strains were listed in Tab. 27, 10 µl of the test solutions, or the controls were added to 490 µl of bacterial suspension adjusted to the corresponding FAU. For determining the mutagenicity with metabolic activation, 17 µl of S9-mix would also be added to each well. The plates were then incubated in the dark at about 37°C and shaken at 125 rpm for 100 min. Next, 2.5 ml of reversion indicator medium (s. Tab. 23) was filled into each well and resuspended. The content of each well of the 24-well plate in 50 µl aliquots was immediately transferred to 48 wells of a 384-well plate. Subsequently, the 384-well plates were incubated continually in the dark at 37°C for 48 h. After the incubation period, the number of positive wells was counted and given in percent. (48 = 100%).

Table 27: Positive controls for different *Salmonella typhimurium* strains with or without S9-mix

Salmonella typhimurium strain	Positive control without S9-mix	Positive control with S9-mix
TA98	4-Nitro-*O*-phenylenediamine (1 mg/ml)	2-Aminoanthracene (5 µg/ml)
TA100	Nitrofurantoin (12.5 µg/ml)	2-Aminoanthracene (80 µg/ml)

6.7 Micronucleus assay

The time to process the plates followed the standard procedure published by Lehmann et al. with some modifications (Lehmann et al., 2006; Lehmann and Metzler, 2004) combined with the guideline OECD 487 (OECD, 2016).

HepG2 C9 (CYP3A4) cells were seeded with a density of 700,000 cells/Petri dish in 2 ml culture medium. After adherence for 24 h, the medium was shifted, and the exposure duration of 24 h for the cell culture to PA congeners (1, 5, 25, 75, 150, and 300 µM) was applied. After that, the medium was replaced with a fresh medium, and the cells were incubated for an additional 72 h to induce cell division, allowing the formation of micronuclei. Then the medium was removed, and cell layers were first rinsed with 2 ml PBS-/- and trypsinized using 300 µl of trypsin-EDTA (0.01%) solution for 10 – 15 min at 37°C with 5% CO_2, then stopped by addition of 700 µl DMEM-HG. The cells were, after resuspension, transferred into micro-reaction vessels and centrifuged at 500 x g for 5 min and the supernatants were removed. After that, the cell pellets were resuspended in 1 ml PBS and then transferred to 15 ml Falcon™ tubes. 4 ml of ethanol was added to each tube and placed in the freezer at -20°C for at least 30 min. After fixation and centrifugation (1000 x g, 10 min), the liquid supernatant was removed, 750 µl of DAPI staining working solution (s. Tab. 28) was added, and after resuspension, pipetted about 10 µl on the microscope slides while always protected from light. Micronucleus were visualized under a light microscope with a UV lamp and a 631.25 immersion oil objective. 1000 nuclei of each sample were inspected for the occurrence of micronuclei. The results were presented as the rate of micronuclei, i.e., number of micronuclei/1000 nuclei. Negative controls were treated with corresponding solvents. MMS (200 µM; s. Tab. 28), a DNA damaging agent, has been used as a positive control to demonstrate the sensitivity of the test system.

Table 28: Solutions for the micronucleus assay

Solution	Substance	Quantity
Staining buffer stored at 4 °C	Tris base	2.42 g
	NaCl	1.75 g
	$CaCl_2$ $(H_2O)_2$	29.4 mg
	$MgCl_2$ $(H_2O)_6$	20.3 mg
	Nodidet® P40	200 µl
	H_2O_{dd}	200 ml
DAPI stock solution (14.3 mM) stored at 4 °C, protected from light	4',6-Diamidino-2'-phenylindole dihydrochloride	10 mg
	H_2O_{dd}	2 ml
DAPI working solution (43 µM) prepared immediately before use,	DAPI stock solution	3 µl
	Staining buffer	1 ml

protected from light		
Positive control: MMS (200 µM) stored at -20 °C	Methyl methanesulfonate DMSO	22 mg 1 ml

6.8 Bicinchoninic acid (BCA) assay for protein quantification

The plates from the BROD assay were rinsed with 0.9% NaCl solution after incubation and stored at -80°C overnight. To lysing the cells, the plates were frozen again. This freeze-thaw cycle was repeated 2-3 times after thawing at room temperature for 15 min. Afterward, 75 µl of bidest. water was added to each well of the plates, and used a culture spatula to homogenize the lysates. A set of diluted standards was prepared as described in Tab. 29. For protein content determination, 25 µl of the lysate and each standard were transferred into a microplate well, 200 µl of the assay working reagent (s. Tab. 29) was added to each well, the plates were covered with an aluminum paper and incubated with gentle shaking at 37 °C for 30 min. For the GSH assay, 20 µl lysate was instead of 25 µl used for further determination. After cooling down to room temperature, the absorbance was measured at 562 nm. The protein content was calculated by comparison to the standard curve with known concentrations of BSA (s. Tab. 30).

Table 29: Solutions for the BCA assay

Solution	Substance	Quantity
BSA stock solution (2 mM) aliquot, stored at -20 °C	Bovine serum albumin H_2O_{dd}	100 mg 50 ml
Assay working reagent prepared immediately before use	BCA reagent A BCA reagent B	50:1 (v/v)

Table 30: Pipetting scheme for the preparation of BSA calibration standards

Calibration standard [Cal Nr.]	Final concentration of BSA [µg/ml]	Volume of BSA stock solution [2 mM] [µl]	Volume of H_2O_{dd} [µl]
A	2000	300	0
B	1500	375	125
C	1000	325	325
D	500	325 from Cal C	325
E	250	325 from Cal D	325
F	125	325 from Cal E	325
G	25	100 from Cal F	400
H	0 (Blank)	0	400

6.9 Data analysis

Each assay was carried out for at least three different cell preparations of each cell type and determined from three independent plate wells. Statistical significance was calculated by Dunnett´s test in GraphPad InStat V3 (GraphPad Software, Inc.) for multiple comparisons with solvent control. The differences between the two groups were analyzed using an unpaired t-test.

In Alamar blue assay, six different analyzable concentrations with approximately half-log intervals between test points were used to investigate a concentration-dependent response. Both results of test substances and controls were corrected for background fluorescence of resazurin reagent alone. For calculation of EC_{50} values, the data means with standard deviations were fitted with exponential or sigmoidal concentration-response curve using OriginLab 2020.

Benchmark Doses (BMDs) in micronucleus assay were analyzed modeling the concentration-response data generated from micronucleus assay via PROAST web application (RIVM/EFSA, version 65.2). Critical effect size (CES) set as 1 (100%), representing a 2-fold increase over the spontaneous micronucleus in vehicle control, helps to minimize the effect of the background counts. In this application, data were fitted with mathematic models from Exponential and Hill families, which are suitable for analyzing continuous data. The model with lower Akeike Information Criterion (AIC) was chosen to calculate the benchmark dose (BMD) that led to a doubling of micronuclei counts over the background as well as their lower (BMDL) and upper (BMDU) 10% confidence limits. Critical effect dose (CED), lower bound (CEDL), and upper bound (CEDU) of CED corresponding to BMD, BMDL, and BMDU, respectively.

REP factors of PA congeners were calculated by comparing to riddelliine, which were represented as the ratio of EC_{50}/BMD of riddelliine.

REFERENCES

Acosta, D., Anuforo, D.C., McMillin, R., Soine, W.H., Smith, R.V., 1979. Comparison of cytochrome P-450 levels in adult rat liver, postnatal rat liver, and primary cultures of postnatal rat hepatocytes. Life Sciences 25, 1413–1418. https://doi.org/10.1016/0024-3205(79)90419-3.

Alderson, T., Clark, A.M., 1966. Interlocus specificity for chemical mutagens in Aspergillus nidulans. Nature 210, 593–595. https://doi.org/10.1038/210593a0.

Allemang, A., Mahony, C., Lester, C., Pfuhler, S., 2018. Relative potency of fifteen pyrrolizidine alkaloids to induce DNA damage as measured by micronucleus induction in HepaRG human liver cells. Food and chemical toxicology : an international journal published for the British Industrial Biological Research Association 121, 72–81. https://doi.org/10.1016/j.fct.2018.08.003.

Ames, B.N., Lee, F.D., Durston, W.E., 1973. An improved bacterial test system for the detection and classification of mutagens and carcinogens. Proceedings of the National Academy of Sciences of the United States of America 70, 782–786. https://doi.org/10.1073/pnas.70.3.782.

Anderson, M.E., 1985. Determination of glutathione and glutathione disulfide in biological samples, in: Meister, A. (Ed.), Glutamate, glutamine, glutathione, and related compounds, vol. 113. Elsevier, pp. 548–555.

ANZFA, 2001. Pyrrolizidine Alkaloids in Food: A Toxicological Review and Risk Assessment.

Arseculeratne, S.N., Gunatilaka, A.A.L., Panabokke, R.G., 1981. Studies on medicinal plants of Sri Lanka: Occurrence of pyrrolizidine alkaloids and hepatotoxic properties in some traditional medicinal herbs. Journal of Ethnopharmacology 4, 159–177. https://doi.org/10.1016/0378-8741(81)90033-7.

Arseculeratne, S.N., Gunatilaka, A.A.L., Panabokke, R.G., 1985. Studies on medicinal plants of sri lanka. part 14: toxicity of some traditional medicinal herbs. Journal of Ethnopharmacology 13, 323–335. https://doi.org/10.1016/0378-8741(85)90078-9.

Bah, M., Bye, R., Pereda-Miranda, R., 1994. Hepatotoxic pyrrolizidine alkaloids in the Mexican medicinal plant Packera candidissima (Asteraceae: Senecioneae). Journal of Ethnopharmacology 43, 19–30. https://doi.org/10.1016/0378-8741(94)90112-0.

Baldwin, S.J., Bloomer, J.C., Smith, G.J., Ayrton, A.D., Clarke, S.E., Chenery, R.J., 1995. Ketoconazole and sulphaphenazole as the respective selective inhibitors of P4503A and 2C9. Xenobiotica; the fate of foreign compounds in biological systems 25, 261–270. https://doi.org/10.3109/00498259509061850.

Benford, D., Bolger, P.M., Carthew, P., Coulet, M., DiNovi, M., Leblanc, J.C., Renwick, A.G., Setzer, W., Schlatter, J., Smith, B., Slob, W., Williams, G., Wildemann, T., 2010. Application of the Margin of Exposure (MOE) approach to

substances in food that are genotoxic and carcinogenic. Food and chemical toxicology : an international journal published for the British Industrial Biological Research Association 48 Suppl 1, S2-24. https://doi.org/10.1016/j.fct.2009.11.003.

Berg, J.M., Tymoczko, J.L., Gatto jr., G.J., Stryer, L., Held, A., Maxam, G., Seidler, L., Häcker, B., Jarosch, B., 2017. Biochemistry 8. Springer Spektrum, Berlin, Heidelberg.

Berry, M.N., Friend, D.S., 1969. High-yield preparation of isolated rat liver parenchymal cells: a biochemical and fine structural study. The Journal of cell biology 43, 506–520. https://doi.org/10.1083/jcb.43.3.506.

BfArM, 1992. Bekanntmachung über die Zulassung und Registrierung von Arzneimitteln (Abwehr von Arzneimittelrisiken - Stufe II) von 5.Juni.1992.

BfArM, 2016. Bekanntmachung zur Prüfung des Gehalts an Pyrrolizidinalkaloiden zur Sicherstellung der Qualität und Unbedenklichkeit von Arzneimitteln, die pflanzliche Stoffe bzw. pflanzliche Zubereitungen oder homöopathische Zubereitungen aus pflanzlichen Ausgangsstoffen als Wirkstoffe enthalten vom 1. März 2016.

BfR, 2011. Analytik und Toxizität von Pyrrolizidinalkaloiden sowie eine Einschätzung des gesundheitlichen Risikos durch deren Vorkommen in Honig.

BfR, 2013. Pyrrolizidinalkaloide in Kräutertees und Tees.

BfR, 2015. International collaborative study for the determination of pyrrolizidine alkaloids in honey and herbal tea by SPE-LC-MS/MS: (BfR-PA-Honey-1.0_2013) (BfR-PA-Tea-1.0_2013). Bundesinstitut für Risikobewertung, Berlin, 91 pp.

Bissell, D.M., Guzelian, P.S., 1979. Ascorbic acid deficiency and cytochrome P-450 in adult rat hepatocytes in primary monolayer culture. Archives of Biochemistry and Biophysics 192, 569–576. https://doi.org/10.1016/0003-9861(79)90127-9.

Bissell, D.M., Hammaker, L.E., Meyer, U.A., 1973. Parenchymal cells from adult rat liver in nonproliferating monolayer culture. I. Functional studies. The Journal of cell biology 59, 722–734. https://doi.org/10.1083/jcb.59.3.722.

Bodi, D., Ronczka, S., Gottschalk, C., Behr, N., Skibba, A., Wagner, M., Lahrssen-Wiederholt, M., Preiss-Weigert, A., These, A., 2014. Determination of pyrrolizidine alkaloids in tea, herbal drugs and honey. Food additives & contaminants. Part A, Chemistry, analysis, control, exposure & risk assessment 31, 1886–1895. https://doi.org/10.1080/19440049.2014.964337.

Bradford, M.M., 1976. A rapid and sensitive method for the quantitation of microgram quantities of protein utilizing the principle of protein-dye binding. Analytical Biochemistry 72, 248–254. https://doi.org/10.1016/0003-2697(76)90527-3.

Brink, N.G., 1966. The mutagenic activity of heliotrine in drosophila. Mutation Research/Fundamental and Molecular Mechanisms of Mutagenesis 3, 66–72. https://doi.org/10.1016/0027-5107(66)90008-X.

Brink, N.G., 1969. The mutagenic activity of the pyrrolizidine alkaloid heliotrine in Drosophila melanogaster II. Chromosome rearrangements. Mutation Research/Fundamental and Molecular Mechanisms of Mutagenesis 8, 139–146. https://doi.org/10.1016/0027-5107(69)90148-1.

Bruggeman, I.M., van der Hoeven, J.C.M., 1985. Induction of SCEs by some pyrrolizidine alkaloids in V79 Chinese hamster cells co-cultured with chick embryo hepatocytes. Mutation Research Letters 142, 209–212. https://doi.org/10.1016/0165-7992(85)90025-9.

Buhler, D.R., Kedzierski, B., 1986. Biological reactive intermediates of pyrrolizidine alkaloids. Advances in experimental medicine and biology 197, 611–620. https://doi.org/10.1007/978-1-4684-5134-4_57.

Bull, L.B., Culvenor, C.C.J., Dick, A.T., 1968. The pyrrolizidine alkaloids : their chemistry-pathogenicity and other biological properties. Amsterdam : North-Holland.

Burke, M.D., Thompson, S., Weaver, R.J., Wolf, C.R., Mayers, R.T., 1994. Cytochrome P450 specificities of alkoxyresorufin O-dealkylation in human and rat liver. Biochemical Pharmacology 48, 923–936. https://doi.org/10.1016/0006-2952(94)90363-8.

Chan, P., 1993. NTP technical report on the toxicity studies of riddelliine (CAS no. 23246 - 96 - 0) administered by gavage to F344/N rats and B6C3F1 mice. Toxicity Report Series 27.

Cheeke, P.R., Pierson-Goeger, M.L., 1983. Toxicity of Senecio jacobaea and pyrrolizidine alkaloids in various laboratory animals and avian species. Toxicology letters 18, 343–349. https://doi.org/10.1016/0378-4274(83)90116-9.

Chen, J.Y., Brockmöller, J., Tzvetkov, M.V., Wang, L.J., Chen, X.J., 2019a. An in vitro study on interaction of anisodine and monocrotaline with organic cation transporters of the SLC22 and SLC47 families. Chinese journal of natural medicines 17, 490–497. https://doi.org/10.1016/S1875-5364(19)30070-6.

Chen, L., Mulder, P.P.J., Louisse, J., Peijnenburg, A. A. C. M., Wesseling, S., Rietjens, I.M.C.M., 2017. Risk assessment for pyrrolizidine alkaloids detected in (herbal) teas and plant food supplements. Regulatory toxicology and pharmacology : RTP 86, 292–302. https://doi.org/10.1016/j.yrtph.2017.03.019.

Chen, L., Ning, J., Louisse, J., Wesseling, S., Rietjens, I.M.C.M., 2018. Use of physiologically based kinetic modelling-facilitated reverse dosimetry to convert in vitro cytotoxicity data to predicted in vivo liver toxicity of lasiocarpine and riddelliine in rat. Food and chemical toxicology : an international journal published for the British Industrial Biological Research Association 116, 216–226. https://doi.org/10.1016/j.fct.2018.04.012.

Chen, L., Peijnenburg, A. A. C. M., Haan, L. D., Rietjens, I.M.C.M., 2019b. Prediction of in vivo genotoxicity of lasiocarpine and riddelliine in rat liver using

a combined in vitro-physiologically based kinetic modelling-facilitated reverse dosimetry approach. Archives of toxicology 93, 2385–2395. https://doi.org/10.1007/s00204-019-02515-5.

Chen, T., Mei, N., Fu, P.P., 2010. Genotoxicity of pyrrolizidine alkaloids. Journal of applied toxicology : JAT 30, 183–196. https://doi.org/10.1002/jat.1504.

Chen, Z.Y., Eaton, D.L., 1991. Differential regulation of cytochrome(s) P450 2B1/2 by phenobarbital in hepatic hyperplastic nodules induced by aflatoxin B1 or diethylnitrosamine plus 2-acetylaminofluorene in male F344 rats. Toxicology and Applied Pharmacology 111, 132–144. https://doi.org/10.1016/0041-008X(91)90142-2.

Chou, M.W., Wang, Y.P., Yan, J., Yang, Y.C., Beger, R.D., Williams, L.D., Doerge, D.R., Fu, P.P., 2003. Riddelliine N-oxide is a phytochemical and mammalian metabolite with genotoxic activity that is comparable to the parent pyrrolizidine alkaloid riddelliine. Toxicology letters 145, 239–247. https://doi.org/10.1016/S0378-4274(03)00293-5.

Chou, M.W., Yan, J., Nichols, J., Xia, Q.S., Beland, F.A., Chan, P.C., Fu, P.P., 2004. Correlation of DNA adduct formation and riddelliine-induced liver tumorigenesis in F344 rats and B6C3F1 mice Cancer Lett. 193 (2003) 119-125. Cancer letters 207, 119–125. https://doi.org/10.1016/j.canlet.2003.12.001.

Chu, P.S., Segall, H.J., 1991. Species difference in the urinary excretion of isatinecic acid from the pyrrolizidine alkaloid retrorsine. Comparative Biochemistry and Physiology Part C: Comparative Pharmacology 100, 683–686. https://doi.org/10.1016/0742-8413(91)90061-W.

Chung, W.G., Buhler, D.R., 2004. Differential metabolism of the pyrrolizidine alkaloid, senecionine, in Fischer 344 and Sprague-Dawley rats. Archives of pharmacal research 27, 547–553. https://doi.org/10.1007/BF02980130.

Chung, W.G., Miranda, C.L., Buhler, D.R., 1995. A cytochrome P4502B form is the major bioactivation enzyme for the pyrrolizidine alkaloid senecionine in guinea pig. Xenobiotica; the fate of foreign compounds in biological systems 25, 929–939. https://doi.org/10.3109/00498259509046664.

Clark, A.M., 1959. Mutagenic activity of the alkaloid heliotrine in Drosophila. Nature 183, 731–732. https://doi.org/10.1038/183731a0.

Clark, A.M., 1976. Naturally occurring mutagens. Mutation Research/Reviews in Genetic Toxicology 32, 361–374. https://doi.org/10.1016/0165-1110(76)90006-3.

COT, 2008. Committee on toxicity of chemicals in in food consumer products and the enviroment (COT). COT Statement on Pyrrolizidine Alkaloids in Food.

Couet, C.E., Hopley, J., Hanley, A.B., 1996. Metabolic activation of pyrrolizidine alkaloids by human, rat and avocado microsomes. Toxicon 34, 1058–1061. https://doi.org/10.1016/0041-0101(96)00056-6.

Coulombe, R.A., Drew, G.L., Stermitz, F.R., 1999. Pyrrolizidine alkaloids crosslink DNA with actin. Toxicology and Applied Pharmacology 154, 198–202. https://doi.org/10.1006/taap.1998.8552.

Countryman, P.I., Heddle, J.A., 1976. The production of micronuclei from chromosome aberrations in irradiated cultures of human lymphocytes. Mutation Research/Fundamental and Molecular Mechanisms of Mutagenesis 41, 321–331. https://doi.org/10.1016/0027-5107(76)90105-6.

Creeper, J.H., MITCHELL, A.A., JUBB, T.F., Colegate, S.M., 1999. Pyrrolizidine alkaloid poisoning of horses grazing a native heliotrope (Heliotropium ovalifolium). Australian Vet J 77, 401–402. https://doi.org/10.1111/j.1751-0813.1999.tb10318.x.

Crews, C., Startin, J.R., Clarke, P.A., 1997a. Determination of pyrrolizidine alkaloids in honey from selected sites by solid phase extraction and HPLC-MS. Food Additives & Contaminants 14, 419–428. https://doi.org/10.1080/02652039709374547.

Crews, C., Startin, J.R., Clarke, P.A., 1997b. Determination of pyrrolizidine alkaloids in honey from selected sites by solid phase extraction and HPLC‐MS. Food Additives & Contaminants 14, 419–428. https://doi.org/10.1080/02652039709374547.

Culvenor, C., Edgar, J.A., Jago, M.V., Outteridge, A., Peterson, J.E., Smith, L.W., 1976. Hepato- and pneumotoxicity of pyrrolizidine alkaloids and derivatives in relation to molecular structure. Chemico-biological interactions 12, 299–324. https://doi.org/10.1016/0009-2797(76)90046-6.

Dalefield, R.R., Gosse, M.A., Bartholomaeus, A., Schyvens, C.G., Müller, U., 2012. Acute toxicity of heliotrine in male Han Wistar rats. Journal Toxicology Research 2, 12–19.

Dalefield, R.R., Gosse, M.A., Müller, U., 2015. Acute toxicity of echimidine in male Han Wistar rats. Journal Toxicology Research 4, 42–47.

Donato, M.T., Gómez-Lechón, M.J., Castell, J.V., 1993. A microassay for measuring cytochrome P450IA1 and P450IIB1 activities in intact human and rat hepatocytes cultured on 96-well plates. Analytical Biochemistry 213, 29–33. https://doi.org/10.1006/abio.1993.1381.

Donato, M.T., Jover, R., Gómez-Lechón, M.J., 2013. Hepatic cell lines for drug hepatotoxicity testing: limitations and strategies to upgrade their metabolic competence by gene engineering. Current drug metabolism 14, 946–968. https://doi.org/10.2174/1389200211314090002.

Donato, M.T., Lahoz, A., Castell, J.V., Gómez-Lechón, M.J., 2008. Cell lines: a tool for in vitro drug metabolism studies. Current drug metabolism 9, 1–11. https://doi.org/10.2174/138920008783331086.

Donato, M.T., Tolosa, L., Gómez-Lechón, M.J., 2015. Culture and functional characterization of human hepatoma HepG2 cells. Methods in molecular biology (Clifton, N.J.) 1250, 77–93. https://doi.org/10.1007/978-1-4939-2074-7_5.

Dorn, S.B., Bolt, H.M., Thevis, M., Diel, P., Degen, G.H., 2008. Induction of micronuclei in V79 cells by the anabolic doping steroids tetrahydrogestrinone and trenbolone. Archives of toxicology 82, 257–263. https://doi.org/10.1007/s00204-007-0241-2.

Drew, R., Miners, J.O., 1984. The effects of buthionine sulphoximine (BSO) on glutathione depletion and xenobiotic biotransformation. Biochemical Pharmacology 33, 2989–2994. https://doi.org/10.1016/0006-2952(84)90598-7.

Dueker, S.R., Lamé, M.W., Segall, H.J., 1992. Hydrolysis of pyrrolizidine alkaloids by guinea pig hepatic carboxylesterases. Toxicology and Applied Pharmacology 117, 116–121. https://doi.org/10.1016/0041-008X(92)90225-H.

Eagling, V.A., Tjia, J.F., Back, D.J., 1998. Differential selectivity of cytochrome P450 inhibitors against probe substrates in human and rat liver microsomes. British journal of clinical pharmacology 45, 107–114. https://doi.org/10.1046/j.1365-2125.1998.00679.x.

Eastman, D.F., Dimenna, G.P., Segall, H.J., 1982. Covalent binding of two pyrrolizidine alkaloids, senecionine and seneciphylline, to hepatic macromolecules and their distribution, excretion, and transfer into milk of lactating mice. Drug metabolism and disposition: the biological fate of chemicals 10, 236–240.

Edgar, J.A., Colegate, S.M., Boppré, M., Molyneux, R.J., 2011. Pyrrolizidine alkaloids in food: a spectrum of potential health consequences. Food additives & contaminants. Part A, Chemistry, analysis, control, exposure & risk assessment 28, 308–324. https://doi.org/10.1080/19440049.2010.547520.

Edgar, J.A., Lin, H.J., Kumana, C.R., Ng, M.M., 1992. Pyrrolizidine alkaloid composition of three Chinese medicinal herbs, Eupatorium cannabinum, E. japonicum and Crotalaria assamica. The American journal of Chinese medicine 20, 281–288. https://doi.org/10.1142/S0192415X92000291.

Edgar, J.A., Molyneux, R.J., Colegate, S.M., 2015. Pyrrolizidine alkaloids: potential role in the etiology of cancers, pulmonary hypertension, congenital anomalies, and liver disease. Chemical research in toxicology 28, 4–20. https://doi.org/10.1021/tx500403t.

Edgar, J.A., Roeder, E., Molyneux, R.J., 2002. Honey from plants containing pyrrolizidine alkaloids: a potential threat to health. Journal of agricultural and food chemistry 50, 2719–2730. https://doi.org/10.1021/jf0114482.

Edgar, J.A., Smith, L.W., 2000. Transfer of pyrrolizidine alkaloids into eggs: food safety implications, in: Tu, A.T., Gaffield, W. (Eds.), Natural and selected synthetic toxins: Biological implications / [editors] Anthony T. Tu, William Gaffield, vol. 745. American Chemical Society, Washington, DC, pp. 118–128.

EFSA Panel on Contaminants in the Food Chain, 2007. Opinion of the scientific panel on contaminants in the food chain [CONTAM] related to the potential increase of consumer health risk by a possible increase of the existing maximum levels for aflatoxins in almonds, hazelnuts and pistachios and derived prod. EFS2 5, 446. https://doi.org/10.2903/j.efsa.2007.446.

EFSA Panel on Contaminants in the Food Chain, 2011. Scientific opinion on pyrrolizidine alkaloids in food and feed. EFS2 9, 2406. https://doi.org/10.2903/j.efsa.2011.2406.

EFSA Panel on Contaminants in the Food Chain, 2016. Dietary exposure assessment to pyrrolizidine alkaloids in the European population. EFS2 14. https://doi.org/10.2903/j.efsa.2016.4572.

EFSA Panel on Contaminants in the Food Chain, 2017. Risks for human health related to the presence of pyrrolizidine alkaloids in honey, tea, herbal infusions and food supplements. EFS2 15. https://doi.org/10.2903/j.efsa.2017.4908.

Ellman, G., Lysko, H., 1979. A precise method for the determination of whole blood and plasma sulfhydryl groups. Analytical Biochemistry 93, 98–102. https://doi.org/10.1016/S0003-2697(79)80122-0.

EMA, 2014. Public statement on the use of herbal medicinal products containing toxic, unsaturated pyrrolizidine alkaloids (PAs), EMA/HMPC/893108/2011.

EMA, 2020. Public statement on the use of herbal medicinal products containing toxic, unsaturated pyrrolizidine alkaloids (PAs) including recommendations regarding contamination of herbal medicinal products with pyrrolizidine alkaloids (Draft), EMA/HMPC/893108/2011 Rev.1.

Eröksüz, Y., Eröksüz, H., Ozer, H., Sener, B., Tosun, F., Akyüz, C., 2001. Toxicity of dietary Heliotropium dolosum seed to mice. Veterinary and human toxicology 43, 152–155.

Evarts, R.P., Marsden, E., Thorgeirsson, S.S., 1984. Regulation of heme metabolism and cytochrome p-450 levels in primary culture of rat hepatocytes in a defined medium. Biochemical Pharmacology 33, 565–569. https://doi.org/10.1016/0006-2952(84)90308-3.

Fahl, W.E., Michalopoulos, G., Sattler, G.L., Jefcoate, C.R., Pitot, H.C., 1979. Characteristics of microsomal enzyme controls in primary cultures of rat hepatocytes. Archives of Biochemistry and Biophysics 192, 61–72. https://doi.org/10.1016/0003-9861(79)90071-7.

Fashe, M.M., Juvonen, R.O., Petsalo, A., Räsänen, J., Pasanen, M., 2015. Species-specific differences in the in vitro metabolism of lasiocarpine. Chemical research in toxicology 28, 2034–2044. https://doi.org/10.1021/acs.chemrestox.5b00253.

Fayer, J.L., Petullo, D.M., Ring, B.J., Wrighton, S.A., Ruterbories, K.J., 2001. A novel testosterone 6β-hydroxylase activity assay for the study of CYP3A-mediated metabolism, inhibition, and induction in vitro. Journal of

Pharmacological and Toxicological Methods 46, 117–123. https://doi.org/10.1016/S1056-8719(02)00168-5.

Field, R.A., Stegelmeier, B.L., Colegate, S.M., Brown, A.W., Green, B.T., 2015. An in vitro comparison of the cytotoxic potential of selected dehydropyrrolizidine alkaloids and some N-oxides. Toxicon : official journal of the International Society on Toxinology 97, 36–45. https://doi.org/10.1016/j.toxicon.2015.02.001.

Frei, H., Lüthy, J., Brauchli, J., Zweifel, U., Würgler, F.E., Schlatter, C., 1992. Structure/activity relationships of the genotoxic potencies of sixteen pyrrolizidine alkaloids assayed for the induction of somatic mutation and recombination in wing cells of Drosophila melanogaster. Chemico-biological interactions 83, 1–22. https://doi.org/10.1016/0009-2797(92)90088-3.

Fries, R. D., Mitsuhashi, M., 1995. Quantification of mitogen induced human lymphocyte proliferation: comparison of alamarBlue assay to 3H-thymidine incorporation assay. Journal of clinical laboratory analysis 9, 89–95. https://doi.org/10.1002/jcla.1860090203.

Fu, P., Xia, Q.S., Ge, L., Chou, M., 2002. Genotoxic Pyrrolizidine Alkaloids — Mechanisms Leading to DNA Adduct Formation and Tumorigenicity. IJMS 3, 948–964. https://doi.org/10.3390/i3090948.

Fu, P.P., Chou, M.W., Xia, Q., Yang, Y.C., Yan, J., Doerge, D.R., Chan, P.C., 2001. GENOTOXIC PYRROLIZIDINE ALKALOIDS AND PYRROLIZIDINE ALKALOID N -OXIDES—MECHANISMS LEADING TO DNA ADDUCT FORMATION AND TUMORIGENICITY. Journal of Environmental Science and Health, Part C 19, 353–385. https://doi.org/10.1081/GNC-100107580.

Fu, P.P., Xia, Q.S., Ge, L., Chou, M.W., 2004. Pyrrolizidine alkaloids--genotoxicity, metabolism enzymes, metabolic activation, and mechanisms. Drug metabolism reviews 36, 1–55. https://doi.org/10.1081/dmr-120028426.

Gao, L., Rutz, L., Schrenk, D., 2020. Structure-dependent hepato-cytotoxic potencies of selected pyrrolizidine alkaloids in primary rat hepatocyte culture. Food and chemical toxicology : an international journal published for the British Industrial Biological Research Association 135, 110923. https://doi.org/10.1016/j.fct.2019.110923.

Geburek, I., Preiss-Weigert, A., Lahrssen-Wiederholt, M., Schrenk, D., These, A., 2020a. In vitro metabolism of pyrrolizidine alkaloids - Metabolic degradation and GSH conjugate formation of different structure types. Food and chemical toxicology : an international journal published for the British Industrial Biological Research Association 135, 110868. https://doi.org/10.1016/j.fct.2019.110868.

Geburek, I., Schrenk, D., These, A., 2020b. In vitro biotransformation of pyrrolizidine alkaloids in different species: part II-identification and quantitative assessment of the metabolite profile of six structurally different pyrrolizidine alkaloids. Archives of toxicology 94, 3759–3774. https://doi.org/10.1007/s00204-020-02853-9.

Gerets, H.H.J., Tilmant, K., Gerin, B., Chanteux, H., Depelchin, B.O., Dhalluin, S., Atienzar, F.A., 2012. Characterization of primary human hepatocytes, HepG2 cells, and HepaRG cells at the mRNA level and CYP activity in response to inducers and their predictivity for the detection of human hepatotoxins. Cell biology and toxicology 28, 69–87. https://doi.org/10.1007/s10565-011-9208-4.

Goldberg, L., 1983. Structure-activity correlation as a predictive tool in toxicology.

Gordon, G.J., Coleman, W.B., Grisham, J.W., 2000. Induction of cytochrome P450 enzymes in the livers of rats treated with the pyrrolizidine alkaloid retrorsine. Experimental and molecular pathology 69, 17–26. https://doi.org/10.1006/exmp.2000.2308.

Green, C.E., Segall, H.J., Byard, J.L., 1981. Metabolism, cytotoxicity, and genotoxicity of the pyrrolizidine alkaloid senecionine in primary cultures of rat hepatocytes. Toxicology and Applied Pharmacology 60, 176–185. https://doi.org/10.1016/0041-008X(91)90221-Y.

Green, M.H.L., Muriel, W.J., 1975. Use of repair-deficient strains of escherichia coli and liver microsomes to detect and characterise DNA damage caused by the pyrrolizidine alkaloids heliotrine and monocrotaline. Mutation Research/Fundamental and Molecular Mechanisms of Mutagenesis 28, 331–336. https://doi.org/10.1016/0027-5107(75)90227-4.

Griffin, D.S., Segall, H.J., 1986. Genotoxicity and cytotoxicity of selected pyrrolizidine alkaloids, A possible alkenal metabolite of the alkaloids, and related alkenals. Toxicology and Applied Pharmacology 86, 227–234. https://doi.org/10.1016/0041-008X(86)90053-0.

Griffith, O.W., 1980. Determination of glutathione and glutathione disulfide using glutathione reductase and 2-vinylpyridine. Analytical Biochemistry 106, 207–212. https://doi.org/10.1016/0003-2697(80)90139-6.

Griffith, O.W., Meister, A., 1979. Potent and specific inhibition of glutathione synthesis by buthionine sulfoximine (S-n-butyl homocysteine sulfoximine). Journal of Biological Chemistry 254, 7558–7560. https://doi.org/10.1016/S0021-9258(18)35980-5.

Guillouzo, A., 1998. Liver cell models in in vitro toxicology. Environmental Health Perspectives 106 Suppl 2, 511–532. https://doi.org/10.1289/ehp.98106511.

Guillouzo, A., Corlu, A., Aninat, C., Glaise, D., Morel, F., Guguen-Guillouzo, C., 2007. The human hepatoma HepaRG cells: a highly differentiated model for studies of liver metabolism and toxicity of xenobiotics. Chemico-biological interactions 168, 66–73. https://doi.org/10.1016/j.cbi.2006.12.003.

Guo, L., Dial, S., Shi, L., Branham, W., Liu, J., Fang, J.L., Green, B., Deng, H., Kaput, J., Ning, B.T., 2011. Similarities and differences in the expression of drug-metabolizing enzymes between human hepatic cell lines and primary human

hepatocytes. Drug metabolism and disposition: the biological fate of chemicals 39, 528–538. https://doi.org/10.1124/dmd.110.035873.

Guzelian, P.S., Bissell, D.M., Meyer, U.A., 1977. Drug metabolism in adult rat hepatocytes in primary monolayer culture. Gastroenterology 72, 1232–1239.

Hamilton, P.B., 1962. Ion exchange chromatography of amino acids--microdetermination of free amino acids in serum. Annals of the New York Academy of Sciences 102, 55–75. https://doi.org/10.1111/j.1749-6632.1962.tb13625.x.

Hammond, A.H., Fry, J.R., 1996. Effects of culture duration, cytochrome P-450 inhibition and glutathione depletion on toxicity of diverse xenobiotics. Toxicology in Vitro 10, 315–321. https://doi.org/10.1016/0887-2333(96)00001-X.

Hartmann, T., 1999. Chemical ecology of pyrrolizidine alkaloids. Planta 207, 483–495. https://doi.org/10.1007/s004250050508.

Hartmann, T., Witte, L. (Eds.), 1995. Chapter 4: Chemistry, Biology and Chemoecology of the Pyrrolizidine Alkaloids. Elsevier.

Hayes, A.W., Kruger, C.L., 2014. Hayes' principles and methods of toxicology. CRC Press Taylor & Francis Group, Boca Raton, xxvi, 2157 pages.

He, X.B., Xia, Q.S., Fu, P.P., 2017. 7-Glutathione-pyrrole and 7-cysteine-pyrrole are potential carcinogenic metabolites of pyrrolizidine alkaloids. Journal of Environmental Science and Health, Part C 35, 69–83. https://doi.org/10.1080/10590501.2017.1298358.

Herzog, N., Katzenberger, N., Martin, F., Schmidtke, K.U., K, J.H., 2015. Generation of cytochrome P450 3A4-overexpressing HepG2 cell clones for standardization of hepatocellular testosterone 6β-hydroxylation activity. JCB 1, 15–26. https://doi.org/10.3233/JCB-15002.

Hessel, S., Gottschalk, C., Schumann, D., These, A., Preiss-Weigert, A., Lampen, A., 2014. Structure-activity relationship in the passage of different pyrrolizidine alkaloids through the gastrointestinal barrier: ABCB1 excretes heliotrine and echimidine. Molecular nutrition & food research 58, 995–1004. https://doi.org/10.1002/mnfr.201300707.

Hilgendorf, C., Ahlin, G., Seithel, A., Artursson, P., Ungell, A.L., Karlsson, J., 2007. Expression of thirty-six drug transporter genes in human intestine, liver, kidney, and organotypic cell lines. Drug metabolism and disposition: the biological fate of chemicals 35, 1333–1340. https://doi.org/10.1124/dmd.107.014902.

Hill, B.D., Gaul, K.L., Noble, J.W., 1997. Poisoning of feedlot cattle by seeds of Heliotropium europaeum. Australian Vet J 75, 360–361. https://doi.org/10.1111/j.1751-0813.1997.tb15717.x.

Hincks, J.R., Kim, H.Y., Segall, H.J., Molyneux, R.J., Stermitz, F.R., Coulombe, R.A., 1991. DNA cross-linking in mammalian cells by pyrrolizidine alkaloids:

Structure-activity relationships. Toxicology and Applied Pharmacology 111, 90–98. https://doi.org/10.1016/0041-008x(91)90137-4.

Hinson, J.A., Roberts, D.W., James, L.P., 2010. Mechanisms of acetaminophen-induced liver necrosis. Handbook of experimental pharmacology, 369–405. https://doi.org/10.1007/978-3-642-00663-0_12.

Hirono, I., Haga, M., Fujii, M., Matsuura, S., Matsubara, N., Nakayama, M., Furuya, T., Hikichi, M., Takanashi, H., Uchida, E., Hosaka, S., Ueno, I., 1979. Induction of hepatic tumors in rats by senkirkine and symphytine. Journal of the National Cancer Institute 63, 469–472.

Hirono, I., Mori, H., Culvenor, C.C., 1976. Carcinogenic activity of coltsfoot, Tussilago farfara l. Gan 67, 125–129.

Hirono, I., Mori, H., Haga, M., 1978. Carcinogenic activity of Symphytum officinale. Journal of the National Cancer Institute 61, 865–869.

Hirono, I., Mori, H., Yamada, K., Hirata, Y., Haga, M., 1977. Carcinogenic activity of petasitenine, a new pyrrolizidine alkaloid isolated from Petasites japonicus Maxim. Journal of the National Cancer Institute 58, 1155–1157. https://doi.org/10.1093/jnci/58.4.1155.

Hirono, I., Ueno, I., Aiso, S., Yamaji, T., Haga, M., 1983. Carcinogenic activity of Farfugium japonicum and Senecio cannabifolius. Cancer letters 20, 191–198. https://doi.org/10.1016/0304-3835(83)90048-4.

Huan, J.Y., Miranda, C.L., Buhler, D.R., Cheeke, P.R., 1998. The roles of CYP3A and CYP2B isoforms in hepatic bioactivation and detoxification of the pyrrolizidine alkaloid senecionine in sheep and hamsters. Toxicology and Applied Pharmacology 151, 229–235. https://doi.org/10.1006/taap.1998.8482.

IARC, 2002. Some traditional herbal medicines, some mycotoxins, naphthalene and styrene.

Javitt, N.B., 1990. HepG2 cells as a resource for metabolic studies: lipoprotein, cholesterol, and bile acids. FASEB journal : official publication of the Federation of American Societies for Experimental Biology 4, 161–168. https://doi.org/10.1096/fasebj.4.2.2153592.

Jeejeebhoy, K., Phillips, M.J., 1976. Isolated mammalian hepatocytes in culture. Gastroenterology 71, 1086–1096.

Jiang, L.L., Jiang, Y., Zhao, D.S., Fan, Y.X., Yu, Q., Li, P., Li, H.J., 2018. CYP3A activation and glutathione depletion aggravate emodin-induced liver injury. Chemical research in toxicology 31, 1052–1060. https://doi.org/10.1021/acs.chemrestox.8b00117.

Jurima-romet, M., Abbott, F.S., Tang, W., Huang, H.S., Whitehouse, l.W., 1996. Cytotoxicity of unsaturated metabolites of valproic acid and protection by vitamins C and E in glutathione-depleted rat hepatocytes. Toxicology 112, 69–85. https://doi.org/10.1016/0300-483X(96)03352-5.

Kakar, F., Akbarian, Z., Leslie, T., Mustafa, M.L., Watson, J., van Egmond, H.P., Omar, M.F., Mofleh, J., 2010. An outbreak of hepatic veno-occlusive disease in Western afghanistan associated with exposure to wheat flour contaminated with pyrrolizidine alkaloids. Journal of toxicology 2010, 313280. https://doi.org/10.1155/2010/313280.

Kapuscinski, J., 1995. DAPI: a DNA-specific fluorescent probe. Biotechnic & histochemistry : official publication of the Biological Stain Commission 70, 220–233. https://doi.org/10.3109/10520299509108199.

Kempf, M., Reinhard, A., Beuerle, T., 2010. Pyrrolizidine alkaloids (PAs) in honey and pollen-legal regulation of PA levels in food and animal feed required. Molecular nutrition & food research 54, 158–168. https://doi.org/10.1002/mnfr.200900529.

Kim, H.Y., Stermitz, F.R., Coulombe, R.A., 1995. Pyrrolizidine alkaloid-induced DNA-protein cross-links. Carcinogenesis 16, 2691–2697. https://doi.org/10.1093/carcin/16.11.2691.

Kim, H.Y., Stermitz, F.R., Li, J.K.K., Coulombe, R.A., 1999. Comparative DNA cross-linking by activated pyrrolizidine alkaloids. Food and Chemical Toxicology 37, 619–625. https://doi.org/10.1016/S0278-6915(99)00025-3.

Kim, H.Y., Stermitz, F.R., Molyneux, R.J., Wilson, D.W., Taylor, D., Coulombe, R.A., 1993. Structural influences on pyrrolizidine alkaloid-induced cytopathology. Toxicology and Applied Pharmacology 122, 61–69. https://doi.org/10.1006/taap.1993.1172.

Kirsch-Volders, M., Elhajouji, A., Cundari, E., van Hummelen, P., 1997. The in vitro micronucleus test: a multi-endpoint assay to detect simultaneously mitotic delay, apoptosis, chromosome breakage, chromosome loss and non-disjunction. Mutation Research/Genetic Toxicology and Environmental Mutagenesis 392, 19–30. https://doi.org/10.1016/S0165-1218(97)00042-6.

Knowles, B.B., Howe, C.C., Aden, D.P., 1980. Human hepatocellular carcinoma cell lines secrete the major plasma proteins and hepatitis B surface antigen. Science (New York, N.Y.) 209, 497–499. https://doi.org/10.1126/science.6248960.

Kowalczyk, E., Kwiatek, K., 2018. Pyrrolizidine alkaloids in honey: determination with liquid chromatography-mass spectrometry method. Journal of veterinary research 62, 173–181. https://doi.org/10.2478/jvetres-2018-0027.

Kuhara, K., Takanashi, H., Hirono, I., Furuya, T., Asada, Y., 1980. Carcinogenic activity of clivorine, a pyrrolizidine alkaloid isolated from Ligularia dentata. Cancer letters 10, 117–122. https://doi.org/10.1016/0304-3835(80)90034-8.

Kumana, C.R., Ng, M., Lin, H.J., Ko, W., Wu, P.C., Todd, D., 1985. Herbal tea induced hepatic veno-occlusive disease: quantification of toxic alkaloid exposure in adults. Gut 26, 101–104. https://doi.org/10.1136/gut.26.1.101.

Labrecque, D.R., Howard, R.B., 1976. Chapter 29 The preparation and characterization of intact isolated parenchymal cells from rat liver, in: Methods in cell biology, vol. 14. Elsevier, Academic Press, Amsterdam [u.a.], pp. 327–340.

Lamba, J.K., Lin, Y.S., Schuetz, E.G., Thummel, K.E., 2002. Genetic contribution to variable human CYP3A-mediated metabolism. Advanced Drug Delivery Reviews 54, 1271–1294. https://doi.org/10.1016/S0169-409X(02)00066-2.

Langer, P.J., Shanabruch, W.G., Walker, G.C., 1981. Functional organization of plasmid pKM101. Journal of Bacteriology 145, 1310–1316.

Lehmann, L., Metzler, M., 2004. Bisphenol A and its methylated congeners inhibit growth and interfere with microtubules in human fibroblasts in vitro. Chemico-biological interactions 147, 273–285. https://doi.org/10.1016/j.cbi.2004.01.005.

Lehmann, L., Wagner, J., Metzler, M., 2006. Estrogenic and clastogenic potential of the mycotoxin alternariol in cultured mammalian cells. Food and Chemical Toxicology 44, 398–408. https://doi.org/10.1016/j.fct.2005.08.013.

Lester, C., Troutman, J., Obringer, C., Wehmeyer, K., Stoffolano, P., Karb, M., Xu, Y., Roe, A., Carr, G., Blackburn, K., Mahony, C., 2019. Intrinsic relative potency of a series of pyrrolizidine alkaloids characterized by rate and extent of metabolism. Food and chemical toxicology : an international journal published for the British Industrial Biological Research Association 131, 110523. https://doi.org/10.1016/j.fct.2019.05.031.

Levin, D.E., Hollstein, M., Christman, M.F., Schwiers, E.A., Ames, B.N., 1982. A new Salmonella tester strain (TA102) with A X T base pairs at the site of mutation detects oxidative mutagens. Proceedings of the National Academy of Sciences of the United States of America 79, 7445–7449. https://doi.org/10.1073/pnas.79.23.7445.

Li, N., Xia, Q.S., Ruan, J.Q., Fu, P.P., Ge, L., 2011. Hepatotoxicity and tumorigenicity induced by metabolic activation of pyrrolizidine alkaloids in herbs. Current drug metabolism 12, 823–834. https://doi.org/10.2174/138920011797470119.

Louisse, J., Rijkers, D., Stoopen, G., Holleboom, W.J., Delagrange, M., Molthof, E., Mulder, P.P.J., Hoogenboom, R.L.A.P., Adebert, M., Reijnenburg, Ad. A.C.M., 2019. Determination of genotoxic potencies of pyrrolizidine alkaloids in HepaRG cells using the γH2AX assay. Food and chemical toxicology 131:110532. https://doi.org/10.1016/j.fct.2019.05.040

Lowry, O.H., Rosebrough, N.J., FARR, A.L., Randall, R.J., 1951. Protein measurement with the Folin phenol reagent. The Journal of biological chemistry 193, 265–275.

Lubet, R.A., Nims, R.W., Mayer, R.T., Cameron, J.W., Schechtman, L.M., 1985. Measurement of cytochrome P-450 dependent dealkylation of alkoxy-phenoxazones in hepatic S9s and hepatocyte homogenates: effects of dicumarol.

Mutation Research Letters 142, 127–131. https://doi.org/10.1016/0165-7992(85)90052-1.

Ma, J., Xia, Q.S., Fu, P.P., Ge, L., 2018. Pyrrole-protein adducts – A biomarker of pyrrolizidine alkaloid-induced hepatotoxicity. Journal of Food and Drug Analysis 26, 965–972. https://doi.org/10.1016/j.jfda.2018.05.005.

Maron, D.M., Ames, B.N., 1983. Revised methods for the Salmonella mutagenicity test. Mutation Research/Environmental Mutagenesis and Related Subjects 113, 173–215. https://doi.org/10.1016/0165-1161(83)90010-9.

Martignoni, M., Groothuis, G.M.M., Kanter, R. D., 2006. Species differences between mouse, rat, dog, monkey and human CYP-mediated drug metabolism, inhibition and induction. Expert Opinion on Drug Metabolism & Toxicology 2, 875–894. https://doi.org/10.1517/17425255.2.6.875.

Maslansky, C.J., Williams, G.M., 1982. Primary cultures and the levels of cytochrome P450 in hepatocytes from mouse, rat, hamster, and rabbit liver. In vitro 18, 683–693. https://doi.org/10.1007/BF02796423.

Mathon, C., Edder, P., Bieri, S., Christen, P., 2014. Survey of pyrrolizidine alkaloids in teas and herbal teas on the Swiss market using HPLC-MS/MS. Analytical and bioanalytical chemistry 406, 7345–7354. https://doi.org/10.1007/s00216-014-8142-8.

Mattocks, A., 1982. Hydrolysis and hepatotoxicity of retronecine diesters. Toxicology letters 14, 111–116. https://doi.org/10.1016/0378-4274(82)90017-0.

Mattocks, A.R., 1971. Hepatotoxic effects due to pyrrolizidine alkaloid N-oxides. Xenobiotica; the fate of foreign compounds in biological systems 1, 563–565. https://doi.org/10.3109/00498257109041530.

Mattocks, A.R., 1986. Chemistry and toxicology of pyrrolizidine alkaloids. Academic, London.

McCann, J., Spingarn, N.E., Kobori, J., Ames, B.N., 1975. Detection of carcinogens as mutagens: bacterial tester strains with R factor plasmids. Proceedings of the National Academy of Sciences of the United States of America 72, 979–983. https://doi.org/10.1073/pnas.72.3.979.

McKinney, J.D., 2000. The practice of structure activity relationships (SAR) in toxicology. Toxicological Sciences 56, 8–17. https://doi.org/10.1093/toxsci/56.1.8.

Meehan, R.R., Forrester, L.M., Stevenson, K., Hastie, N.D., Buchmann, A., Kunz, H.W., Wolf, C.R., 1988. Regulation of phenobarbital-inducible cytochrome P-450s in rat and mouse liver following dexamethasone administration and hypophysectomy. The Biochemical journal 254, 789–797. https://doi.org/10.1042/bj2540789.

Mei, N., Chou, M.W., Fu, P.P., Heflich, R.H., Chen, T., 2004a. Differential mutagenicity of riddelliine in liver endothelial and parenchymal cells of transgenic

big blue rats. Cancer letters 215, 151–158. https://doi.org/10.1016/j.canlet.2004.06.013.

Mei, N., Heflich, R.H., Chou, M.W., Chen, T., 2004b. Mutations induced by the carcinogenic pyrrolizidine alkaloid riddelliine in the liver cII gene of transgenic big blue rats. Chemical research in toxicology 17, 814–818. https://doi.org/10.1021/tx049955b.

Merz, K.H., Schrenk, D., 2016. Interim relative potency factors for the toxicological risk assessment of pyrrolizidine alkaloids in food and herbal medicines. Toxicology letters 263, 44–57. https://doi.org/10.1016/j.toxlet.2016.05.002.

Miranda, C.L., Reed, R.L., Guengerich, F.P., Buhler, D.R., 1991. Role of cytochrome P450IIIA4 in the metabolism of the pyrrolizidine alkaloid senecionine in human liver. Carcinogenesis 12, 515–519. https://doi.org/10.1093/carcin/12.3.515.

Mirsalis, J.C., Steinmetz, K.L., Blazak, W.F., Spalding, J.W., 1993. Evaluation of the potential of riddelliine to induce unscheduled DNA synthesis, S-phase synthesis, or micronuclei following in vivo treatment with multiple doses. Environmental and molecular mutagenesis 21, 265–271. https://doi.org/10.1002/em.2850210310.

Mitchell, J.R., Jollows, D.J., 1975. Metabolic activation of drugs to toxic substances. Gastroenterology 68, 392–410. https://doi.org/10.1016/S0016-5085(75)80025-4.

Mohabbat, O., Shafiq Younos, M., Merzad, A.A., Srivastava, R.N., Ghaos Sediq, G., Aram, G.N., 1976. An outbreak of hepatic veno-occlusive disease in north-western Afghanistan. Lancet (London, England) 308, 269–271. https://doi.org/10.1016/s0140-6736(76)90726-1.

Molyneux, R.J., Gardner, D.L., Colegate, S.M., Edgar, J.A., 2011. Pyrrolizidine alkaloid toxicity in livestock: a paradigm for human poisoning? Food additives & contaminants. Part A, Chemistry, analysis, control, exposure & risk assessment 28, 293–307. https://doi.org/10.1080/19440049.2010.547519.

Moore, D.J., Batts, K.P., Zalkow, L.L., Fortune, G.T., Powis, G., 1989. Model systems for detecting the hepatic toxicity of pyrrolizidine alkaloids and pyrrolizidine alkaloid N-oxides. Toxicology and Applied Pharmacology 101, 271–284. https://doi.org/10.1016/0041-008X(89)90276-7.

Mori, H., Sugie, S., Yoshimi, N., Asada, Y., Furuya, T., Williams, G.M., 1985. Genotoxicity of a variety of pyrrolizidine alkaloids in the hepatocyte primary culture-DNA repair test using rat, mouse, and hamster hepatocytes. Cancer research 45, 3125–3129.

Morrison, M.H., Di Monte, D., Jernström, B., 1985. Glutathione status in primary cultures of rat hepatocytes and its role in cell attachment to collagen. Chemico-biological interactions 53, 3–12. https://doi.org/10.1016/s0009-2797(85)80079-x.

Mulder, P.P.J., López, P., Castellari, M., Bodi, D., Ronczka, S., Preiss-Weigert, A., These, A., 2018. Occurrence of pyrrolizidine alkaloids in animal- and plant-derived food: results of a survey across Europe. Food additives & contaminants.

Part A, Chemistry, analysis, control, exposure & risk assessment 35, 118–133. https://doi.org/10.1080/19440049.2017.1382726.
Mulder, P.P.J., Sánchez, P.L., These, A., Preiss-Weigert, A., Castellari, M., 2015. Occurrence of pyrrolizidine alkaloids in food. EFS3 12. https://doi.org/10.2903/sp.efsa.2015.EN-859.
Mulder, P.P.J., Witte, S.L. D., Stoopen, G.M., van der Meulen, J., van Wikselaar, P.G., Gruys, E., Groot, M.J., Hoogenboom, R.L.A.P., 2016. Transfer of pyrrolizidine alkaloids from various herbs to eggs and meat in laying hens. Food additives & contaminants. Part A, Chemistry, analysis, control, exposure & risk assessment 33, 1826–1839. https://doi.org/10.1080/19440049.2016.1241430.
Müller, L., Kasper, P., Kaufmann, G., 1992. The clastogenic potential in vitro of pyrrolizidine alkaloids employing hepatocyte metabolism. Mutation Research Letters 282, 169–176. https://doi.org/10.1016/0165-7992(92)90091-U.
Müller-Tegethoff, K., Kersten, B., Kasper, P., Müller, L., 1997. Application of the in vitro rat hepatocyte micronucleus assay in genetic toxicology testing. Mutation Research/Genetic Toxicology and Environmental Mutagenesis 392, 125–138. https://doi.org/10.1016/S0165-1218(97)00051-7.
Namkung, M.J., Yang, H.L., Hulla, J.E., Juchau, M.R., 1988. On the substrate specificity of cytochrome P450IIIA1. Molecular pharmacology 34, 628–637.
Nerurkar, P.V., Park, S.S., Thomas, P.E., Nims, R.W., Lubet, R.A., 1993. Methoxyresorufin and benzyloxyresorufin: substrates preferentially metabolized by cytochromes P4501A2 AND 2B, respectively, in the rat and mouse. Biochemical Pharmacology 46, 933–943. https://doi.org/10.1016/0006-2952(93)90504-p.
Ning, J., Rietjens, I.M.C.M., Strikwold, M., 2019. Integrating physiologically based kinetic (PBK) and Monte Carlo modelling to predict inter-individual and inter-ethnic variation in bioactivation and liver toxicity of lasiocarpine. Archives of toxicology 93, 2943–2960. https://doi.org/10.1007/s00204-019-02563-x.
Novotná, A., Krasulová, K., Bartoňková, I., Korhoňová, M., Bachleda, P., Anzenbacher, P., Dvořák, Z., 2014. Dual effects of ketoconazole cis-enantiomers on CYP3A4 in human hepatocytes and HepG2 Cells. PLoS ONE 9, e111286. https://doi.org/10.1371/journal.pone.0111286.
NTP, 1978. (National Toxicology Program) Bioassay of lasiocarpine for possible carcinogenicity. National Cancer Institute carcinogenesis technical report series 39, 1–66.
NTP, 2003. Toxicology and carcinogenesis studies of riddelliine (CAS No. 23246-96-0) in F344/N rats and B6C3F1 mice (gavage studies). National Toxicology Program technical report series, 1–280.
O'Brien, J., Wilson, I., Orton, T., Pognan, F., 2000. Investigation of the Alamar Blue (resazurin) fluorescent dye for the assessment of mammalian cell cytotoxicity.

European journal of biochemistry 267, 5421–5426. https://doi.org/10.1046/j.1432-1327.2000.01606.x.

OECD, 2016. OECD Guideline for the Testing of Chemicals: In Vitro Mammalian Cell Micronucleus Test.

Okuno, S., Maezawa, I., Sakuma, Y., Matsushita, T., Yamaguchi, T., 1988. Effect of the hydroxyl group of the p-hydroxyphenyl moiety of aspoxicillin, a semisynthetic penicillin, on its pharmacokinetic property. J. Antibiot. 41, 239–246. https://doi.org/10.7164/antibiotics.41.239.

Page, B., Page, M., Noel, C., 1993. A new fluorometric assay for cytotoxicity measurements in-vitro. International journal of oncology 3, 473–476.

Pereira, T.N., Webb, R.I., Reilly, P.E., Seawright, A.A., Prakash, A.S., 1998. Dehydromonocrotaline generates sequence-selective N-7 guanine alkylation and heat and alkali stable multiple fragment DNA crosslinks. Nucleic Acids Research 26, 5441–5447. https://doi.org/10.1093/nar/26.23.5441.

Petry, T.W., Bowden, G.T., Huxtable, R.J., Sipes, I.G., 1984. Characterization of hepatic DNA damage induced in rats by the pyrrolizidine alkaloid monocrotaline. Cancer research 44, 1505–1509.

Rao, M.S., Reddy, J.K., 1978. Malignant neoplasms in rats fed lasiocarpine. British journal of cancer 37, 289–293. https://doi.org/10.1038/bjc.1978.38.

Reed, R.L., Ahern, K.G., Pearson, G.D., Buhler, D.R., 1988. Crosslinking of DNA by dehydroretronecine, a metabolite of pyrrolizidine alkaloids. Carcinogenesis 9, 1355–1361. https://doi.org/10.1093/carcin/9.8.1355.

Ridker, P.M., Ohkuma, S., McDermott, W.V., Trey, C., Huxtable, R.J., 1985. Hepatic venocclusive disease associated with the consumption of pyrrolizidine containing dietary supplements. Gastroenterology 88, 1050–1054. https://doi.org/10.1016/s0016-5085(85)80027-5.

Roeder, E., 2000. Medicinal plants in China containing pyrrolizidine alkaloids. Die Pharmazie 55, 711–726.

Roulet, M., Laurini, R., Rivier, L., Calame, A., 1988. Hepatic veno-occlusive disease in newborn infant of a woman drinking herbal tea. The Journal of pediatrics 112, 433–436. https://doi.org/10.1016/s0022-3476(88)80330-5.

Ruan, J.Q., Liao, C.S., Ye, Y., Ge, L., 2014a. Lack of metabolic activation and predominant formation of an excreted metabolite of nontoxic platynecine-type pyrrolizidine alkaloids. Chemical research in toxicology 27, 7–16. https://doi.org/10.1021/tx4004159.

Ruan, J.Q., Yang, M.B., Fu, P., Ye, Y., Ge, L., 2014b. Metabolic activation of pyrrolizidine alkaloids: insights into the structural and enzymatic basis. Chemical research in toxicology 27, 1030–1039. https://doi.org/10.1021/tx500071q.

Rubiolo, P., Pieters, L., Calomme, M., Bicchi, C., Vlietinck, A., Vanden Berghe, D., 1992. Mutagenicity of pyrrolizidine alkaloids in the Salmonella

typhimurium/mammalian microsome system. Mutation Research Letters 281, 143–147. https://doi.org/10.1016/0165-7992(92)90050-R.

Sanderson, B.J.S., Clark, A.M., 1993. Micronuclei in adult and foetal mice exposed in vivo to heliotrine, urethane, monocrotaline and benzidine. Mutation research 285, 27–33. https://doi.org/10.1016/0027-5107(93)90048-K.

Schoental, R., 1975. Pancreatic islet-cell and other tumors in rats given heliotrine, a monoester pyrrolizidine alkaloid, and nicotinamide. Cancer research 35, 2020–2024.

Schoental, R., Cavanagh, J.B., 1972. Brain and spinal cord tumors in rats treated with pyrrolizidine alkaloids. Journal of the National Cancer Institute 49, 665–671.

Schoental, R., Fowler, M.E., Coady, A., 1970. Islet cell tumors of the pancreas found in rats given pyrrolizidine alkaloids from Amsinckia intermedia Fisch and Mey and from Heliotropium supinum L. Cancer research 30, 2127–2131.

Schoental, R., Hard, G.C., Gibbard, S., 1971. Histopathology of renal lipomatous tumors in rats treated with the “natural” products, pyrrolizidine alkaloids and α,β-unsaturated aldehydes. JNCI: Journal of the National Cancer Institute. https://doi.org/10.1093/jnci/47.5.1037.

Schoental, R., HEAD, M.A., Peacock, P.R., 1954. Senecio alkaloids; primary liver tumours in rats as a result of treatment with (1) a mixture of alkaloids from S. jacobaea Lin; (2) retrorsine; (3) isatidine. British journal of cancer 8, 458–465. https://doi.org/10.1038/bjc.1954.49.

Schuler, M., Gudi, R., Cheung, J., Kumar, S., Dickinson, D., Engel, M., Szkudlinska, A., Colman, M., Maduka, N., Sherman, J., Thiffeault, C., 2010. Evaluation of phenolphthalein, diazepam and quinacrine dihydrochloride in the in vitro mammalian cell micronucleus test in Chinese hamster ovary (CHO) and TK6 cells. Mutation research 702, 219–229. https://doi.org/10.1016/j.mrgentox.2010.04.004.

Segall, H.J., Wilson, D.W., Dallas, J.L., Haddon, W.F., 1985. trans-4-Hydroxy-2-hexenal: a reactive metabolite from the macrocyclic pyrrolizidine alkaloid senecionine. Science (New York, N.Y.) 229, 472–475. https://doi.org/10.1126/science.4012327.

Seglen, P.O., 1976. Chapter 4 Preparation of isolated rat liver cells, in: Methods in cell biology, vol. 13. Elsevier, Academic Press, Amsterdam [u.a.], pp. 29–83.

Seglen, P.O., Fosså, J., 1978. Attachment of rat hepatocytes in vitro to substrata of serum protein, collagen, or concanavalin A. Experimental Cell Research 116, 199–206. https://doi.org/10.1016/0014-4827(78)90076-9.

Shi, F., Zhao, P., Li, X.B., Pan, H., Ma, S.P., Ding, L., 2015. Cytotoxicity of luteolin in primary rat hepatocytes: the role of CYP3A-mediated ortho-benzoquinone metabolite formation and glutathione depletion. Journal of applied toxicology : JAT 35, 1372–1380. https://doi.org/10.1002/jat.3106.

Shitara, Y., Sato, H., Sugiyama, Y., 2005. Evaluation of drug-drug interaction in the hepatobiliary and renal transport of drugs. Annual review of pharmacology and toxicology 45, 689–723. https://doi.org/10.1146/annurev.pharmtox.44.101802.121444.

Shull, L.R., Buckmaster, G.W., Cheeke, P.R., 1976. Factors influencing pyrrolizidine (Senecio) alkaloid metabolism: species, liver sulfhydryls and rumen fermentation. Journal of animal science 43, 1247–1253. https://doi.org/10.2527/jas1976.4361247x.

Shumaker, R.C., Robertson, K.A., Hsu, I.C., Allen, J.R., 1976. Neoplastic transformation in tissues of rats exposed to monocrotaline or dehydroretronecine. Journal of the National Cancer Institute 56, 787–790. https://doi.org/10.1093/jnci/56.4.787.

Silva-Neto, J.P., Barreto, R.A., Pitanga, B.P.S., Souza, C.S., v.d. Silva, Silva, A.R., Velozo, E.S., Cunha, S.D., Batatinha, M.J.M., Tardy, M., Ribeiro, C.S.O., Costa, M.F.D., El-Bachá, R.S., Costa, S.L., 2010. Genotoxicity and morphological changes induced by the alkaloid monocrotaline, extracted from Crotalaria retusa, in a model of glial cells. Toxicon 55, 105–117. https://doi.org/10.1016/j.toxicon.2009.07.007.

Smith, L.W., Culvenor, C.C., 1981. Plant sources of hepatotoxic pyrrolizidine alkaloids. Journal of natural products 44, 129–152. https://doi.org/10.1021/np50014a001.

Smith, P.K., Krohn, R.I., Hermanson, G.T., Mallia, A.K., Gartner, F.H., Provenzano, M.D., Fujimoto, E.K., Goeke, N.M., Olson, B.J., Klenk, D.C., 1985. Measurement of protein using bicinchoninic acid. Analytical Biochemistry 150, 76–85. https://doi.org/10.1016/0003-2697(85)90442-7.

Stegelmeier, B.L., Edgar, J.A., Colegate, S.M., Gardner, D.R., Schoch, T.K., Coulombe, R.A., Molyneux, R.J., 1999. Pyrrolizidine alkaloid plants, metabolism and toxicity. Journal of natural toxins 8, 95–116.

Sun, W., Wu, R.R., van Poelje, P.D., Erion, M.D., 2001. Isolation of a family of organic anion transporters from human liver and kidney. Biochemical and biophysical research communications 283, 417–422. https://doi.org/10.1006/bbrc.2001.4774.

Takanashi, H., Umeda, M., Hirono, I., 1980. Chromosomal aberrations and mutation in cultured mammalian cells induced by pyrrolizidine alkaloids. Mutation Research/Genetic Toxicology 78, 67–77. https://doi.org/10.1016/0165-1218(80)90027-0.

Takashima, R., Takasawa, H., Wako, Y., Yasunaga, K., Hattori, A., Kawabata, M., Nakadate, K., Nakagawa, M., Hamada, S.C., 2015. Micronucleus induction in rat liver and bone marrow by acute vs. repeat doses of the genotoxic hepatocarcinogen monocrotaline. Mutation research. Genetic toxicology and

environmental mutagenesis 780-781, 64–70. https://doi.org/10.1016/j.mrgentox.2014.12.008.

Tamta, H., Pawar, R.S., Wamer, W.G., Grundel, E., Krynitsky, A.J., Rader, J.I., 2012. Comparison of metabolism-mediated effects of pyrrolizidine alkaloids in a HepG2/C3A cell-S9 co-incubation system and quantification of their glutathione conjugates. Xenobiotica; the fate of foreign compounds in biological systems 42, 1038–1048. https://doi.org/10.3109/00498254.2012.679978.

Tandon, B.N., Tandon, H.D., Tandon, R.K., Narndranathan, M., Joshi, Y.K., 1976. AN EPIDEMIC OF VENO-OCCLUSIVE DISEASE OF LIVER IN CENTRAL INDIA. Lancet (London, England) 308, 271–272. https://doi.org/10.1016/S0140-6736(76)90727-3.

Tandon, H.D., Tandon, B.N., Mattocks, A.R., 1978. An epidemic of veno-occlusive disease of the liver in Afghanistan. Pathologic features. The American journal of gastroenterology 70, 607–613.

Tong, V., Teng, X.W., Chang, T.K.H., Abbott, F.S., 2005. Valproic acid II: effects on oxidative stress, mitochondrial membrane potential, and cytotoxicity in glutathione-depleted rat hepatocytes. Toxicological Sciences 86, 436–443. https://doi.org/10.1093/toxsci/kfi185.

Treiber, A., Schneiter, R., Delahaye, S., Clozel, M., 2004. Inhibition of organic anion transporting polypeptide-mediated hepatic uptake is the major determinant in the pharmacokinetic interaction between bosentan and cyclosporin A in the rat. The Journal of pharmacology and experimental therapeutics 308, 1121–1129. https://doi.org/10.1124/jpet.103.061614.

Tu, M.J., Li, L.P., Lei, H.M., Ma, Z.Y., Chen, Z.J., Sun, S.Y., Xu, S.Y., Zhou, H., Zeng, S., Jiang, H.D., 2014. Involvement of organic cation transporter 1 and CYP3A4 in retrorsine-induced toxicity. Toxicology 322, 34–42. https://doi.org/10.1016/j.tox.2014.04.007.

Tu, M.J., Sun, S.Y., Wang, K., Peng, X.Y., Wang, R.H., Li, L.P., Zeng, S., Zhou, H., Jiang, H.D., 2013. Organic cation transporter 1 mediates the uptake of monocrotaline and plays an important role in its hepatotoxicity. Toxicology 311, 225–230. https://doi.org/10.1016/j.tox.2013.06.009.

Turpeinen, M., Ghiciuc, C., Opritoui, M., Tursas, L., Pelkonen, O., Pasanen, M., 2007. Predictive value of animal models for human cytochrome P450 (CYP)-mediated metabolism: a comparative study in vitro. Xenobiotica; the fate of foreign compounds in biological systems 37, 1367–1377. https://doi.org/10.1080/00498250701658312.

Uhl, M., Helma, C., Knasmüller, S., 2000. Evaluation of the single cell gel electrophoresis assay with human hepatoma (Hep G2) cells. Mutation Research/Genetic Toxicology and Environmental Mutagenesis 468, 213–225. https://doi.org/10.1016/S1383-5718(00)00051-6.

van Montfoort, J.E., Hagenbuch, B., Groothuis, G.M.M., Koepsell, H., Meier, P.J., Meijer, D.K.F., 2003. Drug uptake systems in liver and kidney. Current drug metabolism 4, 185–211. https://doi.org/10.2174/1389200033489460.

VanDemark, N.L., Mercier, E., Salisbury, G.W., 1945. The Methylene-Blue Reduction Test and its Relation to Other Measures of Quality in Bull Semen. Journal of Dairy Science 28, 121–128. https://doi.org/10.3168/jds.S0022-0302(45)95152-6.

Waizenegger, J., Braeuning, A., Templin, M., Lampen, A., Hessel-Pras, S., 2018. Structure-dependent induction of apoptosis by hepatotoxic pyrrolizidine alkaloids in the human hepatoma cell line HepaRG: Single versus repeated exposure. Food and chemical toxicology : an international journal published for the British Industrial Biological Research Association 114, 215–226. https://doi.org/10.1016/j.fct.2018.02.036.

Wang, C.H., Li, Y., Gao, J.G., He, Y.Q., Xiong, A.Z., Yang, L., Cheng, X.M., Ma, Y.M., Wang, Z.T., 2011. The comparative pharmacokinetics of two pyrrolizidine alkaloids, senecionine and adonifoline, and their main metabolites in rats after intravenous and oral administration by UPLC/ESIMS. Analytical and bioanalytical chemistry 401, 275–287. https://doi.org/10.1007/s00216-011-5075-3.

Wang, J., Lai, L., Tang, Y., 1999. Structural features of toxic chemicals for specific toxicity. J. Chem. Inf. Comput. Sci. 39, 1173–1189. https://doi.org/10.1021/ci990039r.

Wang, T.T., Frandsen, H.L., Christiansson, N.R., Rosendal, S.E., Pedersen, M., Smedsgaard, J., 2019. Pyrrolizidine alkaloids in honey: Quantification with and without standards. Food Control 98, 227–237. https://doi.org/10.1016/j.foodcont.2018.11.033.

Wang, X., Kanel, G.C., DeLeve, L.D., 2000. Support of sinusoidal endothelial cell glutathione prevents hepatic veno-occlusive disease in the rat. Hepatology 31, 428–434. https://doi.org/10.1002/hep.510310224.

Wang, Y.P., Fu, P., Chou, M., 2005a. Metabolic Activation of the Tumorigenic Pyrrolizidine Alkaloid, Retrorsine, Leading to DNA Adduct Formation In Vivo. IJERPH 2, 74–79. https://doi.org/10.3390/ijerph2005010074.

Wang, Y.P., Yan, J., Beger, R.D., Fu, P.P., Chou, M.W., 2005b. Metabolic activation of the tumorigenic pyrrolizidine alkaloid, monocrotaline, leading to DNA adduct formation in vivo. Cancer letters 226, 27–35. https://doi.org/10.1016/j.canlet.2004.11.039.

Wang, Y.P., Yan, J., Fu, P.P., Chou, M.W., 2005c. Human liver microsomal reduction of pyrrolizidine alkaloid N-oxides to form the corresponding carcinogenic parent alkaloid. Toxicology letters 155, 411–420. https://doi.org/10.1016/j.toxlet.2004.11.010.

Wehner, F.C., Thiel, P.G., van Rensburg, S.J., 1979. Mutagenicity of alkaloids in the Salmonella/microsome system. Mutation Research/Genetic Toxicology 66, 187–190. https://doi.org/10.1016/0165-1218(79)90065-X.

Westerink, W.M.A., Schoonen, W.G.E.J., 2007. Phase II enzyme levels in HepG2 cells and cryopreserved primary human hepatocytes and their induction in HepG2 cells. Toxicology in vitro : an international journal published in association with BIBRA 21, 1592–1602. https://doi.org/10.1016/j.tiv.2007.06.017.

White, I.N., Mattocks, A.R., 1972. Reaction of dihydropyrrolizines with deoxyribonucleic acids in vitro. The Biochemical journal 128, 291–297. https://doi.org/10.1042/bj1280291.

White, I.N.H., Mattocks, A.R., Butler, W.H., 1973. The conversion of the pyrrolizidine alkaloid retrorsine to pyrrolic derivatives in vivo and in vitro and its acute toxicity to various animal species. Chemico-biological interactions 6, 207–218. https://doi.org/10.1016/0009-2797(73)90048-3.

WHO-IPCS, 1988. Pyrrolizidine alkaloids. World Health Organization, Geneva.

WHO-IPCS, 1989. Pyrrolizidine alkaloids health and safety guide. WHO, Geneva.

Williams, D.E., Reed, R.L., Kedzierski, B., Dannan, G.A., Guengerich, F.P., Buhler, D.R., 1989. Bioactivation and detoxication of the pyrrolizidine alkaloid senecionine by cytochrome P-450 enzymes in rat liver. Drug metabolism and disposition: the biological fate of chemicals 17, 387–392.

Williams, G.M., Bermudez, E., Scaramuzzino, D., 1977. Rat hepatocyte primary cell cultures. III. Improved dissociation and attachment techniques and the enhancement of survival by culture medium. In vitro 13, 809–817. https://doi.org/10.1007/BF02615128.

Williams, G.M., Mori, H., Hirono, I., Nagao, M., 1980. Genotoxicity of pyrrolizidine alkaloids in the hepatocyte primary culture/DNA-repair test. Mutation Research/Genetic Toxicology 79, 1–5. https://doi.org/10.1016/0165-1218(80)90141-X.

Williams, R.T., 1974. Inter-Species Variations in the Metabolism of Xenobiotics. Biochemical Society Transactions 2, 359–377. https://doi.org/10.1042/bst0020359.

Williams, R.T., 1978. Species Variations in the Pathways of Drug Metabolism. Environmental Health Perspectives 22, 133. https://doi.org/10.2307/3428562.

Winter, C.K., Segall, H.J., Jones, A.D., 1988. Species differences in the hepatic microsomal metabolism of the pyrrolizidine alkaloid senecionine. Comparative Biochemistry and Physiology Part C: Comparative Pharmacology 90, 429–433. https://doi.org/10.1016/0742-8413(88)90022-9.

Wu, G.Y., Fang, Y.Z., Yang, S., Lupton, J.R., Turner, N.D., 2004. Glutathione metabolism and its implications for health. The Journal of nutrition 134, 489–492. https://doi.org/10.1093/jn/134.3.489.

Xia, Q.S., Chou, M.W., Edgar, J.A., Doerge, D.R., Fu, P.P., 2006. Formation of DHP-derived DNA adducts from metabolic activation of the prototype heliotridine-type pyrrolizidine alkaloid, lasiocarpine. Cancer letters 231, 138–145. https://doi.org/10.1016/j.canlet.2005.01.023.

Xia, Q.S., Yan, J., Chou, M.W., Fu, P.P., 2008. Formation of DHP-derived DNA adducts from metabolic activation of the prototype heliotridine-type pyrrolizidine alkaloid, heliotrine. Toxicology letters 178, 77–82. https://doi.org/10.1016/j.toxlet.2008.02.008.

Xia, Q.S., Zhao, Y.W., Tungeln, L.S. V., Doerge, D.R., Ge, L., Cai, L.N., Fu, P.P., 2013. Pyrrolizidine alkaloid-derived DNA adducts as a common biological biomarker of pyrrolizidine alkaloid-induced tumorigenicity. Chemical research in toxicology 26, 1384–1396. https://doi.org/10.1021/tx400241c.

Yamanaka, H., Nagao, M., Sugimura, T., Furuya, T., Shirai, A., Matsushima, T., 1979. Mutagenicity of pyrrolizidine alkaloids in the Salmonella/mammalian-microsome test. Mutation Research/Genetic Toxicology 68, 211–216. https://doi.org/10.1016/0165-1218(79)90152-6.

Yan, J., Nichols, J., Yang, Y.C., Fu, P., Chou, M., 2002. Detection of Riddelliine-Derived DNA Adducts in Blood of Rats Fed Riddelliine. IJMS 3, 1019–1026. https://doi.org/10.3390/i3091019.

Yang, M.B., Ruan, J.Q., Gao, H., Li, N., Ma, J., Xue, J.Y., Ye, Y., Fu, P.P., Wang, J.Y., Ge, L., 2017. First evidence of pyrrolizidine alkaloid N-oxide-induced hepatic sinusoidal obstruction syndrome in humans. Archives of toxicology 91, 3913–3925. https://doi.org/10.1007/s00204-017-2013-y.

Yang, Y., Yan, J., Churchwell, M., Beger, R., Chan, P., Doerge, D.R., Fu, P.P., Chou, M.W., 2001a. Development of a (32)P-postlabeling/HPLC method for detection of dehydroretronecine-derived DNA adducts in vivo and in vitro. Chemical research in toxicology 14, 91–100. https://doi.org/10.1021/tx000149o.

Yang, Y.C., Yan, J., Doerge, D.R., Chan, P.C., Fu, P.P., Chou, M.W., 2001b. Metabolic activation of the tumorigenic pyrrolizidine alkaloid, riddelliine, leading to DNA adduct formation in vivo. Chemical research in toxicology 14, 101–109. https://doi.org/10.1021/tx000150n.

Yokoyama, Y., Sasaki, Y., Terasaki, N., Kawataki, T., Takekawa, K., Iwase, Y., Shimizu, T., Sanoh, S., Ohta, S., 2018. Comparison of Drug Metabolism and Its Related Hepatotoxic Effects in HepaRG, Cryopreserved Human Hepatocytes, and HepG2 Cell Cultures. Biological & pharmaceutical bulletin 41, 722–732. https://doi.org/10.1248/bpb.b17-00913.

Yu, Z.G., Guo, G.F., Wang, B.Z., 2020. Lycopsamine inhibits the proliferation of human lung cancer cells via induction of apoptosis and autophagy and suppression of interleukin-2. Journal of B.U.ON. : official journal of the Balkan Union of Oncology 25, 2358–2363.

CURRICULUM VITAE

	Publications
2021	Geburek I., Rutz L., Gao L., Küpper J.-H., These A., Schrenk D. Metabolic pattern of hepatotoxic pyrrolizidine alkaloids in liver cells. *Chemical Research in Toxicology* 34(4): 1101-1113
	Gao L., Schäfer C., O´Reardon K., Gorgus E., Ruth S.-H. The mutagenic potency of onion juice vs. its contents of quercetin and rutin. *Food and Chemical Toxicology* 148: 111923
2020	Rutz L., Gao L., Küpper J.-H., Schrenk D. Structure-dependent genotoxic potencies of selected pyrrolizidine alkaloids in metabolically competent HepG2 cells. *Archives of Toxicology* 94(12): 4159-4172.
	Schrenk D., Gao L., Ge L., Mahony C., Mulder P.P.J., Peijnenburg A., Pfuhler S., Rietjens I.M.C.M., Rutz L., Steinhoff B., These A. Pyrrolizidine alkaloids in food and phytomedicine: Occurrence, exposure, toxicity, mechanisms, and risk assessment – A review. *Food and Chemical Toxico*logy 136: 111107
	Gao L., Rutz L., Schrenk D. Structure-dependent hepato-cytotoxic potencies of selected pyrrolizidine alkaloids in primary rat hepatocytes culture. *Food and Chemical Toxicology* 135:110923.
2019	Gao L., Schmitz H.-J., Merz K.-H., Schrenk D. Characterization of the cytotoxicity of selected Chelidonium alkaloids in rat hepatocytes. *Toxicology Letters* 311, 91-97.
	Lectures
09.2018	Workshop: Toxicity and risk assessment of pyrrolizidine alkaloids – current status and way toward (Kaiserslautern, Germany) "Toxicological risk assessment of pyrrolizidine alkaloids – investigation of cytotoxicity and mutagenicity of individual congeners"
12.2017	Symposium: Alte Indikationen – neue Wirkmechanismen, zum 35-jährigen Bestehen der Kooperation Phytopharmaka (Cologne, Germany)

	"Vergleichende toxikologische Bewertung ausgewählter Pyrrolizidinalkaloide"
09.2017	Phytotherapiekongress 2017 (Münster, Germany) "Projekt zur vergleichenden toxikologischen Bewertung von PA-Isomeren"
11.2016	Symposium: DNA damage response, genetic instability and cancer (Mainz, Germany) "Pre-trial in a toxicological risk assessment of pyrrolizidine alkaloids"
11.2016	Symposium: Phytopharmaka – von der Tradition zur Evidenz (Bonn, Germany) "*In vitro* Untersuchung der Hepatotoxizität und Genotoxizität ausgewählter Pyrrolizidinalkaloide"
	Posters
02.2019	85rd Annual Meeting of the German Society for Experimental and Clinical Pharmacology and Toxicology (DGPT) and 21th Annual Meeting of Association of Clinical Pharmacology (VKliPha) with Contribution of AGAH (Stuttgart, Germany) Rutz L., Gao L., Merz K.-H., Schrenk D. "Investigations of the hepatotoxic potential of selected pyrrolizidine alkaloids and synthesis of dehydropyrrolizidine alkaloid glutathione adducts"
10.2018	Annual Meeting of the German Pharmaceutical Society – DPhG: Pharmaceutical Science: Structure, Function and Application (Hamburg, Germany) Gao L., Rutz L., Kelber O., Merz K.-H., Schrenk D. "Structure-dependent cytotoxicity of different pyrrolizidine alkaloids in primary rat hepatocytes and HepG2 cells: Role of cytochrome P450 3A"
09.2018	54rd Congress of the European Societies of Toxicology (Brussels, Belgium) Gao L., Rutz L., Kelber O., Merz K.-H., Schrenk D. "Investigation of pyrrolizidine alkaloids – cytotoxicity tests using primary rat hepatocytes and HepG2 cells: Role of cytochrome P450 3A"
04.2018	10th Congress of Toxicology in Developing Countries and 12th Serbian Congress of Toxicology (Belgrade, Serbia) Gao L., Rutz L., Kelber O., Merz K.-H., Schrenk D.

	"Investigation of the relative hepatotoxic and genotoxic potency of selected pyrrolizidine alkaloids"
03.2018	84rd Annual Meeting of the German Society for Experimental and Clinical Pharmacology and Toxicology (DGPT) and 20th Annual Meeting of Association of Clinical Pharmacology (VKliPha) with Contribution of AGAH (Göttingen, Germany) Rutz L., Gao L., Schrenk D. "Investigations of hepatotoxicity in the Alamar blue assay and test for mutagenic potential in the Ames fluctuation assay"
09.2017	53rd Congress of the European Societies of Toxicology (Bratislava, Slovakia) Gao L., Rutz L., Kelber O., Merz K.-H., Keller J., Müller J., Schrenk D. "Toxicological risk assessment of pyrrolizidine alkaloids – Investigation of mutagenicity in the Ames fluctuation assay"
03.2017	83rd Annual Meeting of the German Society for Experimental and Clinical Pharmacology and Toxicology (DGPT) and 19th Annual Meeting of Association of Clinical Pharmacology (VKliPha) with Contribution of AGAH (Heidelberg, Germany) Gao L., Schmitz H.-J., A.-Beckmann M., Schrenk D. "Toxicity of *Chelidonium majus* alkaloids in rat hepatocytes – role of glutathione"